The impact of differential temperatures (30°C versus 45°C) on the methanogenic community in Philippine rice field soil

Dissertation

zur Erlangung des Grades eines

Doktor der Naturwissenschaften

(Dr. rer. nat.)

des Fachbereichs Biologie der Philipps-Universität Marburg

Vorgelegt von

Xin Li

aus Qingdao, China

Marburg, Deutschland, 2022

Die vorliegende Dissertation wurde von 12/2018 bis 12/ 2022 am Max-Planck-Institut für terrestrische Mikrobiologie unter Leitung von PD Dr. Werner Liesack angefertigt.

Vom Fachbereich Biologie der Philipps-Universität Marburg (Hochschulkennziffer 1180) als Dissertation angenommen am

Erstgutachter: PD Dr. Werner Liesack

Zweitgutachter: Prof. Dr. Lennart Randau

Prüfer: Prof. Dr. Andreas Brune

Prüfer: Prof. Dr. Alexander Zizka

Tag der Disputation: _____09.03.2023_____

Table of contents

Summary

Microbial methanogenesis is the largest biogenic source of atmospheric methane (CH_4), which is the second most important anthropogenic greenhouse gas. In particular, water-logged rice paddies contribute approximately 25% to the total annual CH_4 budget in the atmosphere, making them a critical source of anthropogenic CH_4 emissions into earth's atmosphere. The methanogenic degradation of organic matter in anoxic environments, whose final products are methane and carbon dioxide, contributes to the energy flow and circulation of matter in ecosystems and involves a microbial food chain composed of different functional guilds of the domains *Bacteria* and *Archaea*. But a deep understanding of their activity dynamics during the methanogenic organic matter breakdown in Philippine paddy soil has not yet been achieved. In addition, like most other forms of metabolism, methanogenesis is temperature-dependent. The expected increase in global surface temperature due to climate change may have a tremendous effect on the microbial dynamics and methanogenic processes in flooded rice field soil. However, a system-level understanding of the effects of rising temperature on the anaerobic food chain in Philippine paddy soil is still lacking.

Anoxic paddy soil slurries amended with rice straw were used as model system. A multi-methods approach (the combination of metabolite measurements, quantitative analysis of biomarkers, metatranscriptomics analysis, and metagenomics analysis) was applied to decipher the compositional and functional dynamics of the methanogenic community in Philippine rice field soil over an incubation period of 120 days under mesophilic (30 °C) and moderately thermophilic temperatures (45 °C). In particular, we aimed at answering the following questions: (i) who are the major bacterial players at the different trophic levels of the anaerobic food chain; (ii) which methanogenic pathways dominate, and which methanogen groups are prevalent during the 120-day incubation period; and (iii) how does the rising temperature affect the structural and functional dynamics of the methanogenic community?

At mesophilic temperature, qPCR and RT-qPCR, but also metatranscriptomics, revealed two major bacterial and methanogenic activity phases defined as early (days 7 to 21) and late (days 28 to < 60 days) community responses, separated by a significant transient decline in microbial gene and transcript abundances. *Geobacteraceae* was the most abundant bacterial population over incubation time. The two methanogenic activity phases corresponded to greatest transcript abundances of the *Methanosarcinaceae,* but differed in the methanogenic pathways expressed. While three genetically distinct *Methanosarcina* populations contributed

to acetoclastic methanogenesis during the early activity phase, the late activity phase was defined by methylotrophic and acetoclastic methanogenesis performed by only a single *Methanosarcina* population. Mapping of environmental transcripts onto metagenome-assembled genomes (MAGs) revealed a population closely related to *Methanosarcina* sp. MSH10X1 to be the key player in both acetoclastic and methylotrophic methanogenesis. Members of the *Methanocellaceae* were the key players in hydrogenotrophic methanogenesis, while the acetoclastic activity of *Methanotrichaceae* members was detectable only during the very late community response.

At moderately thermophilic temperature, the structure and function (including polymer hydrolysis, syntrophic oxidation of key intermediates, and methanogenesis) of the methanogenic community displayed differential responses compared to mesophilic temperature. *Heliobacteriaceae* replaced *Geobacteraceae* to prevail in bacterial dynamics during the 120-day incubation period. The transcript dynamics of CAZyme-encoding genes showed a different pattern, compared with mesophilic condition. In particular, CAZyme genes involved in the hydrolysis of cellulose and hemicellulose had an increased transcript activity in the late stage. The methanogen community and their dynamics were characterized by acetoclastic-methylotrophic (*Methanosarcinaceae*) and hydrogenotrophic (*Methanocellaceae*) methanogens. The intra-family analysis of *Methanosarcinaceae* identified five genetically distinct *Methanosarcina* populations that differed in the methanogenic pathways expressed. Mapping of environmental transcripts onto *Methanosarcina* reference genomes revealed that two *Methanosarcina* populations mainly contributed to acetoclastic and methylotrophic methanogenesis during the early activity phase. These were closely affiliated to *Methanosarcina flavescens* - *Methanosarcina thermophila* TM-1 and *Methanosarcina barkeri* 3, respectively. The late activity phase was defined only by methylotrophic methanogenesis, which was performed by a single *Methanosarcina* population closely affiliated to *Methanosarcina barkeri* 3. Members of the *Methanocellaceae* were the key players in hydrogenotrophic methanogenesis, while no acetoclastic activity of *Methanotrichaceae* members was observed under moderately thermophilic condition.

In conclusion, the occurrence of methylotrophic methanogenesis, in addition to acetoclastic and hydrogenotrophic methanogenesis, at both mesophilic and moderately thermophilic temperatures is a crucial new finding. Temperature had a differential effect on the structural and functional continuum in which the methanogenic food chain operates. Our study showed that the methanogenic community responses in flooded rice field soils are more complex than previously thought.

Zusammenfassung

Methanogenese ist eine der bedeutendsten biogenen Quellen für atmosphärisches Methan (CH_4). Dieses ist nach Kohlendioxid das zweitwichtigste Treibhausgas. Insbesondere geflutete Reisfelder sind mit einem Beitrag von circa 25% zur jährlichen Methanemission in die Erdatmosphäre eine kritische anthropogene Quelle für Methan. Die methanogene Zersetzung organischen Materials zu Methan und Kohlendioxid in anoxischen Umwelten trägt erheblich zum globalen Stoffumsatz und Energiefluß bei. Die anaerobe Nahrungskette beinhaltet die Aktivität von Mitgliedern der *Bacteria* und *Archaea*, welche in unterschiedlichen funktionellen Gilden strukturiert sind. Jedoch fehlen für philippinischen Reisfeldboden bisher detaillierte Untersuchungen zur Aktivität und Dynamik der an der anaeroben Nahrungskette beteiligten Mikroorganismen. Ferner ist zu erwähnen, dass die mikrobiellen Umsetzungen innerhalb der anaeroben Nahrungskette temperaturabhängig sind. Der im Rahmen des Klimawandels prognostizierte Anstieg der Temperatur an der Erdoberfläche könnte daher einen erheblichen Effekt allgemein auf mikrobielle Aktivitäten haben, aber insbesondere auch auf die methanogenen Prozesse im gefluteten Reisfeldboden. Allerdings liegen bisher nur begrenzt Kenntnisse vor, wie sich eine Temperaturerhöhung im Reisfeldboden auf die Dynamiken der an der anaeroben Nahrungskette beteiligten Mikroorganismen auswirken würde.

In dieser Studie wurden Aufschlämmungen anoxischen Reisfeldbodens, denen Reisstroh zugesetzt wurde, als Modellsystem genutzt. Verschiedene methodische Ansätze wurden kombiniert, um Struktur, Funktion und Dynamik der methanogenen Lebensgemeinschaft im philippinischen Reisfeldboden während einer Langzeitinkubation (120 Tage) vergleichend under mesophilen (30°C) und moderat thermophilen (45°C) Bedingungen aufzuklären. Dazu gehörten die Messung freigesetzter Fermentationsprodukte (Acetat, Propionat, Butyrat) und der Methanbildung, quantitative PCR von Markergenen und deren Transkripte (16S rRNA, *mcrA*) sowie die Analyse des Metatranskriptoms und Metagenoms. Insbesondere sollten die folgenden Fragen beantwortet werden: (i) Welche Mikroorganismen tragen auf den verschiedenen trophischen Ebenen der anaeroben Nahrungskette zur Zersetzung organischen Materials bei? (ii) Welche methanogenen Stoffwechselwege dominieren und von welchen Gruppen an Methanogenen werden diese während der 120 Tage langen Inkubation exprimiert? (iii) Welchen Effekt hat eine Temperaturerhöhung von 30°C auf 45°C auf die Struktur, Funktion und Dynamik der methanogenen Lebensgemeinschaft?

Sowohl die quantitatien Analysen via qPCR und RT-qPCR als auch Metatranskriptomics

ergaben, dass die Langzeitinkubation unter mesophilen (30°C) Bedingungen in zwei methanogene Aktivitätsphasen zu unterteilen ist. Diese sind durch eine frühe (7 – 21 Tage) und späte (28 - 60 Tage) Phase definiert, wobei die beiden Aktivitätsperioden durch eine signifikante Abnahme der quantifizierbaren Kopienzahl an Markergenen (qPCR) und deren Transkripte (RT-qPCR) zeitlich voneinander getrennt sind. Mitglieder der *Geobacteraceae* waren während der gesamten Inkubation die vorherrschende bakterielle Population. Die frühe und späte Aktivitätsphasen korrespondierten in den Metatranskriptom-Analysen zu den höchsten mRNA-Abundanzen der *Methanosarcinaceae*, unterschieden sich aber in den von *Methanosarcina* spp. exprimierten methanogenen Stoffwechselwegen. Während in der frühen Aktivitätsphase drei phylogenetisch unterscheidbare *Methanosarcina*-Populationen zur acetoklastischen Methanogenese beitrugen, war in der späten Aktivitätsphase nur eine einzige phylogenetisch definierte *Methanosarcina*-Population aktiv. Diese exprimierte neben acetoklastischer vor allem auch methylotrophe Methanogenese. Eine basierend auf der metatranskriptomischen mRNA durchgeführte Transkript-Analyse von metagenom-assemblierten Genomen (MAGs) zeigte, dass die besonders in der späten Aktivitätsphase vorherrschende und aktive *Methanosarcina*-Population eng mit dem Stamm MSH10X1 verwandt ist. Die Expression der hydrogenotrophen Methanogenese konnte Mitgliedern der Familie *Methanocellaceae* zugeordnet werden, während acetoklastische Aktivität von Mitgliedern der *Methanotrichaceae* erst ab dem 60. Tag der Langzeitinkubation nachweisbar war.

Die Inkubation unter moderat thermophilen (45°C) Bedingungen hatte erhebliche Effekte auf die Struktur, Funktion und Dynamik der in die anaerobe Nahrungskette involvierte methanogene Lebensgemeinschaft. Insbesondere gilt dies im Vergleich zu den mesophilen (30°C) Bedingungen für die an der Polymer-Hydrolyse, der syntrophen Oxidation von Intermediaten (Propionat, Acetat) und der Expression methanogener Stoffwechselwege beteiligten mikrobiellen Populationen. Mitglieder der Familie *Heliobacteriaceae* repräsentierten während der gesamten Inkubation die vorherrschende bakterielle Population. *Geobacteraceae* waren hingegen nicht mehr nachweisbar. Im Vergleich zu den mesophilen Bedingungen zeigten Gene, welche für kohlenhydrataktive Enzyme (CAZymes) kodieren, eine über die Inkubationszeit wesentlich differenziertere transkriptionelle Aktivität. Gene involviert in die Hydrolye von Xylan und Chitin wurden um den 14. Tag stark exprimiert, während für solche involviert in die Hydrolyse von Cellulose und Hemicellulose am 35. und 60. Tag die höchsten Transkriptmengen nachweisbar waren. Acetoklastische und methylotrophe Methanogenese wurde durch Mitglieder der *Methanosarcinaceae* experimiert, während

Mitglieder der *Methanocellaceae* für die hydrogenotrophe Methanogenese verantwortlich waren. Die weitere Analyse wies fünf phylogenetisch differenzierbare *Methanosarcina* Populationen nach. Eine basierend auf der metatranskriptomischen mRNA durchgeführte Transkript-Analyse von metagenom-assemblierten Genomen (MAGs) zeigte, dass in der frühen Aktivitätsphase jedoch nur zwei *Methanosarcina*-Populationen primär für die Expression der acetoklastischen und methylotrophen Methanogenese verantwortlich waren. Diese wiesen eine enge Verwandtschaft zu *Methanosarcina flavescens* - *Methanosarcina thermophila* TM beziehungsweise zu *Methanosarcina barkeri* 3 auf. Die späte Aktivitätsphase war ausschließlich durch methylotrophe Methanogenese und der mit *Methanosarcina barkeri* 3 eng assoziierten Population charakterisiert. Die Expression der hydrogenotrophen Methanogenese wurde, wie unter mesophilen Bedingungen, Mitgliedern der *Methanocellaceae* zugeordnet, während eine Aktivität von Mitgliedern der *Methanotrichaceae* unter moderat thermophilen Bedingungen nicht nachweisbar war.

Abschließend sei hervorgehoben, dass der Nachweis methylotropher Methanogenese im gefluteten Reisfeldboden, zusätzlich zur acetoklastischen und hydrogenotrophen Methanogenese, sowohl unter mesophilen (30°C) als auch moderat thermophilen (45°C) Bedingungen ein unerwartetes Ergebnis ist. Die Temperaturerhöhung von 30°C auf 45°C hatte erheblichen Effekte auf die anaerobe Nahrungskette und der daran beteiligten methanogenen Lebensgemeinschaft. Ganz offensichtlich ist die Antwort dieser Lebensgemeinschaft auf sich verändernde Umweltbedingungen komplexer als zuvor angenommen.

1 Introduction

Waterlogged rice fields are not only one of the prevailing sources of the global annual methane budget, but they also represent an excellent model system to gain an understanding of the methanogenic food chain in anoxic environments. This chapter of my PhD thesis is intended to give a comprehensive overview about methane as the second-biggest contributor to human-caused climate change after carbon dioxide, rice field soil as a model system for microbial ecology and how the methanogenic food chain contributes to the global methane budget through the anaerobic degradation of bio-polymers. Furthermore, I discuss how the temperature influences the structure and function of certain functional guilds such as fermentative bacteria, syntrophs, and methanogens. The scientific topics are organized by particular subheadings.

1.1 Methane budget

Methane is the second most important anthropogenic greenhouse gas in terms of climate forcing, after carbon dioxide (CO_2). Methane is responsible for approximately 40% of the human-caused warming the world has experienced to date. According to the IPCC (2013), the global warming potential (GWP) of methane, measured over a 100-year time horizon, is 28 times greater than carbon dioxide (CO_2) on a per mass basis, and 10.2 times greater on a per molecule basis. Human activities have caused atmospheric methane concentrations to more than double since 1750. After a period of stability in the early 2000s, methane levels began to increase again in 2007. The annual increase in atmospheric methane during 2021 ((17 parts per billion (ppb)) reported by NOAA was the largest annual increase recorded since systematic measurements began in 1983. Atmospheric methane levels averaged 1,895.7 ppb during 2021, and thus were around 162% greater than pre-industrial levels and 15% higher than the 1984-2006 period (Feng et al., 2022; Lan et al., 2022). Combined with CO_2, this level of methane emissions puts the world on a pathway that leads to a 3-4 ˚C increase in mean global surface temperature by 2100 (**Figure 1.1**).

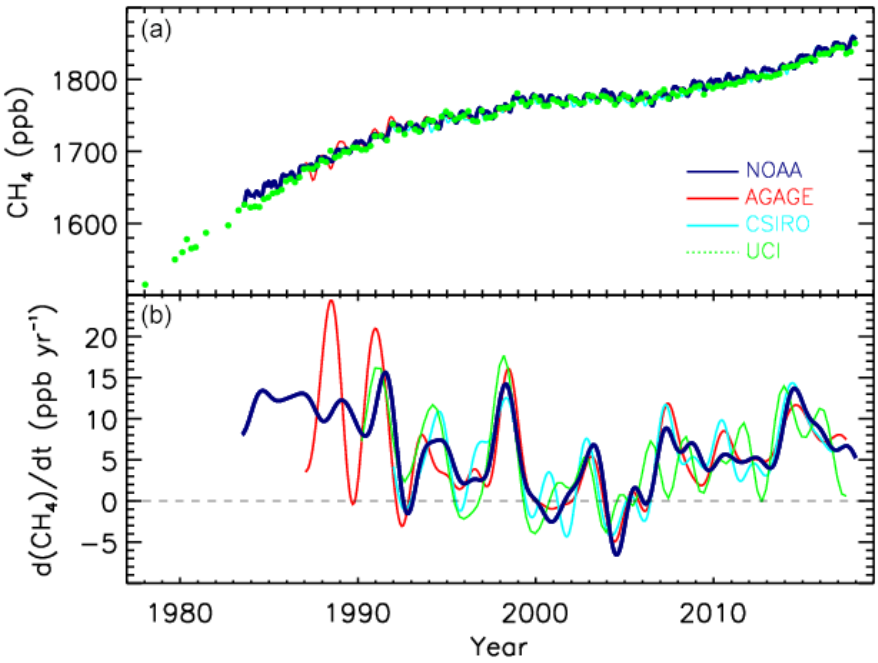

Figure 1.1: Globally averaged atmospheric CH_4 (ppb) (a) and its annual growth rate GATM (ppb yr^{-1}) (b) from four measurement programs: National Oceanic and Atmospheric Administration (NOAA), Advanced Global Atmospheric Gases Experiment (AGAGE), Commonwealth Scientific and Industrial Research Organization (CSIRO), and University of California, Irvine (UCI). Taken from Kirschke et al. (2013).

Studies of atmospheric methane are numerous and vary widely due to the many natural and human sources of this gas. The **Figure 1.2** indicates an estimate of the sinks (i.e., atmospheric loss) of CH_4 over the period from 2000 to 2009. This figure illustrates that the global atmospheric methane budget is determined by a variety of human and natural sources that are balanced in the atmosphere. Methane emissions can generally be grouped into three categories: biogenic, thermogenic, and pyrogenic. Biogenic sources include methane-producing methanogens in anaerobic environments such as natural wetlands, rice paddies, oxygen-poor freshwater reservoirs, digestive systems of ruminants and termites, and organic waste deposits. Methanogenesis by anaerobic methanogens is the largest biogenic source of atmospheric methane (Reeburgh, 2003). This process is considered central to the global carbon cycle and plays a great role in climate regulation, due to the high GWP of methane (IPCC, 2013). The considerable role of methane in global warming makes microbial methane production an important research issue. Moreover, knowledge of the methanogenic degradation pathways allows establishment of mechanistic models for the prediction of future methane release scenarios and development of mitigation strategies.

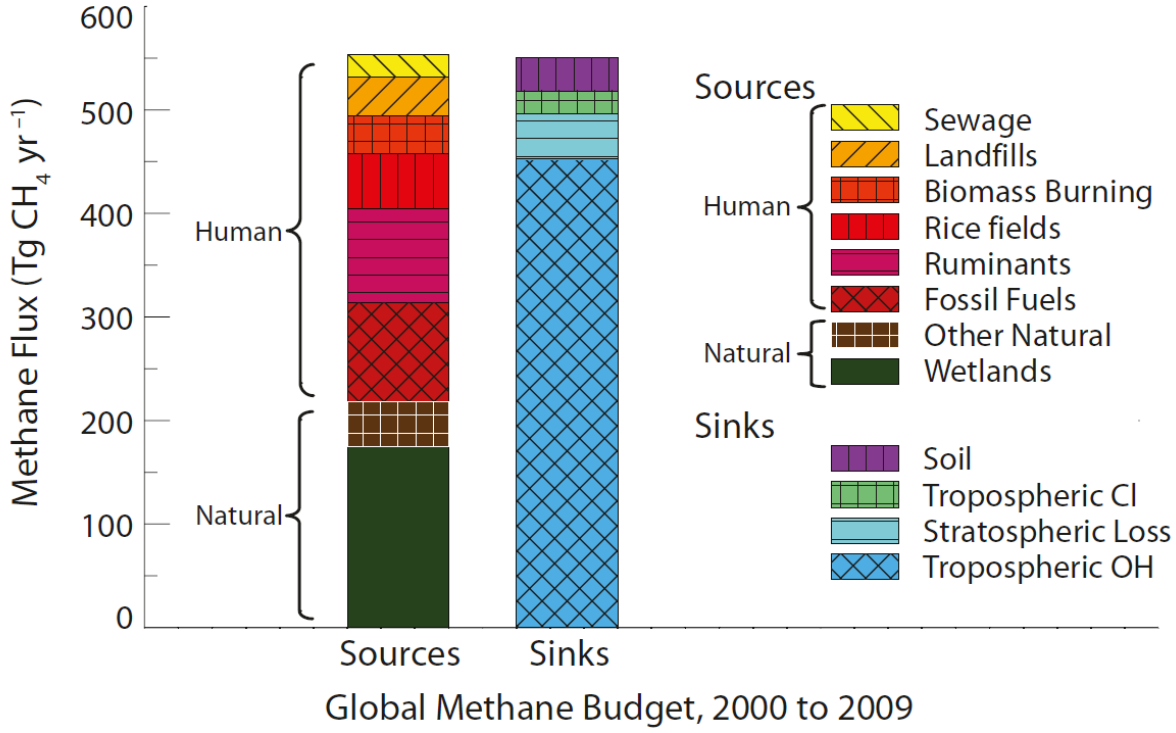

Figure 1.2: Global methane budget. Sources and sinks of atmospheric methane, over the decade 2000–2009, expressed as flux either into or out of the atmosphere. After Conrad (2009) and Kirschke et al. (2013). Human and natural sources, as well as their sources and sinks.

1.2 Rice paddy soil – a suitable model system

Rice is the staple food of approximately half of the world's population and thus the most important agronomic crop plant. In about 75% of this land rice grows under waterlogged conditions (Roger et al., 1993), and such anoxic conditions lead to the emission of methane. Estimations of the annual methane emission rate from flooded rice fields range from 60 to 110 Tg (Prinn, 1994). The higher end of this range represents about 25% of total annual methane emissions into the atmosphere (Cicerone and Oremland, 1988), indicating that flooded rice fields are a significant source of biogenic methane (Prinn, 1994).

Waterlogged rice fields are not only one of the prevailing sources of the global annual methane budget (IPCC 2007, Chen and Prinn, 2005; Bridgham et al., 2013), but they also represent an excellent model system to gain an understanding of the methanogenic food web in anoxic environments, including diversity, structure, and dynamics of microbial communities as well as structure-function relationships between microorganisms. Rice fields are one of the few environmental systems that are regularly exposed to alternate dry/wet and oxic/anoxic cycles. Due to the growing global population, further increase in rice farming worldwide is expected. Therefore, rice field soil will gain more impact on the global methane budget and, in

consequence, more research interest.

Rice paddies are a distinct ecosystem that is flooded seasonally and defined by the biological, physical, and chemical characteristics of a particular site. Waterlogged paddy soil can be considered as a complex ecosystem composed of three individual eco-compartments (oxic surface soil, anoxic bulk soil, and rhizosphere soil plus rhizoplane) characterized by different physiochemical conditions including organic carbon input, oxygen availability, and the presence and accessibility of alternative electron acceptors (e.g., nitrate, Mn^{4+}, Fe^{3+}, and sulfate). Organic carbon present in paddy soil originates from soil organic matter, rice root exudates, and decaying plant material.

In rice, aerial parts of plants take up CO_2, then transform it into sugars through photosynthesis, which are used to produce biomass or storage compounds. Carbon from decaying plant material or rice root exudates, which are composed of sugars, amino acids and fatty acids, can be converted by decomposer microbes into methanogenic substrates (CO_2, hydrogen and acetate). In the anoxic zone, these substrates are transformed into CH_4 by methanogenic archaea. The methane may remain in the soil, escape to the atmosphere by diffusion through the aerenchyma of the rice plants, or be intercepted by methane-consuming bacteria. These utilize methane for oxygen-requiring respiration, thereby yielding CO_2. Hence, methane emission from rice paddies is determined by the balance of methane-producing and methane-consuming microorganisms, the availability of other substrates, and the activity of microbes competing for these compounds — collectively, these processes constitute the methane cycle (Bodelier, 2015) (**Figure 1.3**).

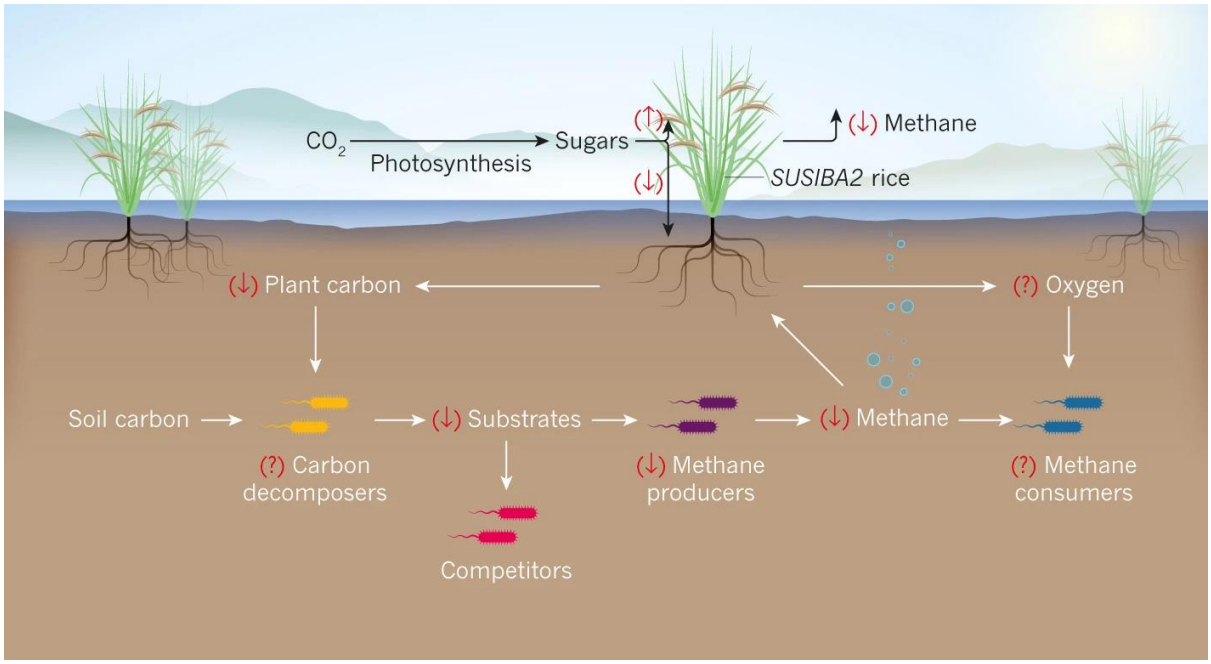

Figure 1.3: Methane cycle in rice paddy soil. Methane emission from rice paddies is determined by the balance of methane-producing and methane-consuming microorganisms, the availability of other substrates, and the activity of microbes competing for these compounds — collectively, these processes constitute the methane cycle. Taken from Bodelier (2015).

Numerous studies have been carried out to understand organic matter decomposition and CH_4 production in rice field soils (e.g., Conrad et al., 2012; Penning and Conrad, 2007; Zhang et al., 2015). In particular, paddy soil slurries amended with rice straw proved to represent an excellent model system to decipher the metabolic processes involved in the anaerobic degradation of plant polymers (Glissmann and Conrad, 2000; Glissmann et al., 2001; Weber et al., 2001a, 2001b; Glissmann and Conrad, 2002). Over recent years, this research had primarily been done on two geographically distinct paddy soils sampled in Italy and the Philippines (e.g., Glissmann and Conrad, 2000; Chin et al., 2004; Conrad et al., 2012; Liu et al., 2018a, 2019). The methanogenic communities in these two soils differ in composition and their response to straw amendments (Liu and Conrad, 2017; Yuan et al., 2020).

Italian rice field soil has frequently been used as a standard model system to investigate methanogenesis in flooded rice paddy soil. Previous studies have revealed that methane production is dominated by acetoclastic and hydrogenotrophic methanogens including *Methanosarcinaceae*, *Methanotrichaceae* and *Methanocellaceae* (Ji et al., 2018a; Peng et al., 2018). Syntrophic bacterial partners, such as *Clostridiaceae*, *Lachnospiraceae*, *Peptococcaceae* and *Ruminococcaceae*, showed co-occurrence patterns with methanogens in

paddy soils (Peng et al., 2018). Several studies in tropical and subtropical rice field soils, like those on the Philippines or from South China, indicated that the structural and functional organization of the anaerobic food chain differs between paddy soils of different geographic locations. Furthermore, microorganisms showed differing responses to environmental factors (Liu et al., 2018; Ma et al., 2012). However, a detailed understanding of these distinctive community responses is not yet achieved.

1.3 The anaerobic degradation of organic matter

The anaerobic breakdown of organic matter, which produces methane and carbon dioxide as end products, plays a crucial role in the movement of energy and substances within ecosystems and is a key part of the global carbon cycle. Anaerobic microbial methane production (AMMP) is the only process that can fully mineralize organic matter.

Anaerobic microbial methane production (AMMP) was the dominant process for recycling dead biomass in the Precambrium (Holland et al., 1986) and, even in our contemporary oxygenated biosphere, it still accounts for about 1-2% of the total carbon cycle (Ehhalt, 1979). AMMP occurs naturally in anoxic ecosystems such as wetlands, flooded rice paddies, freshwater sediments, and the digestive tracts of animals (Hackstein et al., 1996). It also takes place in man-made systems like anaerobic digesters and landfills, which together contribute more than 60% of the global methane budget (Conrad, 2009). In general, AMMP can occur wherever degradable organic matter is present in anoxic conditions. It only occurs under low redox potential and in the absence of energetically more favorable electron acceptors such as oxygen, nitrate, iron, and sulfate.

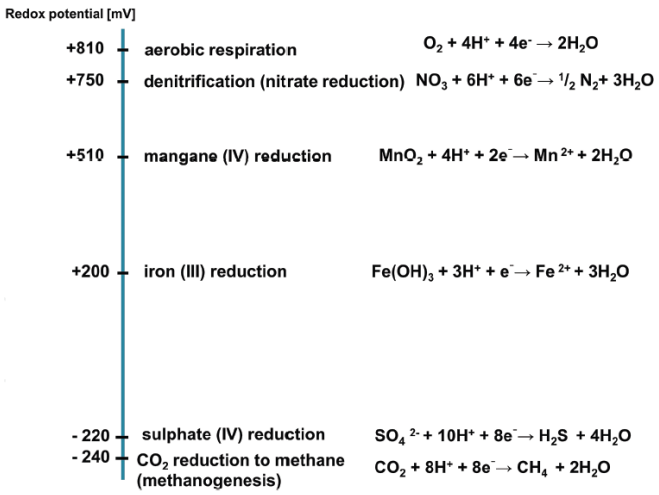

Figure 1.4: Redox potential for different types of terminal electron acceptors in anaerobic respiration and energy gain for microbial cells. Taken from Sikora et al.(2017).

Operation of AMMP is promoted by the activity of a complex microbial community consisting of various guilds including hydrolytic bacteria, fermenting bacteria, syntrophic bacteria and methanogenic archaea that fulfill the following functions (Zinder, 1993; Conrad, 1999; Schink and Stams, 2013): ① hydrolysis of bio-polymers to monomers, ② fermentation of the monomers to simple compounds, usually short-chain fatty acids (e.g., acetate, butyrate, and propionate), alcohols, H_2 and CO_2; ③ syntrophic conversion of short-chain fatty acids and alcohols to acetate, CO_2 and H_2; ④ fermentation of monomers to only acetate (heterotrophic acetogenesis) or ⑤ conversion of H_2 and CO_2 to acetate (chemolithotrophic acetogenesis); ⑥ syntrophic oxidation of acetate to CO_2 and H_2; and ⑦ products such as H_2 and CO_2, acetate and methylated compounds are utilized by methanogens to produce methane (**Figure 1.5**) (Evans et al., 2019; Conrad, 2020a). Thus, the anaerobic degradation of rice straw involves a complex anaerobic food chain.

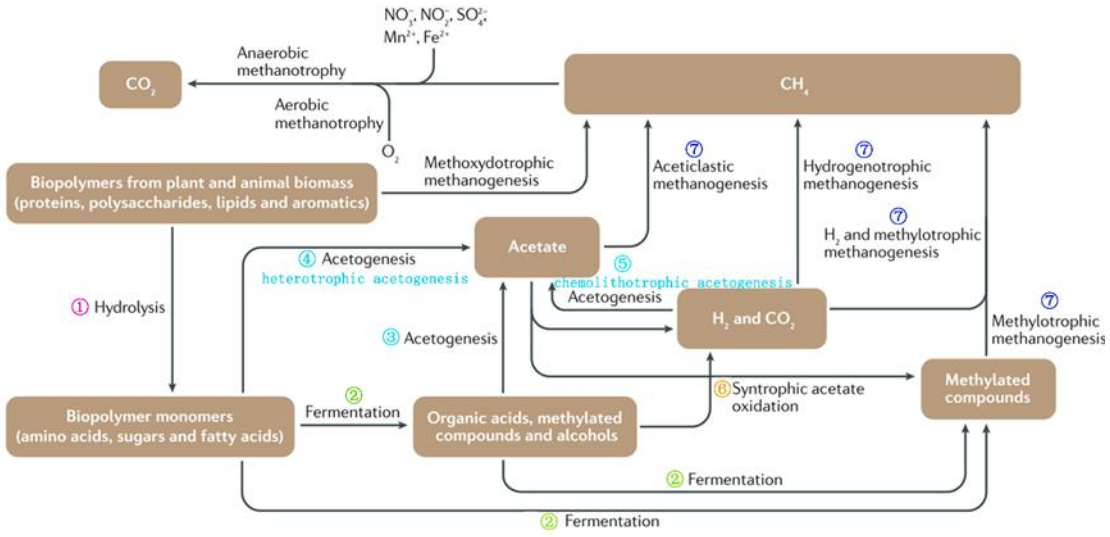

Figure 1.5: Biomass ultimately fuels both the production and consumption of methane (CH_4) before its release to the atmosphere. Complex organic matter is degraded by microorganisms in anoxic environments by a multi-step process including hydrolysis, fermentation, homoacetogenesis and syntrophic acetate oxidation, leading to CO_2 and CH_4 as the end products. Modified after (Evans et al., 2019).

1.3.1 Hydrolysis: rice straw degradation

Hydrolysis is the first step of the anaerobic food web through which polymeric substances (lipids, proteins, carbohydrates) are converted into small molecules (molecular weight < 1000 Da) (e.g., sugars, fatty acids, amino acids). Straw is one of the most abundant stocks of renewable biomass from crop production and one of the major organic carbon sources added to paddy soil as a fertilizer, which is decomposed by anaerobic degradation (Kimura et al., 2004). In consequence, methane production will be enhanced (Yan et al., 2009).

Rice straw, as a lignocellulosic biomass, is comprised of different biopolymers, including cellulose (32–37%), hemicellulose (29–37%), lignin (5–15%), and pectin (2-3%), bound together in a complex structure. Cellulose and hemicelluloses are fiber organics, whereas lignin is a component of the cell wall (Klass, 1998). Inside the lignocellulose complex, cellulose maintains its crystalline fibrous structure and serves as the primary structural component of plant cell walls, providing mechanical strength (Anwar et al., 2014). Hemicellulose is located between the micro- and macro-fibrils of cellulose, while lignin, which can be found in the spaces between fibers and on the surface of cells, provides structural support for the matrix in which cellulose and hemicellulose are embedded.(Harmsen et al., 2010).

The rice straw contains polysaccharides which provide food for the diverse group of microorganisms that break down organic matter into CO_2 and CH_4 (Kimura and Tun, 1999; Weber et al., 2001b, 2001a; Wegner and Liesack, 2016). During microbial hydrolysis, the decomposition of organic matter is facilitated by enzymes produced by hydrolytic microorganisms. The activity and production of these enzymes play a crucial role in the hydrolysis process in anoxic ecosystems. These extracellular hydrolases, such as lipases, proteases, and glucosidases, are found on the surface of microbial membranes or as part of a multi-enzyme complex called the cellulosome (Burgess and Pletschke, 2008). Microorganisms with the ability to break down cellulose, a particularly recalcitrant compound, have developed intricate enzyme systems for this purpose (Himmel et al., 2010). The three main groups of hydrolases involved in anaerobic digestion are esterases, glycosidases, and peptidases, which break down ester bonds, glycoside bonds, and peptide bonds, respectively. The bacteria most frequently involved in hydrolysis belong to the *Firmicutes* (*Clostridia*, *Bacilli*), *Bacteroidetes*, and *Gammaproteobacteria* groups (Wirth et al., 2012; Hanreich et al., 2013; Li et al., 2013). Usually, these bacteria are capable of performing acidogenesis, the second step in organic matter decomposition.

In general, rice straw degradation can be separated into fast and slow microbial processes depending on organic carbon availability. A steady-state governed by methanogenesis and

limited by bio-polymer breakdown is reached due to depletion of the easily accessible organic compounds consisting of glucose and nonstructural carbohydrates after 4-week anaerobic incubation (Glissmann and Conrad, 2002). High turnover rates of intermediates, such as acetate, butyrate and propionate, and rapid-response microbes were detected in the early-stage of rice straw degradation (Wegner and Liesack, 2016; Peng et al., 2018). The later stage was characterized by the degradation of more recalcitrant compounds (e.g., cellulose, lignin, and other structural components). Furthermore, previous long-term incubation studies under anaerobic conditions have shown that bacteria and archaea (methanogens) differ in their successional dynamics during organic matter decomposition (Glissmann and Conrad, 2000; Ji et al., 2018a, 2018b; Kong et al., 2020; Peng et al., 2008; Rui et al., 2009).

1.3.2 Fermentation: acidogenesis

Acidogenesis is the fermentative stage where the products of hydrolysis (organic monomers of sugars and proteins) are converted by acidogenic bacteria to non-gaseous compounds (e.g., alcohols, aldehydes, and short-chain fatty acids) and gases (H_2 and CO_2) (Angenent et al., 2004). The dominant end-products of the fermentation process determine the type of fermentation. Acetogenic bacteria can be either facultative anaerobes or strict anaerobes.

The known species, such as members of *Clostridium* and *Enterobacteriaceae*, have been identified as active fermenters to operate fermentation of sugars (Manyi-Loh et al., 2013; Sikora et al., 2017). It has been reported that representatives of the *Clostridiales* (families *Clostridiaceae*, *Eubacteriaceae*, *Peptococcaceae*, *Peptostreptococcaceae*), *Fusobacterales*, *Synergistetes* (*Aminobacterium colombiense*) and *Cloacimonetes* (Candidatus *Cloacimonas acidaminovorans*) are capable of amino acid fermentation (Sieber et al., 2012; Schink and Stams, 2013).

1.3.3 Syntrophic oxidation of short-chain fatty acids

Syntrophy is a cooperative interaction between two organisms in which they exchange small amounts of intermediate products to work effectively together. The final two steps of the AMMP process, acetogenesis (Phase 5) and methane formation (Phase 7), are closely linked and involve this type of interaction. Acetogenesis provides the necessary substrates for methanogens, which rely on other microbes for the oxidation of short fatty acids into acetate, CO_2, and H_2 that they can use. This process, in which H_2 is transferred between acetogenic bacteria and methanogenic archaea, is an example of syntrophy (Stams and Plugge, 2009; Sieber et al., 2012). Under standard conditions, the oxidation of substances like butyrate,

propionate, and acetate during acidogenesis, accompanied by H_2 production, requires energy (endergonic). However, when coupled with methane production, the conversion becomes energetically feasible (exergonic) due to the low H_2 partial pressure provided by H_2-consuming methanogens.

Acetate is the most abundant intermediate during anaerobic organic matter breakdown (Fey and Conrad, 2000; Glissmann and Conrad, 2000). Generally, it can be directly consumed by acetoclastic methanogens or syntrophically converted to H_2 and CO_2. Syntrophic bacteria use the oxidative Wood-Ljungdahl pathway for the syntrophic oxidation of acetate. This pathway is the reversal of acetogenesis ($4\ H_2 + 2\ CO_2 \rightarrow CH_3COOH + 2\ H_2O$; $\Delta G = -95$ kJ mol^{-1}) (**Figure 1.6**). The research on syntrophically acetate-oxidizing bacteria have been neglected for decades (SAOB). Therefore, only a few species of SAOB have been isolated and little is known about their physiology and biochemistry. To date, recognized acetate-oxidizing bacteria include members of the *Clostridia* such as, for example, *Thermoacetogenium phaeum*, *Clostridium ultunense*, *Clostridium sporomusa*, *Syntrophaceticus schinkii*, *Tepidanaerobacter syntrophicus*, *Tepidanaerobacter acetatoxydans*, *Candidatus* Syntrophonatronum acetioxidans and *Moorella* spp., as well as *Deltaproteobacteria (Geobacter* spp.), and *Thermotogae* (e.g,, *Thermotogae lettingae*) (Schink and Stams, 2013; Worm et al., 2014).

Propionate and butyrate are the two next important intermediates of organic matter conversion under anoxic conditions (Krylova et al., 1997). Acetate, H_2, and CO_2 generated by syntrophic conversion of propionate and butyrate are able to feed acetoclastic and hydrogenotrophic methanogens. Propionate accounts for up to 35% of the methanogenic activity in anaerobic digestors (Mah et al., 1990), 30% in littoral lake sediments (Rothfuss and Conrad, 1993) and rice paddy soils (Krylova et al., 1997; Glissmann and Conrad, 2000; McInerney et al., 2009). The degradation of propionate to acetate, H_2, and CO_2 is highly endergonic under standard conditions ($\Delta G = +76.1$ kJ mol^{-1}), but it can be accomplished by syntrophic cooperation of propionate-oxidizing hydrogen-producing bacteria and hydrogen (or formate)-scavenging partner microorganisms (methanogens), which maintain a low hydrogen partial pressure. Propionate degradation becomes feasible in such syntrophic associations only under methanogenic conditions. *Smithella propionica* converts propionate through a dismutating pathway to acetate and butyrate, after which butyrate is oxidized to acetate (de Bok et al., 2001). All other known bacteria predominantly use the methyl-malonyl-coenzyme A pathway for syntrophic propionate degradation, through which propionate is oxidized to acetate plus CO_2 (**Figure 1.6**). Several members of the *Syntrophomonadaceae* are known as propionate-oxidizing bacteria: *Syntrophobacter* (*S. fumaroxidans*, *S. wolinii*, *S. pfennigii*, *S.*

sulfatireducens), *Pelotomaculum (P. thermopropionicum*, *P. schinkii*, *P. propionicicum)*, *Smithella propionica*, and strains of *Desulfotomaculum thermobenzoicum* (Stams and Plugge, 2009; Sieber et al., 2012; Schink and Stams, 2013).

Butyrate-oxidizing bacteria known so far belong to two groups of bacteria (the family *Syntrophomonadaceae* and the order *Syntrophobacterales*), including *Syntrophomonas. wolfei*, *Syntrophomonas bryantii*, *Syntrophomonas erecta*, *Syntrophomonas curvata*, *Syntrophomonas zehnderi*, and *Thermosyntropha lipolytica* (Stams and Plugge, 2009; Müller et al., 2010; Sieber et al., 2012; Schink and Stams, 2013). All known butyrate-oxidizing bacteria use the beta-oxidation pathway (Wofford et al., 1986; Schink, 1997; McInerney et al., 2007) (**Figure 1.6**).

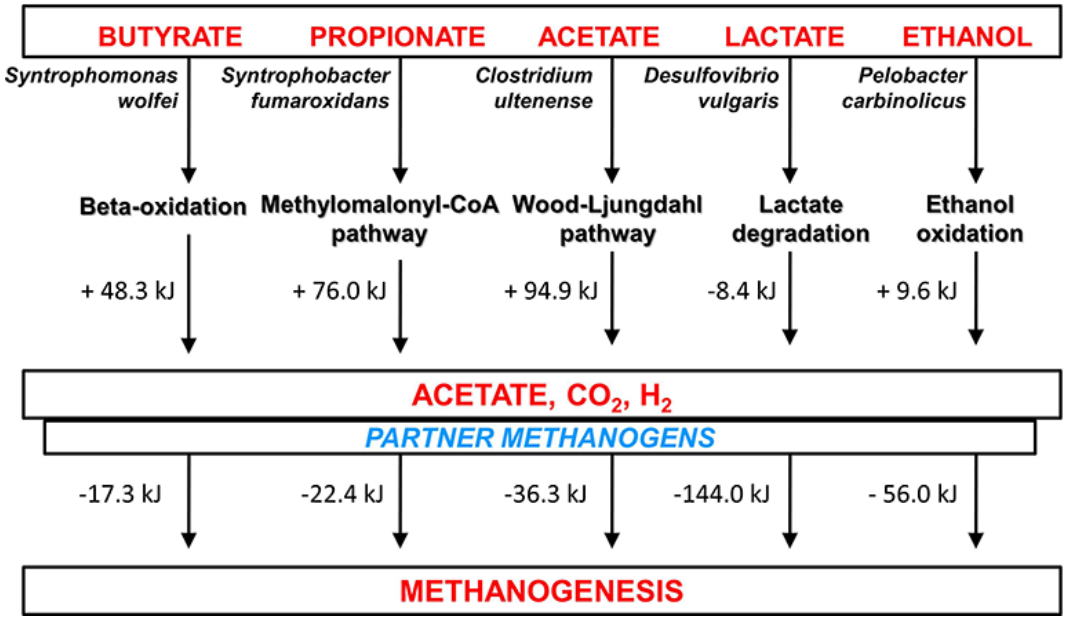

Figure 1.6: Syntrophic metabolism based on reverse electron transfer in syntrophy with hydrogen-consuming methanogens. The ΔG values for acetate, butyrate, propionate and ethanol and those for lactate oxidation, coupled or uncoupled with the methanogen partner. Taken from Sikora et al. (2017).

1.3.4 Methanogenesis

Methanogenesis, the final step in anaerobic decomposition of biopolymers, is a complex process requiring specific enzymes and cofactors not found in other microorganisms. Historically, there are three recognized pathways of methanogenesis that contribute to CH_4 production (substrates in parenthesis): acetoclastic (acetate), hydrogenotrophic (H_2 and CO_2), and methylotrophic (methanol and other methylated compounds) methanogenesis (Thauer, 1998). Most widely distributed among methanogens is hydrogenotrophic methanogenesis, with

its occurrence in six methanogenic orders: *Methanobacteriales*, *Methanococcales*, *Methanomicrobiales*, *Methanosarcinales*, *Methanocellales*, and *Methanopyrales* (Liu and Whitman, 2008; Conrad et al., 2009; Borrel et al., 2013, 2014). They utilize H_2 as an electron donor for reduction of CO_2 to CH_4.

Although approximately two-thirds of global biogenic CH_4 in the atmosphere is through acetate utilization (Liu and Whitman, 2008), acetoclastic methanogenesis is restricted to members of the order *Methanosarcinales*. Acetate enters the cell via an acetate transporter and thereafter is activated to acetyl-CoA, either by acetate kinase (Ack) and transacetylase (Pta) in *Methanosarcinaceae* or by acetyl-CoA synthetase (Acs) in *Methanotrichaceae* (formerly *Methanosaetaceae*) (Berger et al., 2012; Welte and Deppenmeier, 2014). *Methanosarcinaceae* and *Methanotrichaceae* may be an excellent example of how two family-level groups compete for the same substrate. *Methanosarcinaceae* is prevailing in acetoclastic methanogenesis at relatively high acetate concentrations, but after acetate declines to a very low level, the late-responding *Methanotrichaceae* significantly increases in competitiveness and acetoclastic activity. It was reported that the threshold acetate concentration for methanogenesis by pure cultures of *Methanosarcina* strains is > 0.2-1.2 mM (Min and Zinder, 1989; Jetten et al., 1990; Großkopf et al., 1998). With a higher maximum rate of acetate utilization and maximum growth rate ($Y * k$), a higher half-saturation coefficient (*KS*), and a higher yield coefficient compared with *Methanotrichaceae*, elevated acetate concentrations are favorable for growth and activity of *Methanosarcinaceae*. By contrast, *Methanotrichaceae* are superior at low acetate concentrations due to the investment of energy to activate acetate, thereby leading to a lower *k* and *KS* (Jetten et al., 1992; Großkopf et al., 1998; Conklin et al., 2006).

The recognized methylotrophic methanogens, which belong to the order *Methanosarcinales* and are able to utilize methanol and methylated amines, possess enzyme systems with three components for this purpose: a substrate-specific methyltransferase (MtaB) that transfers the methyl group to a corrinoid protein (MtaC), and a second methyltransferase (MtaA) that directs the methyl group into the methanogenic pathway at the stage of methyl-CoM (**Figure 1.7**).

However, next to these three historically known pathways, further methanogenic substrates and pathways have been discovered. Several phylogenetically distinct methanogenic lineages (*Methanosphaera*, *Methanimicrococcus*, *Methanomassiliicoccus*, *Methanonatronarchaeum*) have evolved H_2-dependent methylotrophic methanogenesis but are incapable of operating either hydrogenotrophic or methylotrophic methanogenesis. Genomic analysis of the deeply branching *Methanonatronarchaeum* showed that it has a specific

membrane-bound hydrogenase complex belonging to the rarely observed class 4 g of multisubunit hydrogenases, which may provide reducing equivalents for anabolism. Additionally, it has been suggested that certain *Methanosarcinales* strains can incorporate methylated sulfur compounds (such as methanethiol, dimethyl sulfide, and methylmercaptopropionate) into adapted methylotrophic methanogenesis pathways. Recently, it was also reported that *Methermicoccus shengliensis* can use methoxylated aromatic compounds to produce methane. Also, tertiary amines like choline (N,N,N-trimethylethanolamine) or betaine (N,N,N-trimethylglycine) have been shown to be substrates for methanogenesis in *Methanococcoides* and *Methanolobus* strains.

To date, the microbial contribution to CH_4 emission from rice paddies emphasizes the roles of acetoclastic and hydrogenotrophic methanogens, while the methylotrophic pathway is less frequently considered.

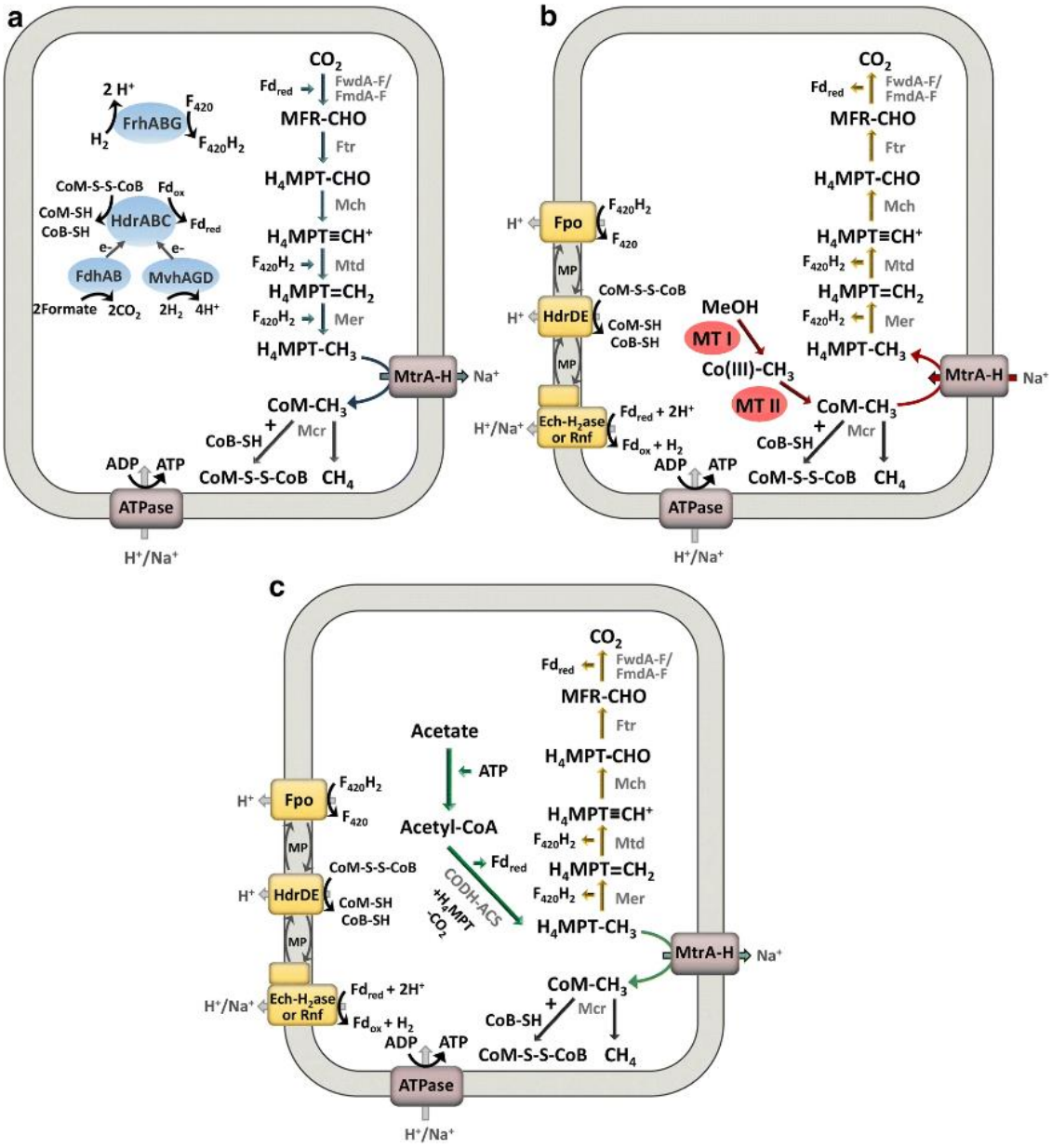

Figure 1.7 Hydrogenotrophic (a), methylotrophic (b) and acetoclastic (c) methanogenesis pathways. FwdA-F/FmdA-F: formylmethanofuran dehydrogenase, Ftr: formylmethanofuran-tetrahydromethanopterin formyl-transferase, Mch: methenyl-tetrahydromethanopterin cyclohydrolase, Mtd: methylenetetrahydromethanopterin dehydrogenase, Mer: 5,10-methylenetetrahydromethanopterin reductase, MtrA-H: tetrahydromethanopterin S-methyl-transferase, McrABCDG methyl-coenzyme M reductase, FrhABG: coenzyme F_{420}-reducing hydrogenase, HdrABC: soluble heterodisulfide reductase, MvhAGD: F_{420}-non-reducing hydrogenase, FdhAB: formate dehydrogenase, FpoA-O: $F_{420}H_2$ dehydrogenase, HdrDE: membrane-bound heterodisulfide reductase, Ech-H_2ase: energy-converting hydrogenase, Rnf: Na^+-translocating ferredoxin:NAD^+ oxidoreductase complex, ATPase: ATP synthase, CODH-ACS: Acetyl-CoA decarbonylase/synthase, MTI and MTII: methyltransferase, CoB: coenzyme B, CoM: coenzyme M, H_4MPT: tetrahydromethanopterin, MFR: methanofuran, Fd: ferredoxin, $F_{420}H_2$: reduced coenzyme F_{420}, MP: methanophenazine, CO(III): cobalamin binding protein. Taken from Kurth et al. (2020).

1.4 Temperature effect on methanogenesis

The ratio at which methanogenic pathways contribute to total CH_4 production depends on the relative net production rates of the methane precursors acetate, H_2 and methylated compounds. The relative turnover rates of methane precursors, and thus the resulting ratio of acetoclastic, hydrogenotrophic and methylotrophic methanogenesis, are complex and depend on many different factors in the environment (e.g., temperature, quality of organic matter and pH).

Like most other forms of metabolism, methanogenesis is temperature-dependent (Min and Zinder, 1989; Westermann et al., 1989). Temperature is a general factor regulating microbial dynamics (Wiegel, 1990) and also markedly controlling methanogenic processes (Yvon-Durocher et al., 2014). Microbial community responses to increasing temperatures can be quite complex (Roussel et al., 2015). The responses of microbial communities to rising temperatures can be complex, as temperature not only impacts the thermodynamics and kinetics of individual processes, but also influences population dynamics and the overall structure of the microbial community (Roussel et al., 2015; Conrad et al., 2009).

Temperature is a key factor in the production of methane by the methanogenic community in rice field soil, with CH_4 being produced over a wide temperature range of up to 55 °C (Yao and Conrad, 2000; Conrad et al., 2009). Studies have shown that temperature not only affects the rate of methane production, but also the composition and function of methanogenic communities in rice field soils in various locations including Italy, China, Japan, the Philippines, and Thailand. (Fey and Conrad, 2000; Ramakrishnan et al., 2001; Krüger et al., 2002; Peng et al., 2008; Watanabe et al., 2009; Conrad et al., 2012; Liu et al., 2018).

The pathways of CH_4 production and the composition of the methanogenic community in rice field soil tend to change gradually at mesophilic temperatures up to 37 °C. Within this range, methane production is typically characterized by acetoclastic and hydrogenotrophic methanogenesis (Fey and Conrad, 2000); However, the communities have been shown to significantly alter their methanogenic activities at temperatures above 40–42 °C (Wu et al., 2006; Peng et al., 2008; Conrad et al., 2009; Yue et al., 2015). At these moderately thermophilic temperatures, methane production is dominated by hydrogenotrophic methanogenesis (Conrad et al., 2009). This temperature-induced change has also been observed in Chinese natural wetlands (Yue et al., 2015). The in situ temperature in paddy soil is usually lower than or around 30 °C(Schutz et al., 1990), but rice fields in southeastern China have reached present-day temperatures above 40 °C (Rui et al., 2009). Additionally, the expected increase in global surface temperature by 2–4 °C by 2050 makes the effects of temperature on the structure and function of soil microbial communities an important research topic (Collins et al., 2013).

The previous studies have addressed that acetoclastic and hydrogenotrophic methanogenesis contribute to methane production at a ratio of about 2:1 (Smith and Mah, 1966). The contribution of hydrogenotrophic methanogenesis has been found to decrease with decreasing temperature in both lake sediments (Schulz and Conrad, 1996; Glissman et al., 2004) and rice field soil (Fey and Conrad, 2000), within the physiological range of about 4 to 40 °C. At low temperatures, H_2-consuming chemolithotrophic acetogenic bacteria are more competitive than methanogens (Conrad et al., 1989; Nozhevnikova et al., 1994; Fu et al., 2018), leading to increased acetate production and suppression of hydrogenotrophic methanogens in methanogenic environments such as rice field soil or lake sediments(Nozhevnikova et al., 2007). This occurs even though hydrogenotrophic methanogenesis is more thermodynamically favorable than chemolithotrophic acetogenesis.(Conrad and Wetter, 1990; Kotsyurbenko et al., 2001).

The microbial communities responsible for AMMP are diverse and complex, and can vary depending on the specific methanogenic environment, such as rice field soil, lake sediments, acidic peat, animal guts, anaerobic digestors, landfills, or saline environments. Generally, the community of methanogenic archaea contains both putatively hydrogenotrophic taxa (*Methanomicrobiales*, *Methanobacteriales*, *Methanocellales*, *Methanosarcinales*) and putatively acetoclastic taxa (*Methanosarcinaceae*, *Methanotrichaceae*) (Oren, 2014), enabling both hydrogenotrophic and acetoclastic methanogenesis. However, at elevated temperatures (40-50 °C), methane production in waterlogged rice field soils and other anoxic environments with methanogenic activity is typically driven by hydrogenotrophic methanogenesis under moderately thermophilic conditions (Schulz et al., 1997; Fey et al., 2001). However, in some cases, paddy soils have also been found to harbor moderately thermophilic acetoclastic methanogens (Wu et al., 2006). In these soils, AMMP does not change with temperature increase above 40 °C (Liu et al., 2018a) and both acetoclastic and hydrogenotrophic methanogenesis occur at a common ratio.

1.5 The potential of meta-omics to study microbial community dynamics

Current knowledge of microbial ecology and physiology using culture-dependent techniques is limited and incomplete due to the inability to cultivate most of the microorganisms. It has been predicted that less than 1% of all microorganisms in natural environments can be cultivated as a pure culture (Amann et al., 1995). More information on methanogenic communities is now being obtained using culture-independent techniques, which are the basis for studying microbial ecology (**Figure 1.8**).

The initial use of rRNA as a phylogenetic marker was a landmark development in molecular microbial ecology (Woese and Fox, 1977; Lane et al., 1985), in particular after PCR-based 16S rRNA gene sequencing techniques (Sanger sequencing) became available. This approach made it possible to uncover the diversity of uncultured microorganisms directly in the environment for the first time (Liesack and Stackebrandt, 1992; Borneman et al., 1996). However, this method is costly and time-consuming. Next, fingerprinting techniques including denaturing gradient gel electrophoresis (DGGE), thermal gradient gel electrophoresis (TGGE), and terminal restriction fragment length polymorphism (T-RFLP) analysis allowed it to overcome methodological limitations and to create microbial community profiles with high throughput. Later, the rapid development of next-generation sequencing (NGS) platforms promoted research into structure and function of microbial communities and the interaction among microbes. The first NGS platform was released by 454 Life Technologies in 2004 based on pyrosequencing (Ronaghi et al., 1996; Ronaghi, 2001), followed by Illumina sequencing (Bentley et al., 2008) and other platforms.

More recently, the increasing number of culture-independent techniques and bioinformatic tools (meta-omics) have helped to develop a deeper understanding of microbial communities. Meta-omics, including metagenomics, metatranscriptomics, metaproteomics and metabolomics, work based on the analysis of environmental extracts of total DNA, RNA, proteins and metabolites, respectively (Koch et al., 2014; Vanwonterghem et al., 2014; Abram, 2015; Heyer et al., 2015; Ravin et al., 2015). Metagenomics allows us to detect the metabolic potential by describing the gene pool present in a microbial community or ecosystem. Metatranscriptomics does analyze community-wide mRNA and thus provides information on the microbial genes being expressed at the time of sampling. Metaproteomics is focused on proteins expressed within a microbiome to explore microbial function. Metabolomics involves the analysis of intermediates and end-products of metabolic pathways and thus provides direct evidence for microbial activity. The data generated by these novel methodologies have provided significant insights into the structure and function of microbial communities in various ecosystems. In addition, meta-omic approaches combined with isotope labeling techniques will allow us to develop a fundamental understanding of the processes leading to methane production.

Other cultivation-independent techniques include amplicon sequencing of marker genes, fluorescence in-situ hybridization (FISH), terminal restriction fragment length polymorphism (T-RFLP) analysis, and real-time quantitative PCR (qPCR). Marker genes frequently used in amplicon sequencing, T-RFLP analysis, and qPCR are the 16S rRNA gene for *Bacteria* and

mcrA for methanogens.

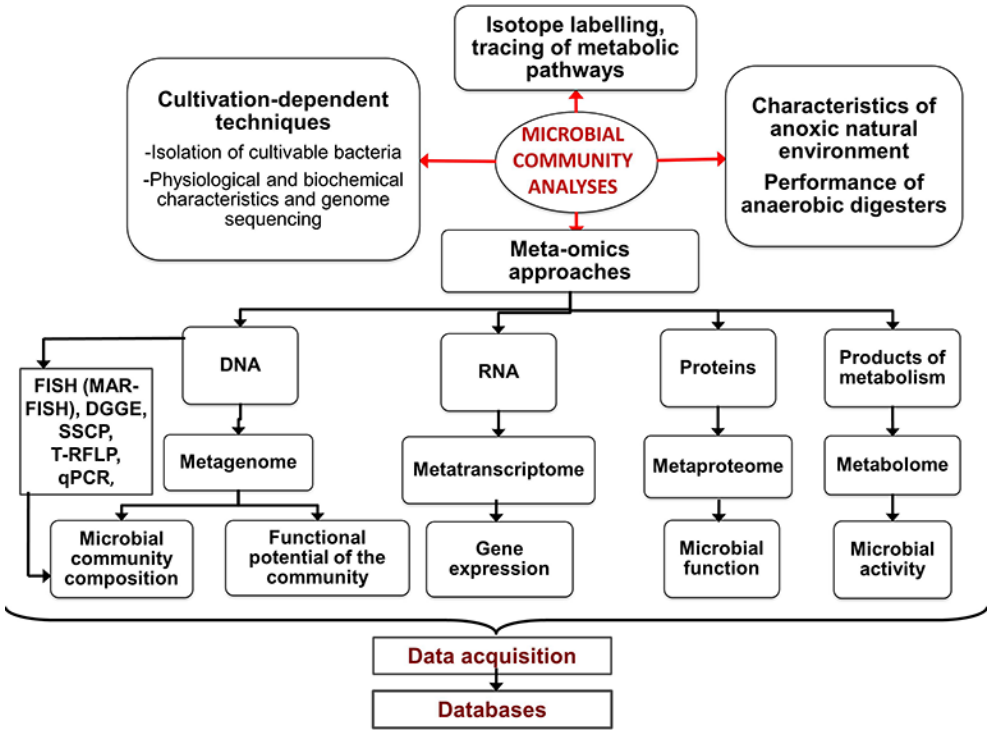

Figure 1.8: Culture-independent approaches to analyze methanogenic communities (Sikora et al., 2017).

1.6 Aim of the project

Anaerobic degradation of organic matter, whose final products are methane and carbon dioxide, contributes to the energy flow and circulation of matter in ecosystems. It plays a key role in the global carbon cycle. The methanogenic degradation of organic matter in anoxic environments (waterlogged rice paddies and anoxic wetlands) follows common principles and involves a microbial food chain composed of different functional guilds of the domains *Bacteria* and *Archaea* (Ferry, 2011). These microbial guilds participate in a cascade of anaerobic degradation steps that involve biopolymer hydrolysis, fermentation, syntrophic oxidation of fatty acids, homoacetogenesis, and methanogenesis (Conrad, 1999). Comprehensive research on the methanogenic decomposition of organic matter has already been done in previous years (Glissman et al., 2004; Conrad et al., 2009; Wegner and Liesack, 2016). Indeed, studies on the methanogenic community dynamics in Italian paddy soil even involved systems-level metatranscriptome analyses on both rRNA (structure) and mRNA (function) levels, but only for the early stage of rice straw degradation (Peng et al., 2018). This study showed that the anaerobic food chain is driven by the functional interplay of a complex microbial community,

with polymer hydrolysis being the rate-limiting step. The methanogen community and their dynamics were characterized by acetoclastic (*Methanosarcinaceae*) and hydrogenotrophic methanogens (*Methanocellaceae*). By contrast, the research on the methanogenic community in Philippine rice field soil is hitherto limited to the analysis of total DNA using primarily PCR-amplicon sequencing of particular biomarkers. This methodological approach, however, can only address particular aspects of the community potential and provides information neither on the microbial groups actually active nor on their functional gene expression at the time of sampling (e.g., Liu et al., 2018, 2019; Yuan et al., 2020; Conrad et al., 2021). A deeper understanding of key functional guilds and populations participating in the methanogenic organic matter breakdown in Philippine paddy soil is not yet achieved.

In addition, the expected increase in global surface temperature due to climate change may have a tremendous effect on the structure and function of the anaerobic food chain in flooded rice field soil (Conrad and Wetter, 1990; Schulz et al., 1997; Fey et al., 2001; Peng et al., 2018; Liu et al., 2019). In previous research, the methanogenic communities in Italian and Philippine paddy soils showed different responses to rising temperature. At moderately thermophilic temperature (40-50°C), the methane production in Italian rice field soil was dominated solely by hydrogenotrophic methanogens (Conrad et al., 2009; Peng et al., 2018). By contrast, a mix of both acetoclastic and hydrogenotrophic methanogens had been detected in the Philippine paddy soil (Liu et al., 2018a, 2019). However, a system-level understanding of the effects of rising temperature on the anaerobic food web in Philippine paddy soil has not yet been achieved. This prompted us to apply a multi-methods approach to disentangle the compositional and functional dynamics of the methanogenic community in Philippine rice field soil over an incubation period of 120 days under mesophilic and moderately thermophilic temperatures. In particular, we aimed at answering the following questions: (i) who are the major bacterial players at the different trophic levels (i.e., hydrolysis, fermentation, syntrophic conversion) of the anaerobic food web; (ii) which methanogenic pathways dominate and which methanogen groups are prevalent during the 120-day incubation period; and (iii) how does the rising temperature affect the structural and functional dynamics of the methanogenic community? Anoxic paddy soil slurries amended with rice straw were used as model system. Central to our research was the combination of metabolite measurements and metatranscriptomic analysis of total RNA, thereby allowing for simultaneously unraveling changes in structure (rRNA) and functioning (mRNA) of the methanogenic community. In addition, we applied quantitative polymerase chain reaction (qPCR), reverse transcription qPCR (RT-qPCR) of biomarkers (16S rRNA, *mcrA*), and targeted metagenomics to assemble draft genomes of key methanogens. The

observed community dynamics led us divide the long-term incubation period into three successional phases defined as early phase (days 3 to 21), intermediate phase (days 21 to 28), and late phase (days 28 to 120).

2 Methodology

2.1 Materials

2.1.1 Soil sample

Soil was obtained from the International Rice Research Institute (IRRI) in Los Banos, Philippines, about 66 km south of Manila (14°09′45″N, 121°15′35″E, 21 m a.s.l.) (Weller et al., 2014; Breidenbach and Conrad, 2015), in 2012. The main physicochemical characteristics of Philippine rice paddy soil were: total C (0.20%), total N (1.90%), and pH 6.30 (Liu et al., 2018; Fu et al., 2019).

2.1.2 Instruments used

Items	Manufacturer	City - State
GC-8A gas chromatograph	Shimadzu	Duisburg, Germany
FastPrep®-24 bead beater	MP Biomedicals	California, USA
NanoDrop® ND-1000 UV-Vis spectrophotometry	NanoDrop Tech. Inc.	USA
Qubit® 2.0 Fluorometer	Invitrogen	California, USA
Experion automated electrophoresis system	Bio-Rad	Hercules, USA
C1000 Touch™ Thermal Cycler	Bio-Rad	Hercules, USA
Magnetic stand	Invitrogen	California, USA
CFX Connect Real-Time PCR detection system	Bio-Rad, USA	Hercules, USA

2.1.3 Chemicals and reagents used

Items	Manufacturer	City- State
DEPC-treated water	Ambion	Austin, USA
Tris-HCl	Sigma	Steinheim, Germany
Phenol-chloroform-isoamyl alcohol (pH 8.0)	Carl Roth	Karlsruhe, Germany
RNase-free TE buffer	Applichem	Darmstadt, Germany
SeaKem LE Agrose	Lonza	Basel, Switzerland
Ethanol (Nuclease-free)	Applichem	Darmstadt, Germany

2.1.4 Kits used

Items	Manufacturer	City - State
DNeasy® PowerLyzer® PowerSoil	QIAGEN	Hilden, Germany
Qubit dsDNA BR Assay Kit	Thermo Fisher Scientific	Massachusetts, USA
RNeasy® PowerSoil Total RNA Kit	QIAGEN	Hilden, Germany
DNase I	Ambion	Austin, USA
RNA Clean and Concentrator kit	Zymo Research	California, USA
Experion™ RNA HighSens Analysis Kit	Bio-Rad	California, USA
Experion™ DNA 12K HighSens Analysis Kit	Bio-Rad	California, USA
Qubit™ RNA HS Assay Kit	Thermo Fisher Scientific	Massachusetts, USA
GoScript Reverse Transcription System and random primers	Promega	Mannheim, Germany
Oligonucleotides (primers)	Eurofins	Constance, Germany
Sybr Green kit	Sigma-Aldrich	Missouri, USA
AMPure XP Beads	New England Biolabs	Ipswich, USA
NEBNext® Ultra II Directional RNA Library Prep Kit for Illumina®	New England Biolabs	Ipswich, USA

2.2 Methods

2.2.1 Sample collection and experimental design

Air-dried soil was stored at room temperature. Soil processing followed a standard procedure, including mechanical crushing, sieving (< 2 mm) prior to its immediate use, and preparation of straw-amended slurries (Ma et al., 2012; Ji et al., 2018b; Bei et al., 2021). Briefly, soil slurries were set up in 125-ml pressure bottles by thoroughly mixing 40 g dry soil, 0.5 g rice straw (1 cm pieces) and 50 ml of deionized and autoclaved water. This amount of rice straw is commonly used in paddy soil slurry studies (Wegner and Liesack, 2016; Peng et al., 2018). It corresponds to 37.5 t ha^{-1}, which is about three times higher than under field conditions (Schütz et al., 1989). The bottles were sealed with butyl rubber stoppers and flushed with N_2 for 15 min to establish anoxic conditions. The slurries were then incubated at 30 °C or 45 °C for 120 days.

Destructive sampling was performed after 3, 7, 11, 14, 21, 28, 35, 60, and 120 days of incubation, with three replicate slurries per time point. Slurry material was sampled from each replicate, promptly shock-frozen using liquid nitrogen, and then stored for molecular analysis at − 80 °C. The pore water samples were taken and kept at -20 °C until metabolite analysis.

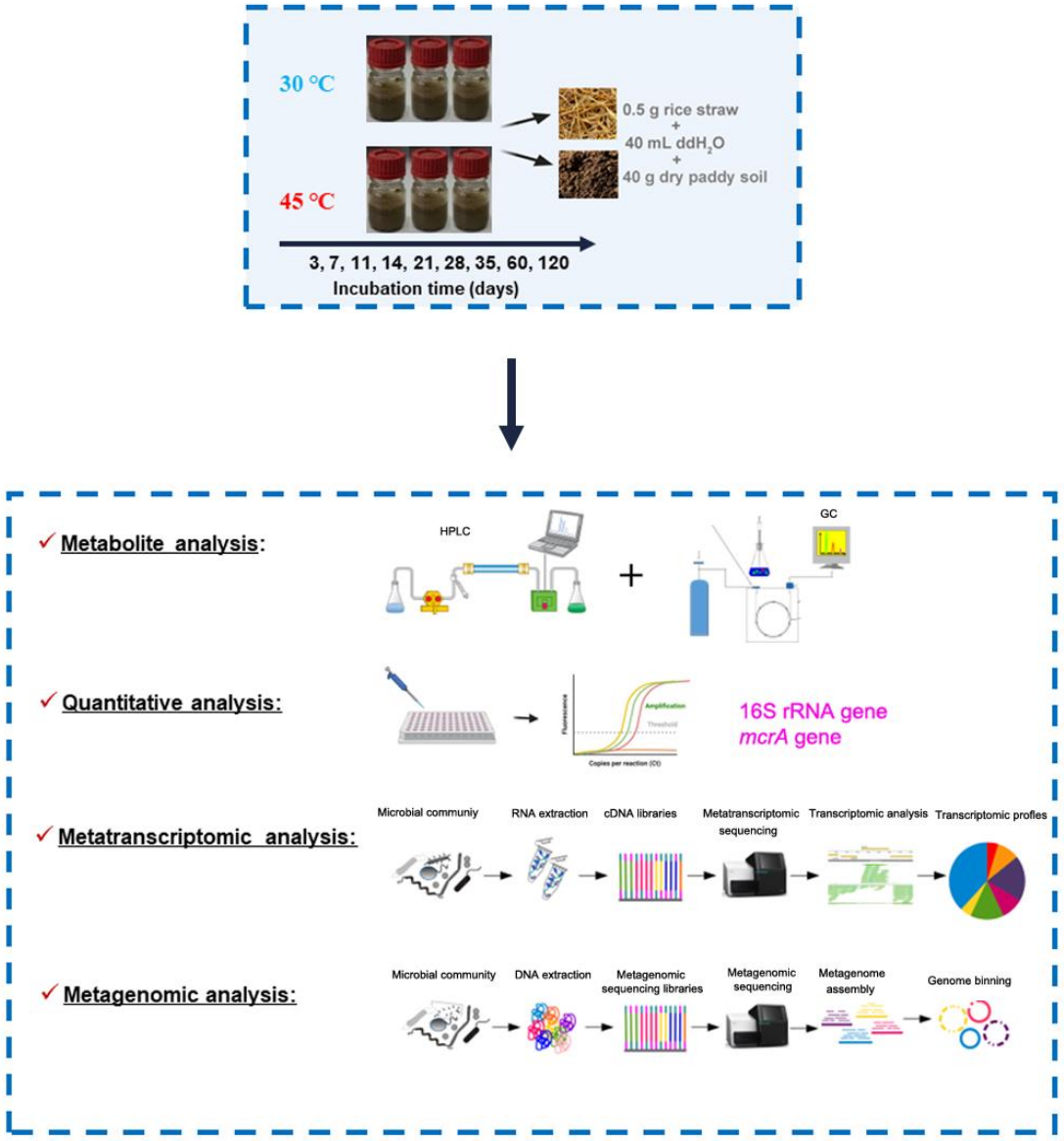

Figure 2.1: Overview of the experimental design

2.2.2 Metabolite measurements

Concentrations of acetate, propionate, and butyrate in the liquid sample of the soil slurry incubations were measured by HPLC equipped with an ion-exclusion column (Aminex HPX-87-H, BioRad, München, Germany) and coupled to an UV–Vis detector (Sykam,

Fuerstenfeldbruck, Germany) (Krumböck and Conrad, 1991). In addition, gas samples were taken from the same set of slurries for process measurements. A GC-8A gas chromatograph (Shimadzu, Duisburg, Germany) containing a Haysep Q column was used to measure methane and CO_2. Data were analyzed with PeakSimple software (SRI Instruments, Bad Honnef, Germany) and calculated by linear regression (Wegner and Liesack, 2016; Peng et al., 2018; Abdallah et al., 2019). Hydrogen was detected using a H_2 microsensor with piercing needle (Unisense A/S, Denmark) (Hakobyan et al., 2020).

2.2.3 DNA and RNA extraction

Total DNA was extracted from soil slurries using the DNeasy® PowerLyzer® PowerSoil kit (QIAGEN, Hilden, Germany) according to the manufacturer`s instructions. Agarose gel (1%) electrophoresis and fluorometry were used to check for the integrity and quantity of each DNA extract. Fluorometric measurements were done on a Qubit 2.0 Fluorometer using the Qubit dsDNA BR Assay Kit (Thermo Fisher Scientific, MA, USA).

The RNeasy® PowerSoil Total RNA Kit (QIAGEN, Hilden, Germany) was used for the extraction of total RNA. The extraction procedure followed the manufacturer's instructions. The RNA extracts were treated with DNase I (Ambion, Austin, USA) and purified using the RNA Clean and Concentrator kit (Zymo Research, CA, USA). The integrity of purified RNA was assessed using the Experion™ RNA HighSens Analysis Kit (Bio-Rad, CA, USA), while the yield was determined with the Qubit™ RNA HS Assay Kit (Thermo Fisher Scientific, MA, USA).

2.2.4 Quantitative PCR (qPCR) and Reverse Transcription quantitative PCR (RT-qRCR)

Primer sets and temperature profiles for quantitation of bacterial 16S rRNA and *mcrA* genes (qPCR) and their transcripts (RT-qPCR) are shown in Table 1. The *mcrA* gene is a standard biomarker to detect and quantify methanogens in environmental samples (e.g., Stubner, 2004; Wegner and Liesack, 2016; Abdallah et al., 2019). In RT-qPCR, randomly reverse-transcribed RNA was generated using the GoScript Reverse Transcription System (Promega, Mannheim, Germany) according to the manusfacturer`s instructions. The standard curve for quantifying bacterial 16S rRNA genes and transcripts were constructed using genomic DNA of *Escherichia coli* (calibration range from 10 to 10^9 copies). The standard curve for quantifying *mcrA* genes and transcripts was constructed using a *mcrA* fragment cloned into the pGEM®-T Easy plasmid (Promega, WI, USA) (calibration range from 10 to 10^8 copies) (Abdallah et al., 2019). The *mcrA* fragment used for cloning was obtained from genomic DNA of *Methanosarcina barkeri*

(Steinberg and Regan, 2009). The qPCR reactions were carried out on an iCycler Real-Time PCR Detection System (CFX Connect™, Bio-Rad). The PCR efficiency was at least 85% (R^2 > 0.98). The presence of unspecific products was checked by melt curve analysis.

Table 2.1: Forward and reverse primers for qPCR and RT-qPCR

Target	Oligo. name	Oligonucleotide sequence (5'- 3')	Reference
16S rRNA gene	520F	AYTGGGYDTAAAGNG	(Stubner, 2004)
	802R	TACNVGGGTATCTAATCC	(Stubner, 2004)
Universal *mcrA* gene	mlas-mod – F	GGYGGTGTMGGDTTCACMCARTA	(Steinberg and Regan, 2009)
	mcrA-rev - R	CGTTCATBGCGTAGTTVGGRTAGT	(Steinberg and Regan, 2009)

2.2.5 Illumina library preparation and sequencing

Metatranscriptomics: A total of 27 RNA samples (three replicate slurries × 9 time points) were subjected to cDNA library preparation using the NEBNext® Ultra II Directional RNA Library Prep Kit for Illumina® (New England Biolabs, USA). The cDNA library synthesis procedure strictly followed the manufacturer`s instructions. cDNA integrity and yield were checked on a Bio-Rad analyzer using the Experion™ DNA 12K Analysis Kit (Bio-Rad). The 27 cDNA libraries were sequenced (RNA-Seq) on the NovaSeq 6000 platform in paired-end mode (2×150 bp) by Novogene Genomics Service (Novogene Co., Ltd, UK).

Metagenomics: DNA extracts from the triplicate slurries of a given time point were mixed in equal amounts prior to metagenomic library construction. A total of three metagenomic libraries (one each for the incubation time points 21, 28, and 35 days) were constructed using the TruSeq DNA Library Prep Kit according to the manufacturer`s instructions (Illumina). The metagenomic libraries were sequenced on an Illumina HiSeq-2500 platform in paired-end mode (2×250 bp) at the Max Planck Genome Centre Cologne, Germany.

2.2.6 Computational analysis of metatranscriptomic datasets

2.2.6.1 Pre-processing

The quality filtration of raw reads was performed using Trimmomatic (Bolger et al., 2014). Default settings were applied with the exception that minimum sequence length was set at 100 bp. Quality control of the filtered reads was visualized using FastQC. Analysis of 16S rRNA and putative mRNA reads was carried out using a bioinformatic pipeline reported previously

(Peng et al., 2018). Briefly, reads mapping to rRNA and non-coding RNA were filtered by SortMeRNA 2.0 against SILVA (release 128) (Quast et al., 2012) and RFAM reference databases (Kopylova et al., 2012). The remaining reads were considered putative mRNA. The sequencing statistics are shown in Table S1.

2.2.6.2 Analysis of 16S rRNA

Illumina rRNA-derived reads were assembled to near full-length 16S rRNA sequences over 40 iterations using EMIRGE with SILVA 132 SSU rRNA database (Miller et al., 2011). This assembly approach was done separately for each of the 27 RNA sequence datasets. Taxonomic assignment was performed using BLASTN algorithm implemented in DIAMOND applying an e-value cutoff of 1e-5 for database searches against the SILVA 132 SSU database (release 2020). MEGAN6 Ultimate Edition v6.20 (Computomics, Tübingen, Germany) was used for downstream analysis (Huson et al., 2016). The abundance estimate of each assembled 16S rRNA sequence type was conducted using BBMap v38.62 (Bushnell, 2014). The minimum identity for each sequence type was set to 0.97 (Lawson et al., 2017; Tran et al., 2018). All nearly full-length 16S rRNA sequences (> 1200 bp), which were affiliated with the family *Methanosarcinaceae*, were extracted and used to build a phylogenetic tree. The sequence alignment was done using MUSCLE (Edgar, 2004) and manually refined. A neighbor-joining tree was constructed in MEGAX using 500 bootstrap replications (Kumar et al., 2018). Reference sequences were downloaded from GTDB (https://gtdb.ecogenomic.org/). The phylogenetic tree was visualized by iTOL (https://itol.embl.de/) (Pruesse et al., 2012).

2.2.6.3 Analysis of mRNA

Trinity (version 2.2.0) was used for *de novo* metatranscriptome assembly (Haas et al., 2013). Total mRNA reads from all 27 cDNA libraries were pooled into one transcriptomic dataset for subsequent contig assembly using Trinity scripts (Smith-Unna et al., 2016). A total of 472,280 quality-checked contigs were obtained. The mRNA reads from each sample were individually mapped back onto the contigs using Bowtie (Langmead et al., 2009). A FPKM matrix of mRNA reads that mapped onto a particular contig was produced for all relevant contigs using RSEM (Li and Dewey, 2011) within Trinity (version 2.2.0). Taxonomic assignment and functional annotation of the mRNA contigs were carried out using BLASTX algorithm implemented in DIAMOND (v0.9.25), applying an e-value cutoff of 1e-5 for database searches against NCBI's non-redundant protein (nr) database (release 2020) (Buchfink et al., 2015). In order to investigate the gene expression of particular metabolic pathways, related mRNA reads were

extracted using MEGAN6 Ultimate Edition (Huson et al., 2016; Peng et al., 2018).

Analysis of carbohydrate-active enzymes (CAZymes): mRNA reads were queried against dbCAN database (release 2020) with DIAMOND in blastx mode applying the default e value cutoff of 1e-3 to analyze for CAZymes. Functional CAZyme modules (e.g., degradation of cellulose, xylan, chitin, and other hemicelluloses) were defined by grouping related enzymatic functions based on their enzyme commission numbers. A mapping file for functional annotation was created using all available entries in dbCAN. The mapping file was stored as indexed sqlite database object and queried using a custom Python script. The resulting annotations are based on matching dbCAN top hits for mRNA reads queried against the mapping file and defined CAZyme modules. The functional annotation of CAZyme-affiliated mRNA reads to CAZyme functional modules were achieved using custom Python scripts described by Peng et al. (2018). The taxonomic assignment of these subsets was performed using BLASTX algorithm implemented in DIAMOND against NR database.

2.2.7 Computational analysis of metagenomic datasets

2.2.7.1 Assembly and binning

Raw reads were quality-filtered using Trimmomatic v0.38 (Bolger et al., 2014). Metagenomic assembly and binning were done using the MetaWRAP pipeline (Uritskiy et al., 2018). The three metagenomic datasets obtained for each incubation time point were processed separately. The quality-filtered reads were first assembled to larger contigs using metaSPAdes v3.13.0 (Nurk et al., 2017). Metagenomic binning was performed on contigs longer than 1000 bp with MetaBAT v2.12.1 (Kang et al., 2015) and MaxBin v2.2.5 (Wu et al., 2016). Completeness and contamination of metagenome-assembled genomes (MAGs) were assessed by CheckM v1.0.17 (Parks et al., 2015). The sequencing statistics are shown in Table S2.

2.2.7.2 Genome annotation

Open reading frames (ORFs) in each MAG were identified using Prokka v1.14.5 (Seemann, 2014). The ORFs were then queried against the nr protein database (June 2020) using DIAMOND v0.9.25 with an e-value of 1e-5 (Buchfink et al., 2015). Functional annotation was performed based on the Kyoto Encyclopedia of Genes and Genomes (KEGG) classification database (January 2021) using the lowest common ancestor (LCA) algorithm in MEGAN Ultimate Edition v6.20 (Huson et al., 2016). In order to determine the expression level of metabolic pathways and related genes in MAGs, mRNA reads were mapped onto the MAGs using BBMap v38.62 pipeline (minimum sequence identity set to 0.97) (Bushnell, 2014;

Lawson et al., 2017; Tran et al., 2018). Competitive mapping was done using BBMap v38.62 in BBsplit (Bushnell, 2014). The mRNA reads obtained in triplicate datasets from 9 incubation time points were mapped to *Methanosarcina* reference genomes simultaneously to determine which genome they match best.

2.2.7.3 Phylogenetic analyses

CheckM v1.0.17 was used to perform taxonomic assignment of MAGs (Parks et al., 2015). FastANI was used to calculate genome average nucleotide identity (ANI) values (Jain et al., 2018). Whole-genome sequences were visualized and compared using CGView software (Stothard and Wishart, 2005). The 16S rRNA genes in MAGs were predicted using CheckM. Subsequently, a genus-level 16S rRNA gene tree for *Methanosarcina* spp. was constructed in MEGAX using the neighbor-joining algorithm and 500 bootstrap replications. Reference sequences were extracted from *Methanosarcina* genomes downloaded from GTDB.

2.2.8 Reverse-transcription quantitative PCR (RT-qPCR) and absolute microbiome profiling (AMP)

RT-qPCR combined with high-throughput sequencing was used to evaluate the absolute abundance of marker genes encoding methanogenesis (Zhang et al., 2022). Transcript copy numbers of the *mcrA* gene was used as a standard to calculate the absolute abundance of other methanogenic marker genes:

$$Transcript\ copy\ numbers\ of\ target\ gene = \frac{\mathrm{x}}{\mathrm{a}} \times \mathrm{b}$$

where **x** are metatranscriptomic transcript abundance of target gene (%), **a** and **b** are metatranscriptomic transcript abundance of *mcrA* (%) and transcript copy numbers of *mcrA* quantified by RT-qPCR, respectively.

2.2.9 Statistical analysis

All means ± standard errors (SE) are based on the analytical results obtained from three independent replicate slurries (metabolite measurements, qPCR, RT-qPCR, and metatranscriptomic community dynamics on rRNA and mRNA level). Significant differences in qPCR and RT-qPCR measurements across the nine incubation time points were determined using the One-Way ANOVA. The resulting *P* values were corrected for multiple testing using the Benjamini-Hochberg false discovery rate method ($P_{FDR} < 0.05$) (Benjamini and Hochberg, 1995). In metatranscriptomic analysis, the relative abundance values for taxon-specific 16S

rRNA and mRNA transcripts (domain, families), and for mRNA transcripts assigned to particular KEGG categories (functional gene expression analysis), were normalized to Transcripts Per Kilobase Million (TPM). This was done to normalize for varying sequencing depths. Tukey's Honest Squared Difference test (Tukey HSD) in STAMP was used to determine significant difference in taxon-specific rRNA/mRNA abundance and functional gene expression across the whole incubation period (significant with $p < 0.05$) (Parks et al., 2014). The DESeq2 package v1.24.0 in R (v3.6.1) was used to further test for significant differences in taxon-specific rRNA abundance and in the mRNA abundance of key pathway genes between two sampling time points (Love et al., 2014). In particular, it was tested whether the taxon-specific rRNA abundance in a particular sampling time point significantly differed from the original abundance at the first sampling (day 3) or vice versa whether the relative rRNA abundance at day 3 significantly differed from those of all other sampling time points. The same analysis approach was applied to the mRNA abundance of key pathway genes. All *P* values generated with STAMP and DESeq2 were corrected for multiple testing using the Benjamini-Hochberg method to control the false discovery rate (FDR), with $P_{FDR} < 0.05$.

2.3 Data accession

The metatranscriptomic sequence data can be accessed at the National Center for Biotechnology Information (NCBI) under BioProject PRJNA907538 (30 ℃) and PRJNA907721 (45 ℃). The metagenomic sequence data can be accessed at the National Center for Biotechnology Information (NCBI) under BioProject PRJNA907625 (30 ℃) and PRJNA907738 (45 ℃).

3 / 4

The temperature effect on the metatranscriptome and metagenome of the methanogenic community in Philippine rice field soil

3 Methanogenic Community Dynamics at Mesophilic Temperature

3.1 Metabolite turnover

Metabolite measurements in the straw-amended slurries were made over the complete incubation period of 120 days. Acetate transiently accumulated and reached its peak concentration (10.57 mM) at day 7. Thereafter, acetate concentration sharply decreased within 7 days to 1.42 mM on day 14 and then showed a steady-state between production and consumption, ranging from 0.83 to 1.30 mM until day 120 (**Figure 3.1a**). Concurrently, the butyrate concentration peaked at day 7 (2.88 mM) and then sharply decreased to low, but detectable, steady-state levels (0.08 to 0.18 mM) (**Figure 3.1b**). Propionate strongly accumulated from day 3 (0.57 mM) onwards, with a peak concentration at day 14 (4.84 mM). Subsequently, its concentration rapidly decreased towards day 35 (0.65 mM), and then propionate showed a steady-state at low but clearly detectable levels (0.35 mM) (**Figure 3.1c**). First CH_4 production was detectable around day 3 (2.5 KPa), but its headspace concentration increased significantly towards day 21 (73.44 KPa). Then the CH_4 production rate was decreased between days 21 and 28 (**Figure 3.1d**), but increased again from days 28 to 35. The greatest CH_4 production rate was observed between days 11 and 21 concomitantly to the decline of acetate and butyrate to low steady-state concentrations, but also related to the net consumption of propionate (**Figure 3.1d**).

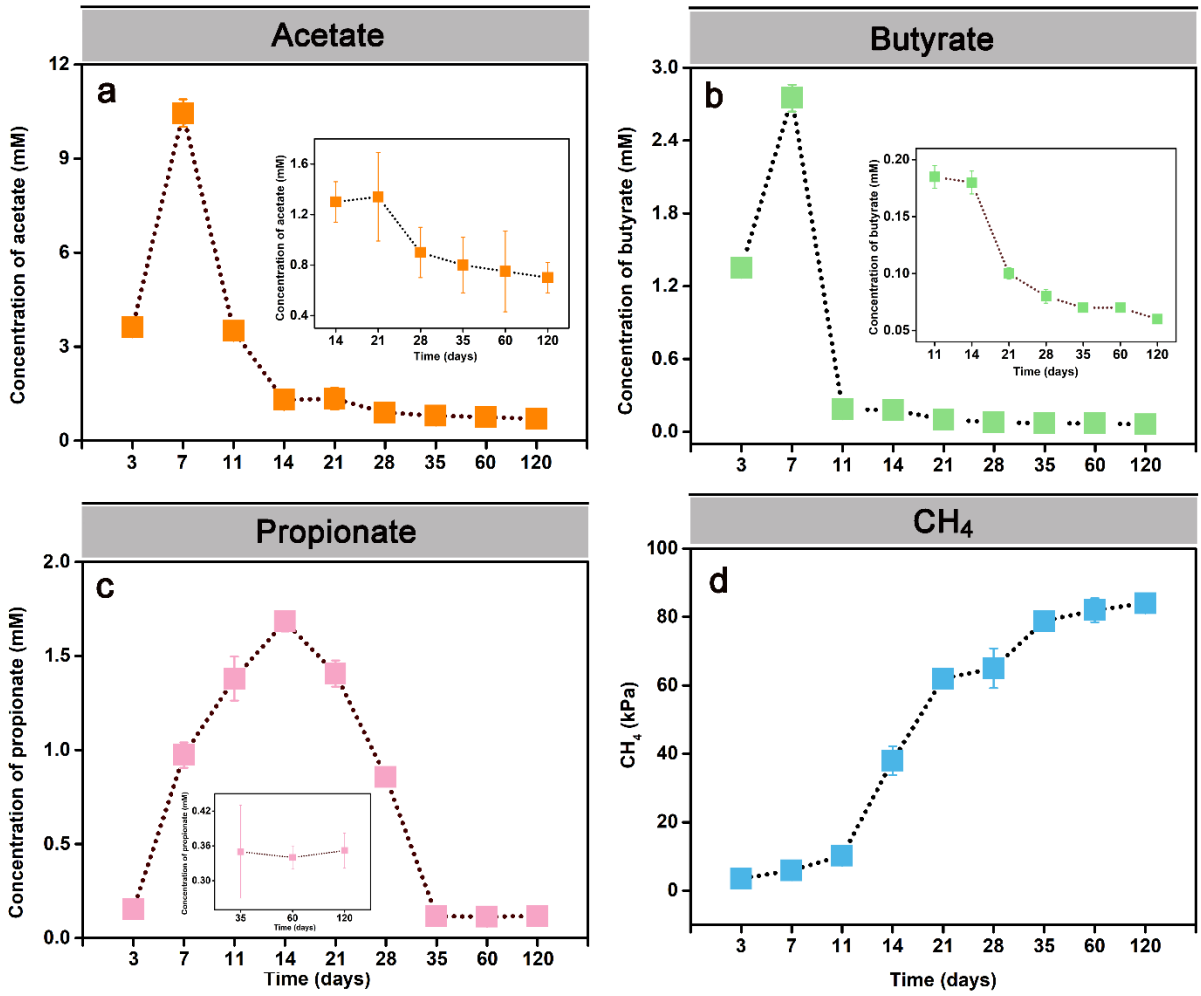

Figure 3.1: Measurement of intermediates and methane in the paddy soil slurries over the 120-day incubation period at 30 °C. Intermediate turnover of acetate (**a**), butyrate (**b**), propionate (**c**), and methane production (**d**). Data are means ± SE (n = 3).

3.2 qPCR and RT-qPCR

The gene and transcript copies of bacterial 16S rRNA and methanogenic *mcrA* were quantified over the 120-day incubation period (**Figure 3.2**). Changes in the copy numbers of bacterial 16S rRNA genes and transcripts (**Figure 3.2a,c**) and *mcrA* genes and transcripts (**Figure 3.2b,d**) showed an M-like up and down over incubation time.. Bacterial 16S rRNA gene and transcript copy numbers peaked first on day 21 (1.2×10^{10} genes vs. 4.8×10^{11} transcripts g^{-1} dry soil) and again on day 35 (1.2×10^{10} genes vs. 4.2×10^{11} transcripts g^{-1} dry soil), with an intermediate decrease on day 28 (5.7×10^{9} 16S rRNA genes vs. 2.7×10^{11} transcripts g^{-1} dry soil) (**Figure 3.2a,c**).

Likewise, the *mcrA* gene and transcript copy numbers peaked first on day 21 (2.9×10^{9} *mcrA* genes vs. 9.2×10^{10} transcripts g^{-1} dry soil) and again on day 35 (3.4×10^{9} *mcrA* genes

vs. 6.5 × 10^{10} transcripts g^{-1} dry soil), with an intermediate decrease on day 28 (1.3 × 10^{9} *mcrA* genes vs. 3.8 × 10^{10} transcripts g^{-1} dry soil) (**Figure 3.2b and d**).

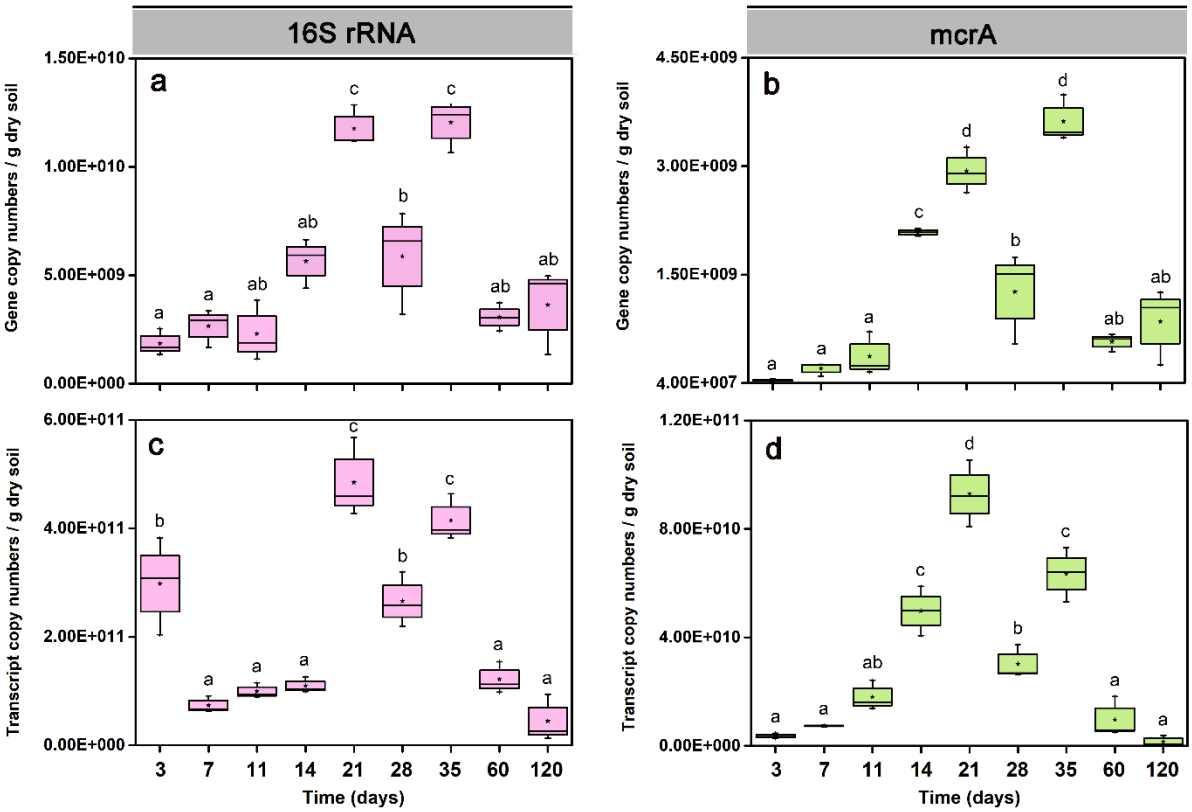

Figure 3.2: Copy number quantification of bacterial 16S rRNA and methanogenic *mcrA* genes (qPCR) and their transcripts (RT-qPCR) in Philippine paddy soil slurries over the 120-day incubation period. Copy numbers of bacterial 16S rRNA genes and transcripts per gram dry paddy soil (**a** and **c**). Copy numbers of *mcrA* genes and transcripts per gram dry paddy soil (**b** and **d**). Data are means ± SE (n = 3). Differences between two incubation time points were determined using the One-Way ANOVA ($P_{FDR} < 0.05$). Exact copy numbers are shown in Tables S3.1, S3.2 (genes) and S3.3, S3.4 (transcripts).

3.3 The bacterial metatranscriptome (16S rRNA, mRNA)

3.3.1 Taxon-specific dynamics

The family-level population dynamics varied over incubation time (**Figure 3.3**). At the rRNA level, the relative abundance of *Geobacteraceae* peaked between days 7 and day 11 (**Figure 3.3a**). Thereafter, the abundance of *Clostridiaceae and Peptococcaceae* peaked at day 21, while *Lachnospiraceae* showed the maximum abundance on day 28 (**Figure 3.3a,c**). In the late stage (days 35 to 120), *Heliobacteriaceae* and *Anaerolineaceae* showed increased rRNA abundance, being together with *Geobacteraceae* the predominant bacterial populations (**Figure 3.3a,c**).

Like on 16S rRNA level, the mRNA abundance of the *Geobacteraceae* peaked at day 7 (22% of total community-wide mRNA and 36% of total bacterial mRNA) followed by a rapid decline towards day 21 and another abundance increase thereafter again (**Figures 3.3b and S3.4a**). The *Peptococcaceae* reached their mRNA peak abundance at day 21 (**Figures 3.3d and S3.4a**). Likewise, *Clostridiaceae* (day 21) and *Lachnospiraceae* (day 28) showed peak mRNA abundances consistent with those observed on rRNA level. The *Acidobacteriaceae* and *Anaerolineaceae* displayed higher mRNA abundances in the late (days 35 to 120) than early phase (days 3 to 21) (days 3 to 21) (**Figure 3.3d**). In addition, putative syntrophic populations, such as *Peptococcaceae* and *Heliobacteriaceae*, reached a second peak abundance during the late stage (**Figures 3.3b, d and S3.4a**).

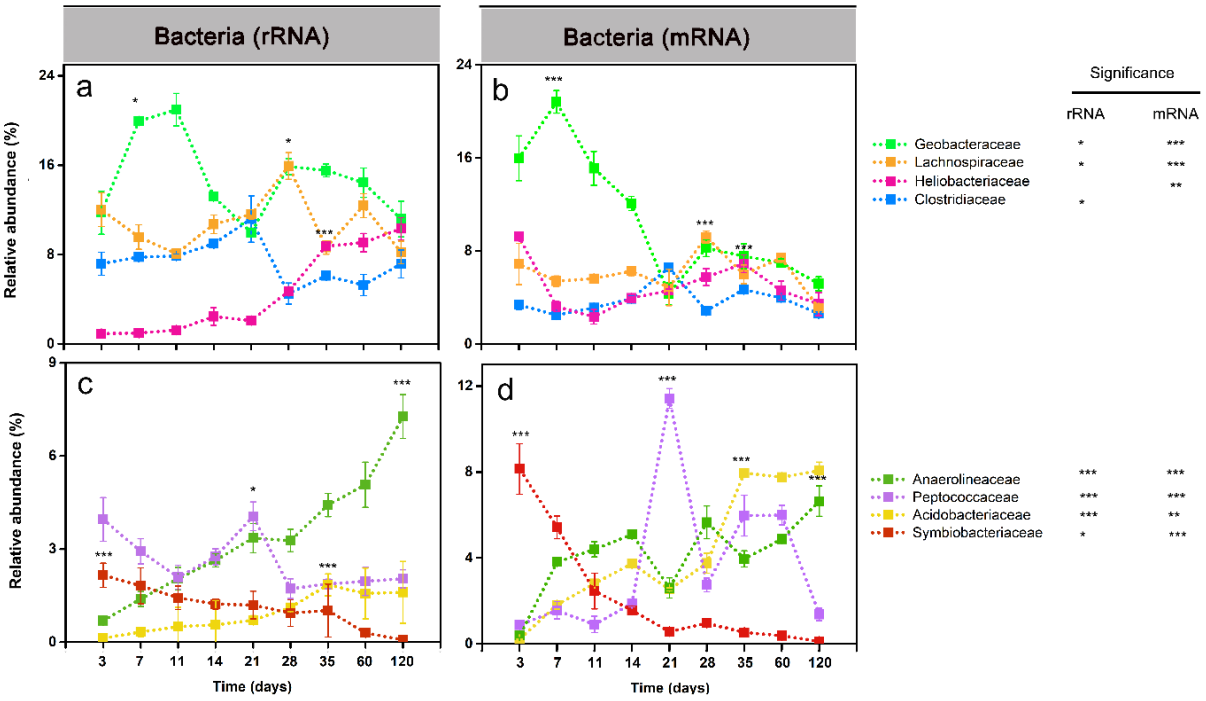

Figure 3.3: Relative abundance changes of dominant bacterial (a-d) families (> 2%) on rRNA and mRNA level, respectively. The percentage abundances are given in relation to total community-wide bacterial and archaeal 16S rRNA and mRNA, respectively. Data are means ± SE (n = 3). Asterisks * (P_{FDR}≤0.05), ** (P_{FDR}≤0.01), and *** (P_{FDR}≤0.001) indicate significant difference. Asterisks shown aside the taxonomic names indicate that in STAMP, the relative rRNA or mRNA abundances significantly changed through the whole incubation period. Asterisks directly shown in the plots indicate that in DESeq2, the rRNA or mRNA abundance in that particular sampling time point significantly differed from the original abundance at the first sampling (day 3) or vice versa that the relative rRNA or mRNA abundance at day 3 (*Symbiobacteriaceae*) significantly differed from all other sampling time points. Significance values (P_{FDR}) are only indicated on rRNA and mRNA level for the taxon-specific abundance peak. The complete set of P_{FDR} values obtained by DESeq2 analysis for all sampling

time points is shown in Tables S3.5 (rRNA) and S3.6 (mRNA).

3.3.2 Carbohydrate-active enzymes (CAZymes)

A total of 13,632 mRNA contigs were annotated to encode CAZymes involved in degrading cellulose (e.g., cellulases, cellulose-1,4-beta-cellobiosidase), xylan (e.g., endo-1,4-beta-xylanase), other hemicelluloses (e.g., alpha- and beta-glactosidase), and chitin (chitinases), (**Figure 3.4a**). The majority of CAZyme transcripts was taxonomically assigned to *Firmicutes, Proteobacteria*, and *Actinobacteria*. Except for chitinases, the CAZyme transcript abundance of *Firmicutes* steadily decreased with incubation time, while that of the *Planctomycetes* increased. The CAZyme transcript abundance of *Proteobacteria* varied during the slurry incubations. The CAZyme transcript abundance of *Actinobacteria* was particularly high during the final incubation period (day 120), with the exception of CAZyme transcripts involved in degrading other hemicellulases (**Figure 3.4b**).

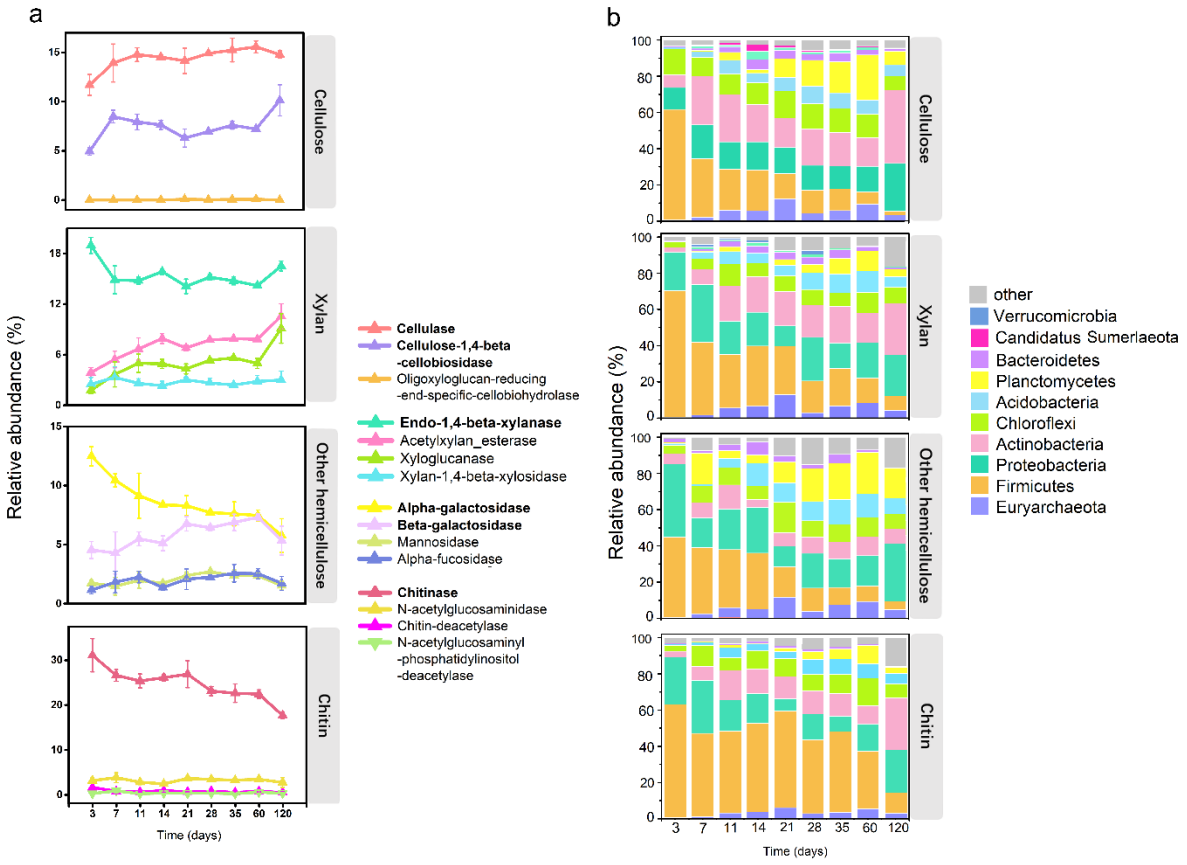

Figure 3.4: Metatranscriptomic expression dynamics of CAZymes-encoding genes involved in the breakdown of cellulose, xylan, and other hemicelluloses, and chitin (a), and their phylum-level affiliation over the 120-day incubation period (b). The analysis involved multiple CAZyme families of glycosyl hydrolases

(GHs) and carbohydrate-binding modules (CBMs). They are specified in Table S3.7

3.4 The methanogenic metatranscriptome (16S rRNA, mRNA)

Methanosarcinaceae, *Methanocellaceae*, and *Methanotrichaceae* were the prevailing methanogenic families throughout slurry incubation (**Figure 3.5a,b**). The *Methanosarcinaceae* was the dominant methanogen group, showing a two-peak abundance dynamics. Both its rRNA and mRNA abundances peaked first around days 11 and 14, then decreased until day 28, but increased thereafter again and reached a second activity peak between days 35 and 60. The *Methanocellaceae* were first detectable at day 11. Upon an abundance peak on day 21, the relative rRNA and mRNA abundances steadily decreased towards day 120. Significant transcript levels of the *Methanotrichaceae* were only detectable on mRNA level during the late stage, with the peak abundance at day 120.

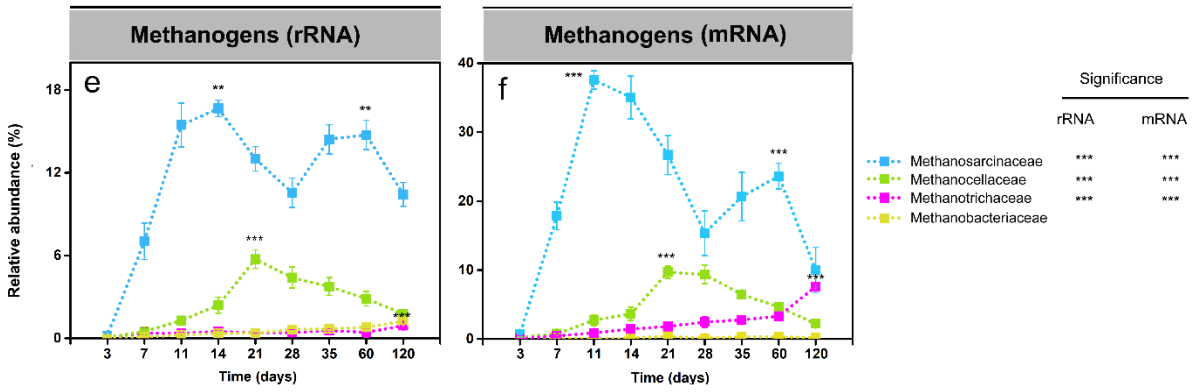

Figure 3.5: Relative abundance changes of the dominant methanogenic (a and b) families (> 2%) on rRNA and mRNA level, respectively. The percentage abundances are given in relation to total community-wide bacterial and archaeal 16S rRNA and mRNA, respectively. Data are means ± SE (n = 3). Asterisks * (P_{FDR}≤0.05), ** (P_{FDR}≤0.01), and *** (P_{FDR}≤0.001) indicate significant difference. Asterisks shown aside the taxonomic names indicate that in STAMP, the relative rRNA or mRNA abundances significantly changed through the whole incubation period. Asterisks directly shown in the plots indicate that in DESeq2, the rRNA or mRNA abundance in that particular sampling time point significantly differed from the original abundance at the first sampling (day 3). Significance values (P_{FDR}) are only indicated on rRNA and mRNA level for the taxon-specific abundance peak. The complete set of P_{FDR} values obtained by DESeq2 analysis for all sampling time points is shown in Tables S3.5 (rRNA) and S3.6 (mRNA).

3.5 Defining dominant *Methanosarcina* populations

Assembled from the rRNA Illumina reads, near full-length 16S rRNA sequences grouped into four distinct *Methanosarcina* populations (I to IV). These differed in their abundance dynamics

(**Figure 3.6**). The Group II population was closely affiliated to *Methanosarcina* sp. MSH10X1 and predominant throughout slurry incubation. *Methanosarcina* Group IV was the second most abundant population and had a close affiliation to *M. horanabensis*. The Group II and Group IV populations showed opposite 16S rRNA abundance dynamics, with both Group IV peak abundance and Group II minimal abundance at day 11 (34% [Group IV] versus 51% [Group II] of total *Methanosarcina* 16S rRNA (**Figure 3.6b**). The *Methanosarcina* Group I and Group III populations displayed low but relatively stable transcript abundances (collectively < 20% of total *Methanosarcina* 16S rRNA) throughout slurry incubation (**Figure 3.6b**).

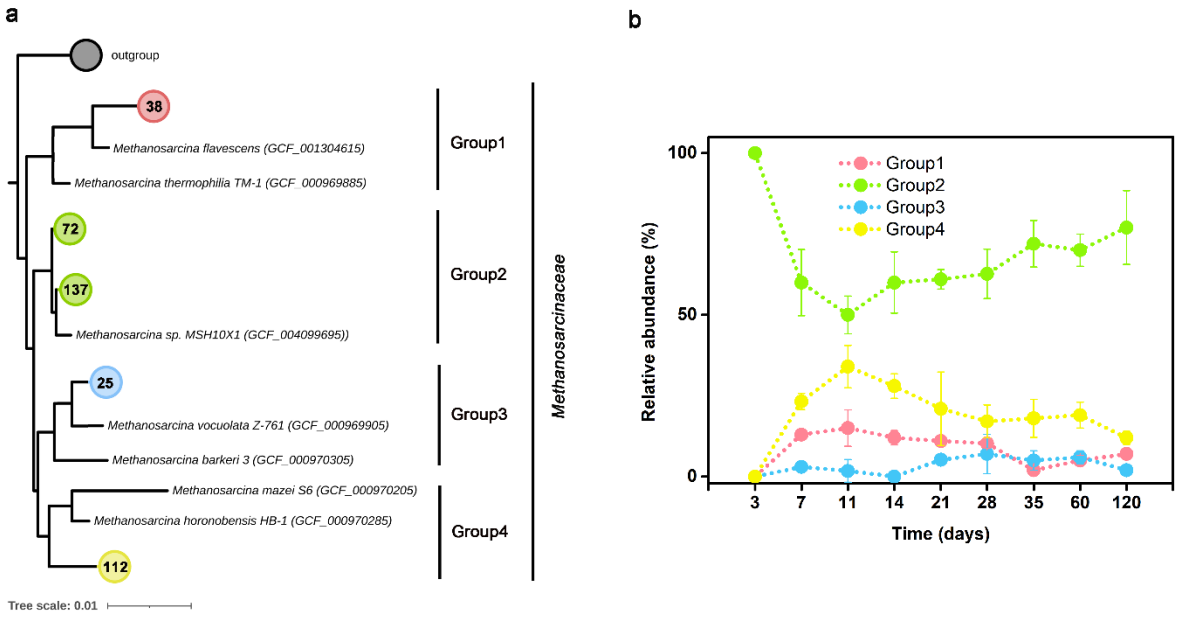

Figure 3.6: Phylogenetic tree of the four *Methanosarcina* populations detected in the paddy soil slurries at mesophilic temperature (30 °C) (a) and their relative abundance dynamics over incubation time (b). (a) The Neighbor-joining tree was constructed based on near full-length 16S rRNA sequences (> 1200 bp) assembled by EMIRGE from the metatranscriptomic datasets (415 sequences) and reference sequences extracted from *Methanosarcina* genomes in GTDB. **(b)** The relative abundance dynamics of the four distinct *Methanosarcina* populations (Groups I to IV) were inferred from the assembled 16S rRNA sequences. Data are means ± SE (n = 3).

3.6 Mapping-independent expression analysis of methanogenic pathways

The collective mRNA abundance of major methanogenesis pathways (**Figure 3.7a**) and the transcript abundance of particular pathway marker genes (**Figure 3.7b**) varied with incubation time. Acetoclastic methanogenesis was the dominant methane production pathway with the greatest transcript abundance (36.4% of total mRNA assigned to KEGG level 3 methane metabolism) in the early stage. This involved the mRNA peak abundance of the following

pathway marker genes: c*dhAB*, *cdhCDE*, *ack*, *pta* (**Figure 3.7b**). The changes in their transcript level over incubation time agreed well with the overall abundance dynamics of the *Methanosarcinaceae* (**Figures 3.5b, 3.7c**). Transcripts of genes (*acs*) indicative of *Methanotrichaceae*-driven acetoclastic methanogenesis steadily increased in relative abundance during the late stage. Their peak abundance was at day 120, while those indicative of *Methanosarcinaceae*-driven acetoclastic methanogenesis had significantly declined (**Figures 3.5b, 3.7c**).

Members of the *Methanocellaceae* were the prevailing H_2-CO_2-utilizing methanogens, with the key genes involved in hydrogenotrophic methanogenesis (*fwd*, *ftr*, *mch*, *mtd*, *mer*) being most expressed by this family-level group (**Figure 3.7b,c**). The gene expression dynamics indicative of hydrogenotrophic methanogenesis agreed well with the overall abundance dynamics of the *Methanocellaceae* (**Figures 3.5b, 3.7b**).

In addition, transcripts of genes (*mtaA*, *mtaBC*, *mtbA*, *mtbBC*, *mtmBC*, *mttBC*) indicative of methylotrophic methanogenesis were detected, with *mtaBC* exhibiting the greatest transcript abundance throughout slurry incubation. The relative abundance of transcripts involved in methylotrophic methanogenesis increased from day 3 and reached the first peak abundance (5.8% of total mRNA assigned to KEGG level 3 methane metabolism) on day 14, but then decreased towards day 21 (2.1%). Thereafter, the relative expression level of this pathway increased again and reached a second peak abundance in relative transcript abundance (3.4% of total mRNA assigned to KEGG level 3 methane metabolism) around day 60 (**Figure 3.7a, b**). This two-peak (14 and 60 days) abundance dynamics of methylotrophic mRNA agreed well with the overall abundance dynamics of *Methanosarcina*-affiliated rRNA (**Figure 3.5a**) and mRNA (**Figure 3.5b**), in both early and late stages. Indeed, the taxonomic assignment of transcripts involved in methylotrophic methanogenesis showed that they were entirely expressed by the *Methanosarcinaceae* (**Figure 3.7c**).

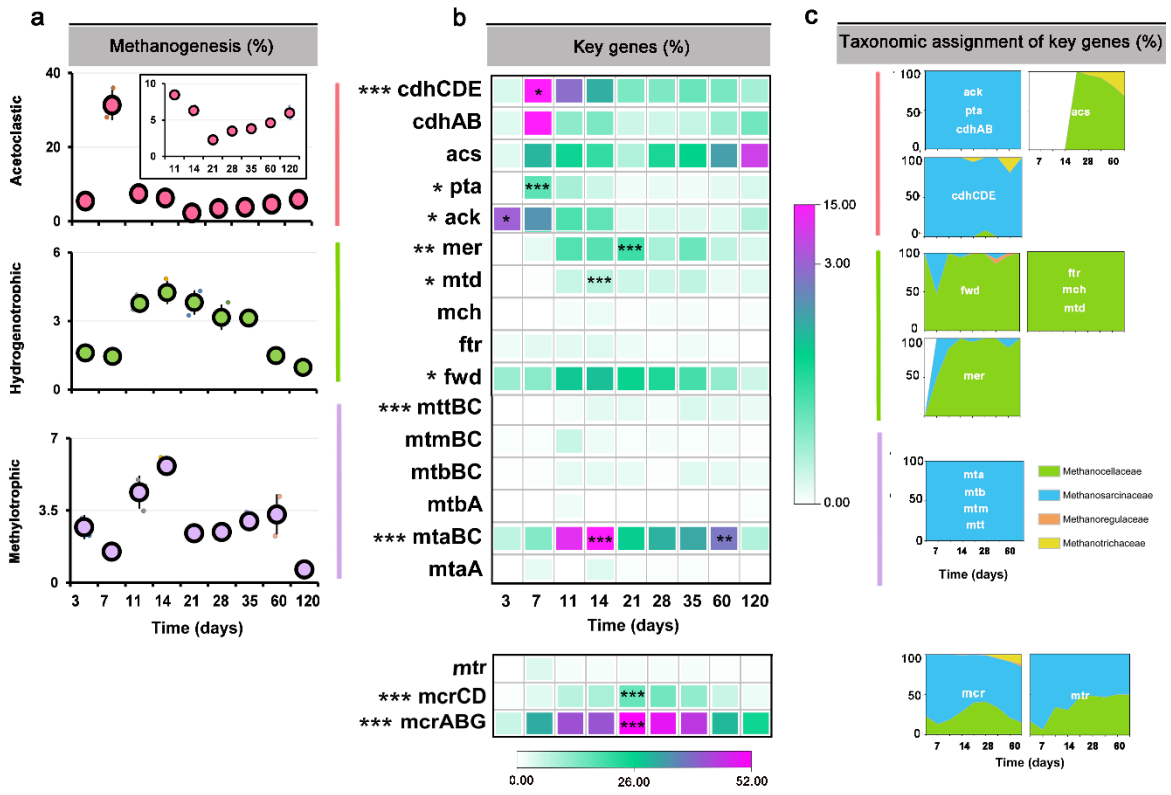

Figure 3.7: Relative mRNA abundance dynamics of individual methanogenic pathways over incubation time (a), transcript dynamics of related key pathway genes (b), and taxonomic assignment of the transcripts (c). The relative abundance values are given in relation to total mRNA affiliated to the KEGG level 3 category 'methane metabolism'. The relative expression levels were calculated based on TPM values. Data are means ± SE (n = 3). Asterisks * (P_{FDR}≤0.05), ** (P_{FDR}≤0.01), and *** (P_{FDR}≤0.001) indicate significant difference. Asterisks shown aside the gene names indicate that in STAMP, the relative mRNA abundance significantly changed through the whole incubation period. Asterisks directly shown in the heatmap (b) indicate that in DESeq2, the mRNA abundance in that particular sampling time point significantly differed from the original abundance at the first sampling (day 3) or vice versa that the relative mRNA abundance (*ack*) at day 3 significantly differed from all other sampling time points. Significance values (P_{FDR}) are only indicated for the peak transcript abundance(s) of each key pathway gene. The complete set of P_{FDR} values obtained in DESeq2 analysis for all sampling time points is shown in Table S3.8.

3.7 Gene expression of methanogenic pathways by *Methanosarcina* Group II

3.7.1 *Methanosarcina* MAGs

In order to be able to map KEGG-annotated transcripts onto genomes of *Methanosarcina* Group II population, we conducted a metagenomic analysis. Metagenomic sequencing yielded a total of 54,672,109 reads after quality control (**Table S2.2**). The assembly of quality-filtered reads generated a total of 781,362 contigs greater than 1,000 bp and 21,770 contigs greater than 5,000 bp. This resulted in three medium-quality metagenome-assembled *Methanosarcina*

genomes, ranging in completeness from 62% to 82.5% (**Table S3.9**). These will be referred to as *Methanosarcina* MAGs. One each was obtained from slurry material sampled at days 21, 28, and 35. The three MAGs shared high average nucleotide identity (ANI) values (> 95%). When compared to *Methanosarcina* genomes in GTDB, the three MAGs shared greatest ANI values with *Methanosarcina* sp. MSH10X1 (> 85%) (**Figure 3.8a**). In addition, the three MAGs shared high nucleotide sequence identities of their *mcrA* genes (98%). When compared to *Methanosarcina* reference genomes, the three MAGs also shared greatest *mcrA* nucleotide sequence identity values with *Methanosarcina* sp. MSH10X1 (> 94%) (**Figure 3.8b**). The inclusion of a near full-length 16S rRNA gene sequence (1,400 nt) from MAG_21 in the *Methanosarcina* 16S rRNA tree confirmed that the three MAGs belong to *Methanosarcina* Group II and are most closely related to *Methanosarcina* sp. MSH10X1 (**Figure 3.9**). Their predicted genome size (3.42 Mbp) was highly similar to that one of strain MSH10X1 (3.56 Mbp) (**Figure S3.6**). Comparative genomics revealed that the three MAGs share their majority of functionally annotated genes with the reference genomes of *Methanosarcina* Groups I to IV (922 common genes), while they encode 141 unique genes (**Figure 3.10, Tables S3.10, S3.11**). A synteny analysis showed that the *mta* gene cluster in the *Methanosarcina* MAGs displays higher similarity with that of *Methanosarcina* sp. MSH10X1 than to those of the other reference genomes (**Figure S3.7**). The *Methanosarcina* MAGs and the genome of strain MSH10X1 contained five gene copies of *mtaA* and three gene copies of *mtaBC.*

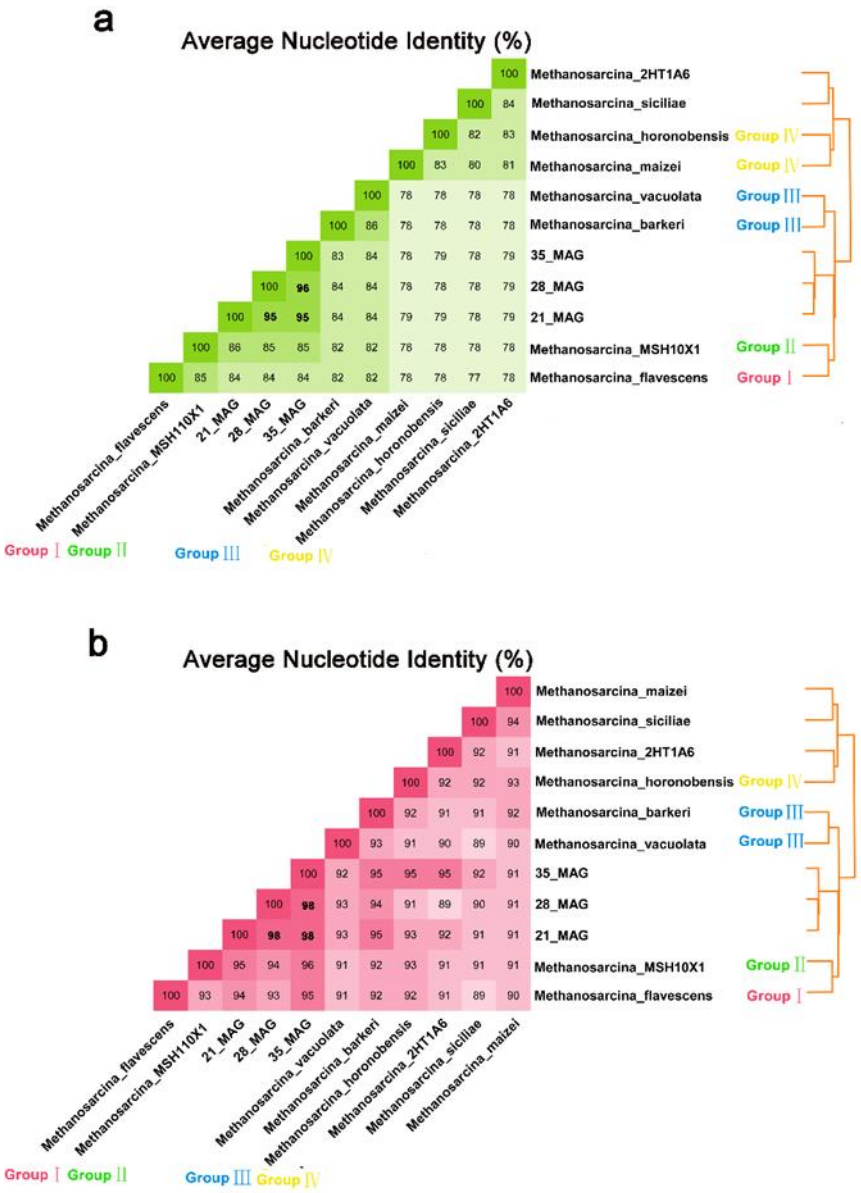

Figure 3.8: (a) Average nucleotide identity (ANI) values calculated for the three *Methanosarcina* MAGs (21, 28, 35) and reference genomes downloaded from GTDB. (b) Nucleotide identity values of the *mcrA* gene sequence calculated for the same set of MAGs and *Methanosarcina* reference genomes.

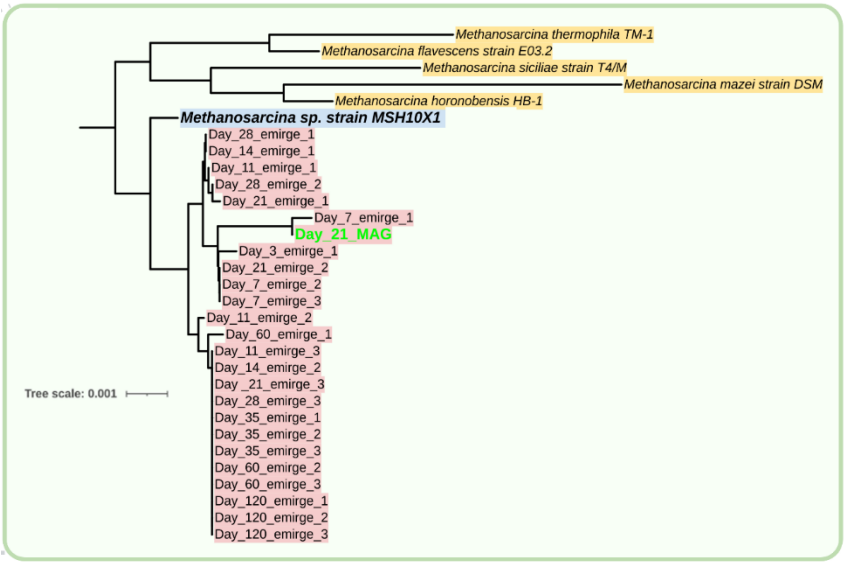

Figure 3.9: Neighbor-joining tree of the 16S rRNA gene sequence from MAG_21 in relation to 16S rRNA (gene) sequences obtained in this study and from *Methanosarcina* reference genomes.

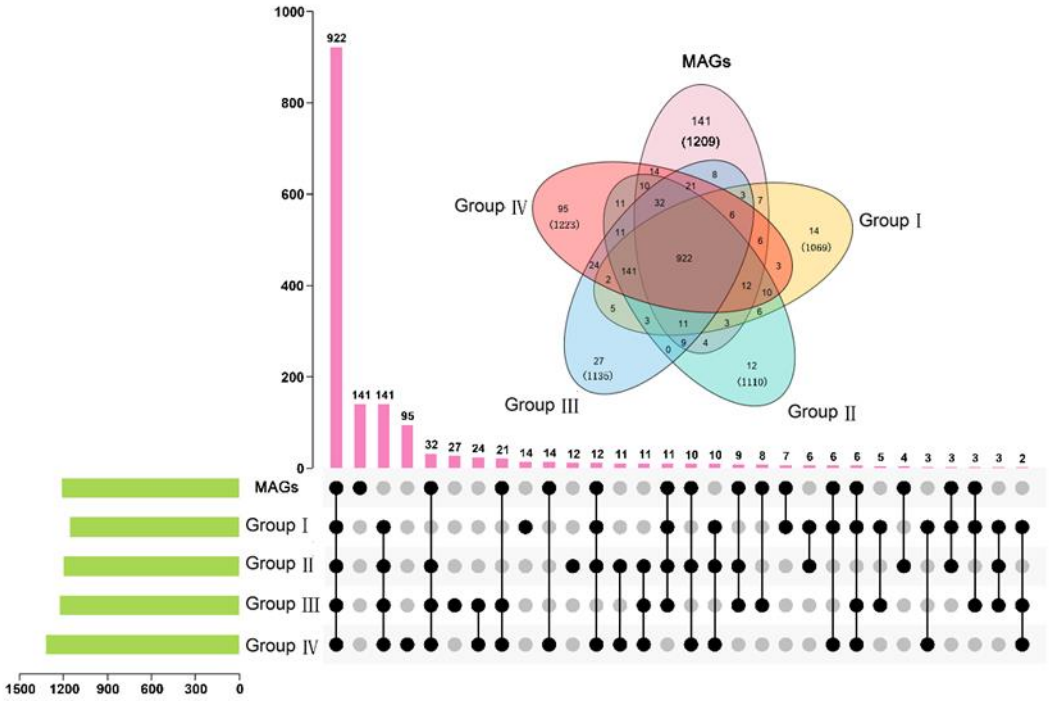

Figure 3.10: Venn diagram showing the distribution of functionally annotated genes among the three *Methanosarcina* MAGs (21, 28, 35) and the reference genomes of *Methanosarcina* Groups I (*M. flavescens*), II (strain MSH10X1), III (*M. barkeri*), and IV (*M. horonobensis*). The bar columns (pink) show the distribution pattern of particular sets of characterized genes among the MAGs and Group I to IV reference genomes. The green columns indicate the totally predicted number of characterized genes in the MAGs and Group I to IV reference genomes. The black and grey dots indicate presence and absence of this particular set of characterized genes in the particular reference genome (Group I to IV), respectively.

3.7.2 Mapping-dependent gene expression analysis

KEGG-annotated transcripts were mapped onto the three MAGs (**Figures 3.11 and 3.12**). On KEGG level 2, transcripts involved in energy metabolism showed greatest mapping efficiency (54% to 86% of total mapped mRNA) throughout slurry incubation, while transcripts involved in mRNA translation were mapped with high frequency (30-32% of total mapped mRNA) particularly during the first week of slurry incubation (**Figure 3.11a**). On KEGG level 3, transcripts involved in methane metabolism were dominantly mapped (51% to 80% of total mapped mRNA) onto the MAGs throughout slurry incubation (**Figure 3.11b**). On KEGG level 4, transcripts involved in acetoclastic methanogenesis and methylotrophic methanogenesis were mapped with high frequency (**Figure 3.12a)**. Overall, the transcript mapping frequency of the methylotrophic pathway (5.1-7.2% of total mapped mRNA) was lower than that of the acetoclastic pathway (7.5-12.4% of total mapped mRNA). Among the total variety of methanogen mRNA, *mtaABC* transcripts showed the greatest mapping frequency (**Figure 3.12b**).

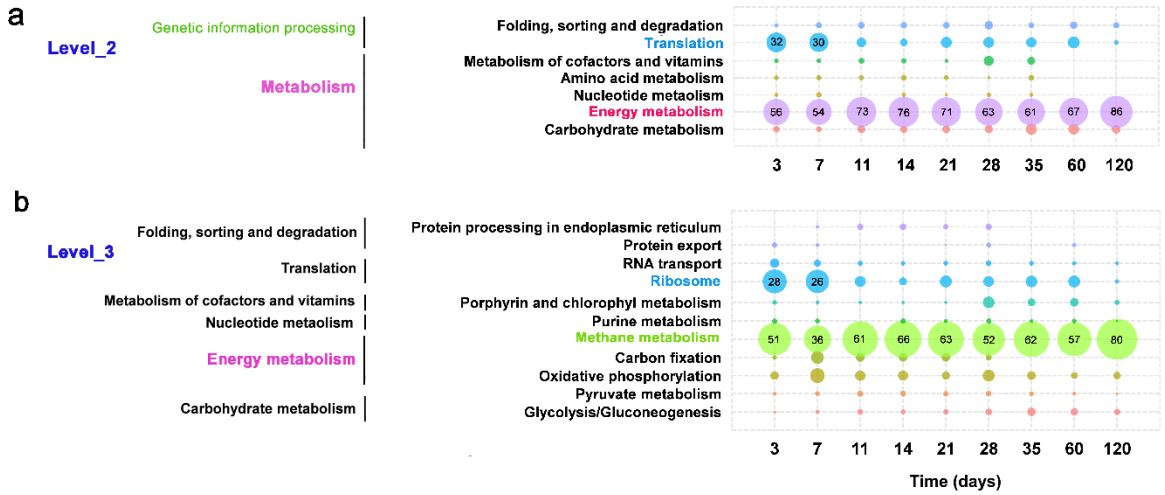

Figure 3.11: Relative abundances of mRNA mapped onto the three *Methanosarcina* MAGs (21, 28, 35) and affiliated with particular KEGG categories on level 2 (a) and 3 (b). The triplicate metatranscriptomes of a given sampling time point were individually mapped onto a particular MAG as follows: (i) triplicate metatranscriptomes of days 3, 7, 11, 14, and 21 onto MAG_21; (ii) triplicate metatranscriptomes of day 28 onto MAG_28; and (iii) triplicate metatransciptomes of days 35, 60, and 120 onto MAG_35. The relative mapping efficiencies were calculated based on the normalized number of mRNA reads that could be mapped onto each ORF of a given *Methanosarcina* MAG. The dot sizes indicate relative mapping efficiencies.

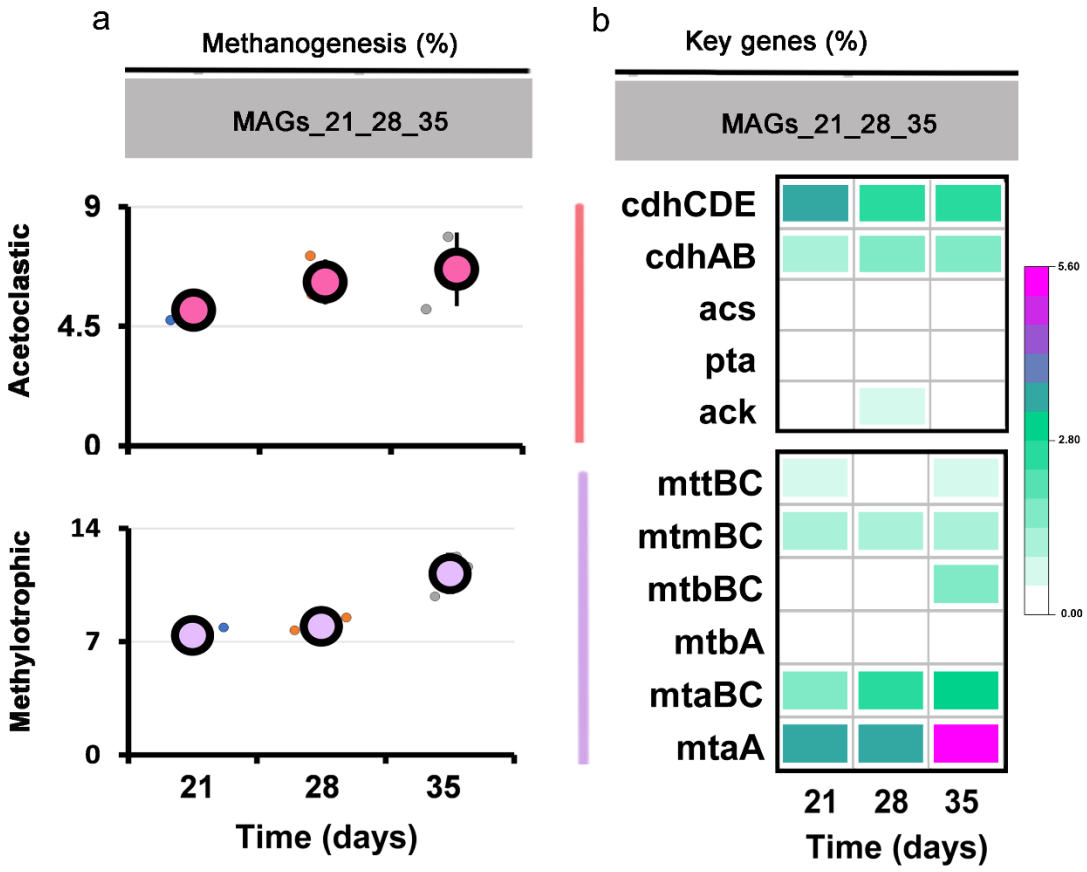

Figure 3.12: Methanogen transcripts mapped onto the *Methanosarcina* MAGs (21, 28, 35). (a) Mapping efficiency of total mRNA involved in acetoclastic and methylotrophic methanogenesis. (b) Mapping efficiency of mRNA encoding particular key genes of the acetoclastic and methylotrophic methanogen pathways. The percentage values are given in relation to the total mRNA that were mapped onto the MAGs. The mapping efficiencies were calculated based on TPM values (means ± SE, n = 3). The complete set of P_{FDR} values obtained in DESeq2 analysis for all sampling time points is shown in Table S3.12.

3.8 Competitive transcript mapping onto the four reference genomes

Simultaneous mRNA mapping against the composite reference genomes of *Methanosarcina* Groups I to IV revealed that the vast majority of transcripts involved acetoclastic and methylotrophic methanogenesis were mapped onto the genome of *Methanosarcina* sp. MSH10X1 (Group II), with the exception of day 7. On that day, a certain number of transcripts of the acetoclastic pathway were also mapped onto the genomes of *Methanosarcina flavescens* (Group I) and *Methanosarcina horonobensis* (Group IV) (**Figure 3.13**).

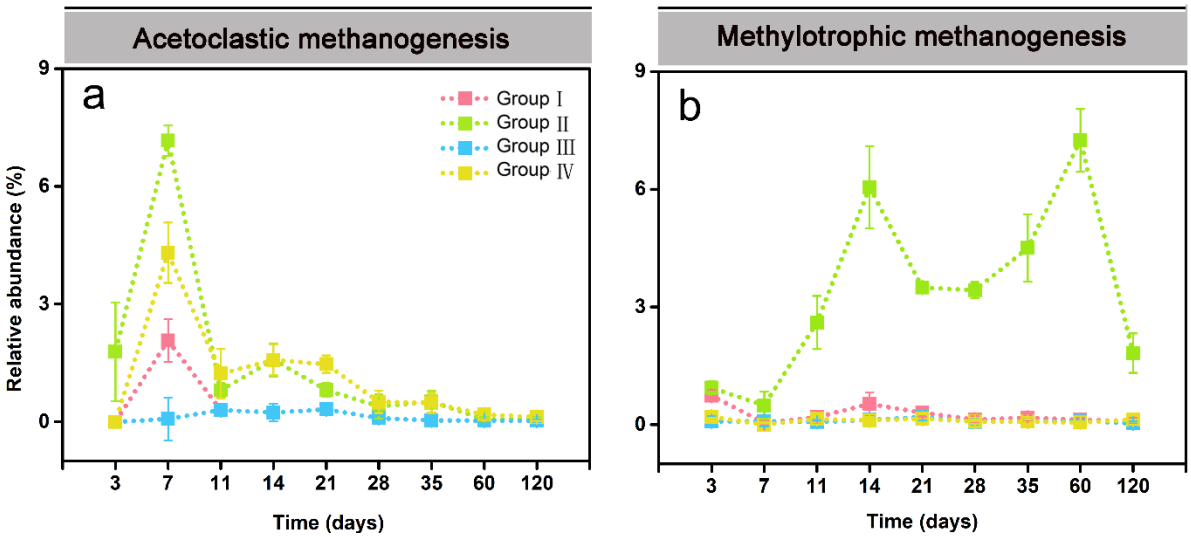

Figure 3.13: Relative transcript dynamics of acetoclastic and methylotrophic methanogen pathways inferred from transcript mapping simultaneously onto a mix of *Methanosarcina* Group I to IV reference genomes (competitive mapping approach). The relative mapping efficiencies were calculated based on TPM values. Data are means ± SE (n = 3).

4 Methanogenic Community Dynamics at Moderately Thermophilic Temperature

4.1 Metabolite turnover

Metabolite measurements in the straw-amended slurries were made over the complete incubation period of 120 days. Acetate transiently accumulated and reached its peak concentration (8.24 mM) at day 7. Thereafter, acetate concentration sharply decreased within 7 days to 0.93 mM on day 14 and then showed a steady-state between production and consumption, ranging from 0.44 to 0.93 mM until day 120 (**Figure 4.1a**). Concurrently, butyrate concentration peaked at day 7 (1.72 mM) and then sharply decreased (**Figure 4.1b**). Propionate strongly accumulated from day 3 (0.58 mM) onwards, with a peak concentration at day 14 (1.26 mM). Subsequently, its concentration rapidly decreased towards day 21 (0.47 mM), and then propionate showed a steady-state at low but clearly detectable levels, ranging from 0.36 to 0.51 mM until day 120 (**Figure 4.1c**). First CH_4 production was detectable around day 7 (1.98 KPa), but increased significantly towards day 28 (62.55 KPa). Then the CH_4 production rate was decreased between days 28 and 35 (**Figure 4.1d**), but increased again from days 35 to 60.

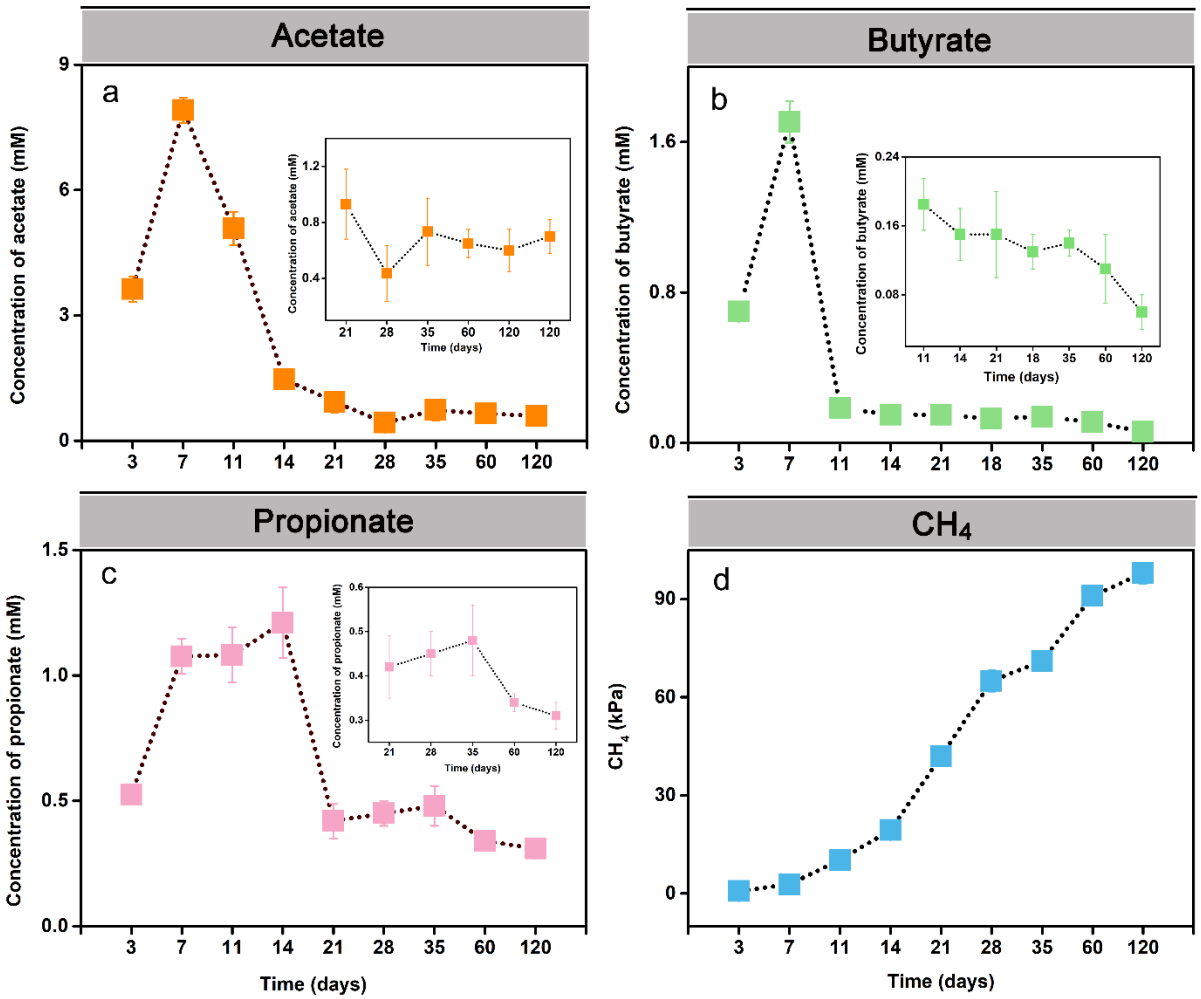

Figure 4.1: Measurement of intermediates and methane in the paddy soil slurries over the 120-day incubation period at 45 °C. Intermediate turnover of acetate (**a**), (**b**) butyrate, propionate (**c**), and methane production (**d**). Data are means ± SE (n = 3).

4.2 qPCR and RT-qPCR

The gene and transcript copies of bacterial 16S rRNA and methanogenic *mcrA* were quantified over the 120-day incubation period (**Figure 4.2**). Changes in the copy numbers of bacterial 16S rRNA genes (**Figure 4.2a**) and *mcrA* genes (**Figure 4.2b**) over incubation time showed an opposite trend. Changes in the copy numbers of bacterial 16S rRNA transcripts (**Figure 4.2c**) and *mcrA* transcripts (**Figure 4.2d**) over incubation time showed 'M-plots'.

The copy numbers of bacterial 16S rRNA genes (**Figure 4.2a**) sharply decreased from day 3 towards day 11 (2.3×10^{10} to 7.6×10^{9} genes g^{-1} dry soil), and then increased to day 21 slightly (9.4×10^{9} genes g^{-1} dry soil). Thereafter, the copy numbers declined from day 21 to day 28 and then maintained in a steady-state (ranging from 4.1×10^{9} to 2.7×10^{9} genes g^{-1} dry

soil). By contrast, the *mcrA* gene copy numbers showed a significant and steady increase over incubation time (**Figure 4.2b**). They increased from day 3 and peaked first on day 21 (7.1×10^8 to 6.2×10^9 genes g^{-1} dry soil), decreased between days 21 and 28, and increased again from day 35 until day 120 (5.2×10^9 to 1.1×10^{10} genes g^{-1} dry soil).

The copy numbers of bacterial 16S rRNA transcripts showed two abundance peaks with one on day 21 and the other on day 35 (7.3×10^{11} vs. 4.8×10^{11} transcripts g^{-1} dry soil), and an intermediate decline on day 28 (3.2×10^{11} transcripts g^{-1} dry soil). Likewise, the *mcrA* transcript copy numbers (**Figure 4.2d**) peaked first on day 21 (1.9×10^{11} transcripts g^{-1} dry soil) and again on day 35 (1.6×10^{11} transcripts g^{-1} dry soil), with an intermediate decline on day 28 (4.2×10^{10} transcripts g^{-1} dry soil). After day 35, the transcript copy numbers of both bacterial 16S rRNA and *mcrA* strongly decreased towards day 120 (**Figure 4.2c, d**).

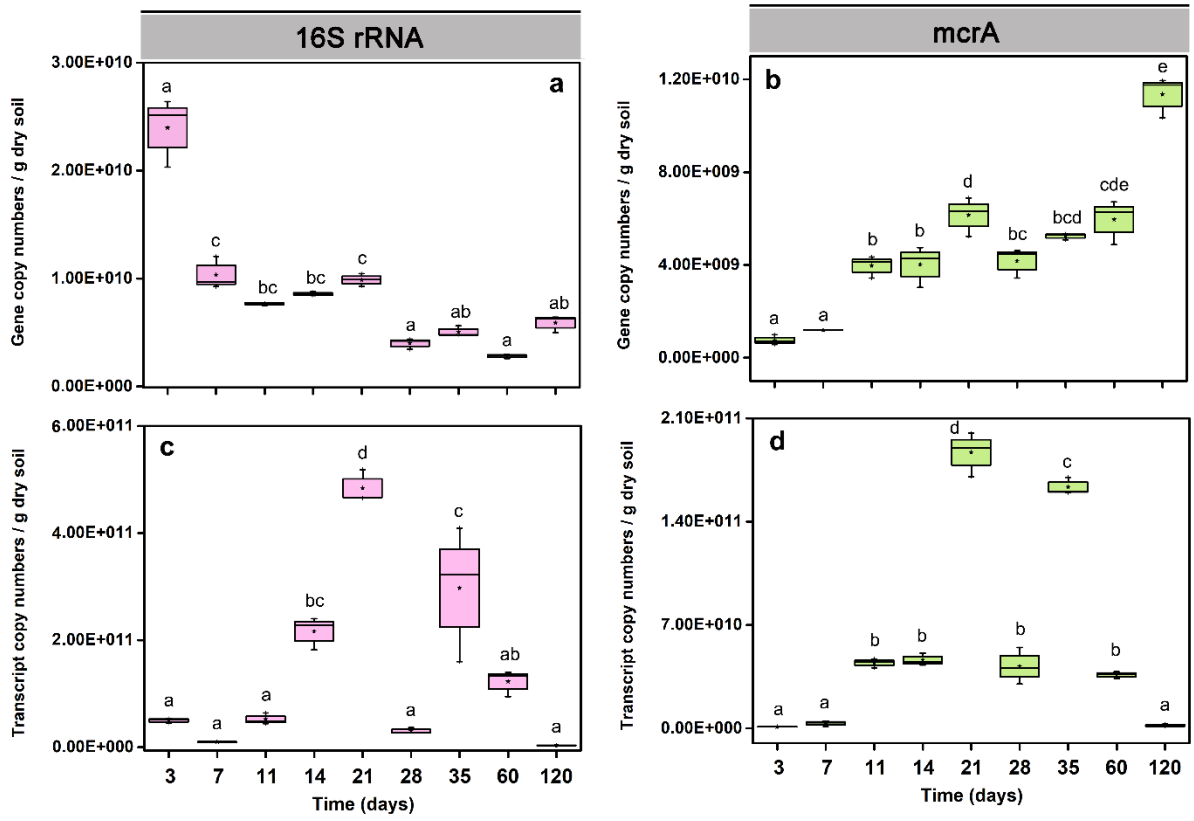

Figure 4.2: Copy number quantification of bacterial 16S rRNA and methanogenic *mcrA* genes (qPCR) and their transcripts (RT-qPCR) in Philippine paddy soil slurries over the 120-day incubation period. Copy numbers of bacterial 16S rRNA genes and transcripts per gram dry paddy soil (**a** and **c**). Copy numbers of *mcrA* genes and transcripts per gram dry paddy soil (**b** and **d**). Data are means ± SE (n = 3). Differences between two incubation time points were determined using the One-Way ANOVA ($P_{FDR} < 0.05$). Exact copy numbers are shown in Tables S4.1, S4.2 (genes) and S4.3, S4.4 (transcripts).

4.3 The bacterial metatranscriptome (16S rRNA, mRNA)

4.3.1 Taxon-specific dynamics

At the 16S rRNA level, *Bacillaceae* and *Peptococcaceae* were the most abundant bacterial families on day 3. *Symbiobacteriaceae*, *Clostridiaceae,* *Ruminococcaceae* and *Lachnospiraceae* reached their abundance peak on day 7 (**Figures 4.3a, c**). Thereafter, the relative abundance of *Heliobacteriaceae* peaked on day 21 (56% of total rRNA) (**Figure 4.3a**). In the late stage, *Thermoanaerobacteraceae* showed increased 16S rRNA abundance, being together with *Heliobacteriaceae* the predominant bacterial population (**Figure 4.3a**).

Like on 16S rRNA level, the mRNA abundance of the *Heliobacteriaceae* peaked at day 21 (38% of total community-wide mRNA) followed by a rapid decline towards day 28 and an abundance increase again thereafter with the second abundance peak on day 35 (**Figure 4.3b**). The *Peptococcaceae* reached their mRNA abundance peak on day 28 (**Figure 4.3b**). In addition, *Clostridiaceae*, *Ruminococcaceae*, and *Lachnospiraceae* showed consistent transcript dynamics on rRNA and mRNA level (**Figure 4.3c,d**). In the late stage, *Bacillaceae* and *Peptococcaceae* displayed increased mRNA abundances (**Figure 4.3b**).

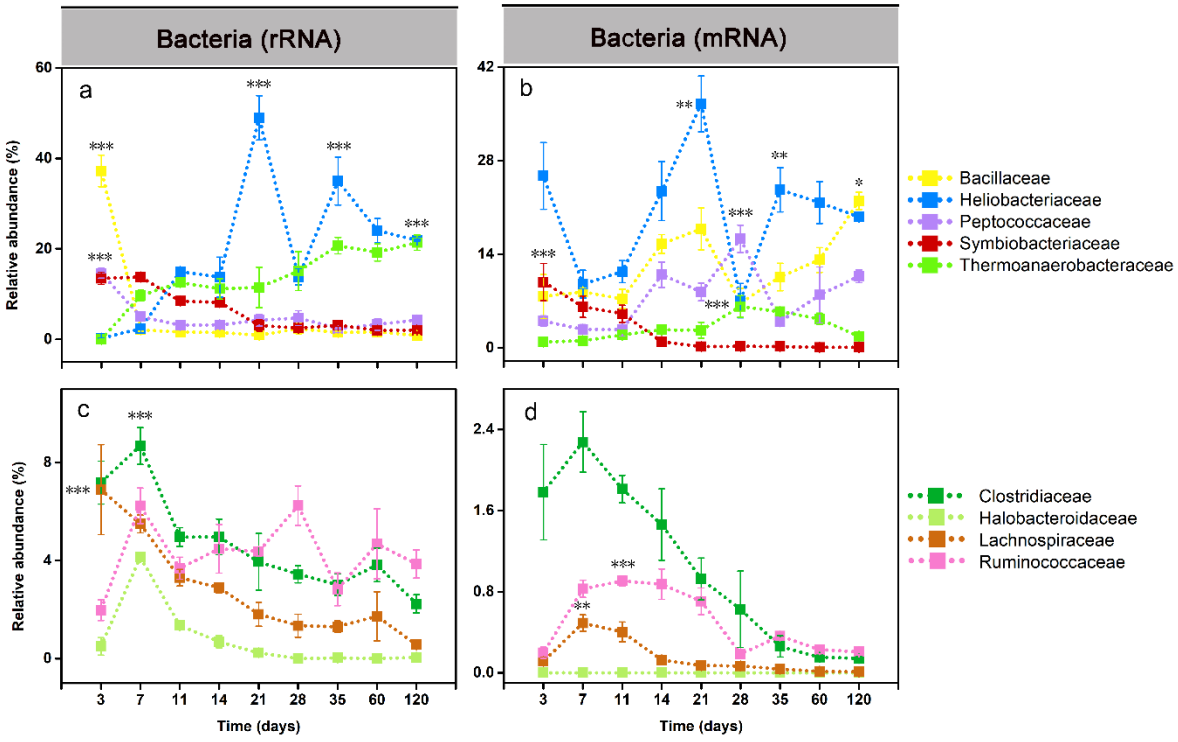

Figure 4.3: Relative abundance changes of dominant bacterial (a-d) families (> 2%) on rRNA and mRNA level, respectively. The percentage abundances are given in relation to total bacterial and archaeal 16S rRNA and mRNA, respectively. Data are means ± SE (n = 3). Asterisks * (P_{FDR}≤0.05), ** (P_{FDR}≤0.01), and *** (P_{FDR}≤0.001) indicate significant difference. Asterisks directly shown in the plots indicate that in DESeq2, the rRNA or mRNA abundance in that particular sampling time point significantly differed from the original abundance at the first sampling (day 3) or vice versa that the relative rRNA or mRNA abundance at day 3 (*Bacillaceae, Symbiobacteriaceae and Lachnospiraceae*) significantly differed from all other sampling time points. Significance values (P_{FDR}) are only indicated on rRNA and mRNA level for the taxon-specific abundance peak. The complete set of P_{FDR} values obtained by DESeq2 analysis for all sampling time points is shown in Tables S4.5 (rRNA) and S4.6 (mRNA).

4.3.2 Carbohydrate-active enzymes (CAZymes)

A total of 18,452 mRNA contigs were annotated to encode CAZymes involved in degrading cellulose (e.g., cellulases, cellulose-1,4-beta-cellobiosidase), xylan (e.g., endo-1,4-beta-xylanase), other hemicelluloses (e.g., alpha- and beta-glactosidase), and chitin (chitinases) (**Figure 4.4a**). The majority of CAZyme transcripts was taxonomically assigned to *Firmicutes,* followed by *Proteobacteria* and *Actinobacteria*. CAZyme transcripts involved in cellulose breakdown and affiliated to *Firmicutes* steadily increased in relative abundance with incubation time. CAZyme transcripts involved in xylan and chitin breakdown and affiliated to *Firmicutes* reached peak abundant at day 14 and then maintained high transcript level until 120 d (>82% of total CAZyme transcripts). The CAZyme transcript abundance of *Proteobacteria* varied during the slurry incubations. The CAZyme transcript abundance of *Actinobacteria* was particularly high during the early incubation period (days 3 to 11) (**Figure 4.4b**).

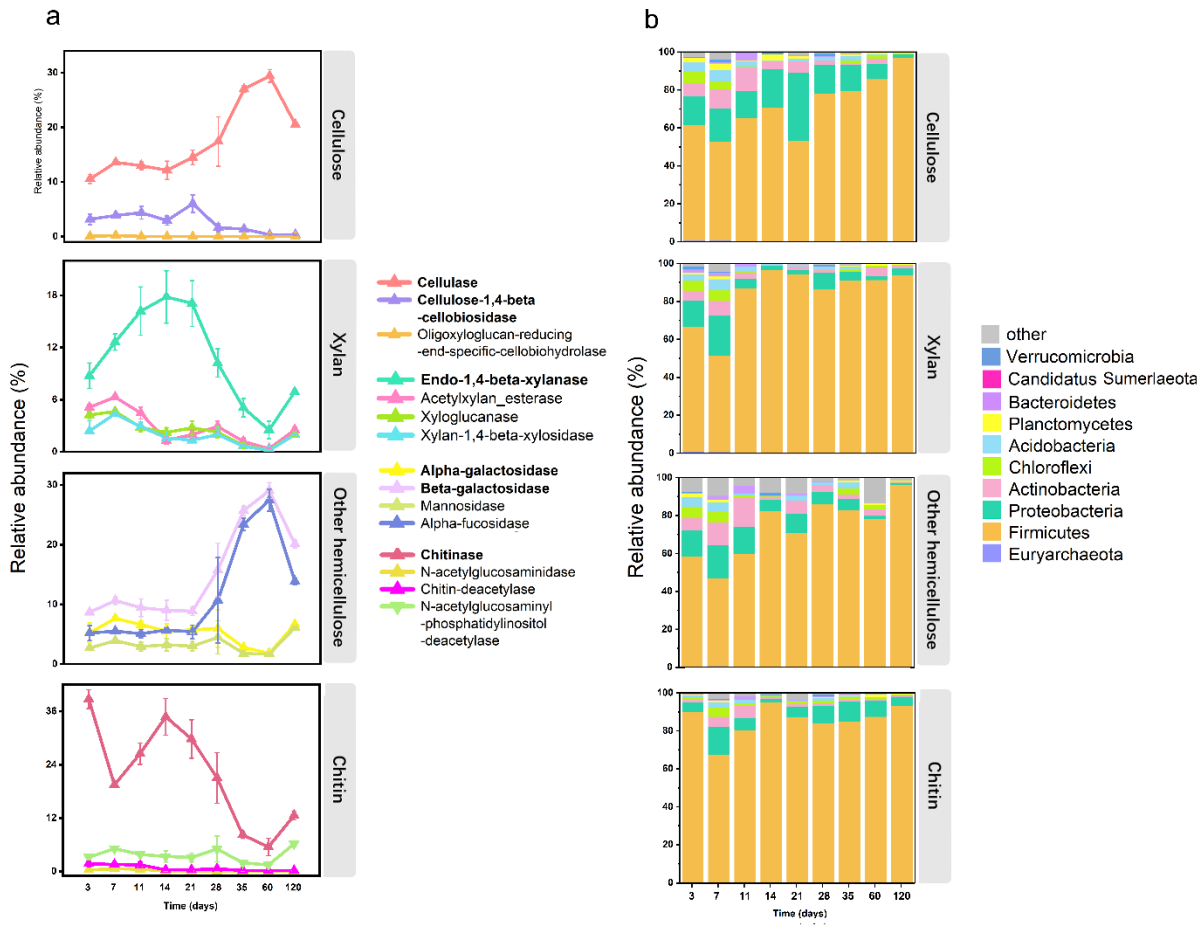

Figure 4.4: Metatranscriptomic expression dynamics of CAZymes-encoding genes involved in the breakdown of cellulose, xylan, other hemicelluloses, and chitin (a), and their phylum-level affiliation over the 120-day incubation period (b). The analysis involved multiple CAZyme families of glycosyl hydrolases (GHs) and carbohydrate-binding modules (CBMs).

4.4 The methanogen metatranscriptome (16S rRNA, mRNA)

Metatranscriptomic analysis revealed the presence of two methanogenic families on both rRNA and mRNA level throughout slurry incubations: *Methanosarcinaceae* and *Methanocellaceae* (**Figure 4.5**). The *Methanosarcinaceae* was the dominant methanogen group on both rRNA and mRNA level. At the rRNA level, its abundance peaked first around day 14, then fluctuated between days 14 and 35, but increased thereafter again from day 35 towards day 120 (**Figure 4.5a**). At the mRNA level, *Methanosarcinaceae* reached its first peak abundance on day 11 followed by a decline until day 21, and then reached a second peak abundance on day 28 (**Figure 4.5b**). Members of the *Methanocellaceae* were first detectable on day 21. Upon a peak abundance on day 35, the relative mRNA abundance steadily decreased towards day 120. Significant transcript levels of the *Methanobacteriaceae* were detectable from day 21 on both

rRNA and mRNA level.

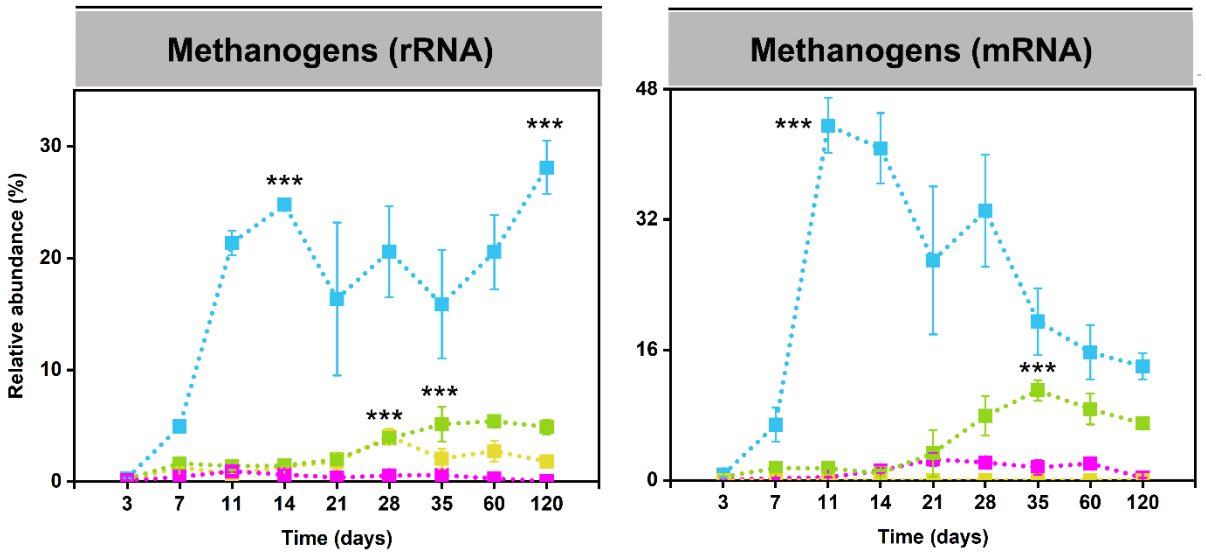

Figure 4.5: Relative abundance changes of dominant methanogenic families (> 2%) on rRNA and mRNA level (a and b), respectively. The percentage abundances are given in relation to total bacterial and archaeal 16S rRNA and mRNA, respectively. Data are means ± SE (n = 3). Asterisks * (P_{FDR}≤0.05), ** (P_{FDR}≤0.01), and *** (P_{FDR}≤0.001) indicate significant difference. Asterisks directly shown in the plots indicate that in DESeq2, the rRNA or mRNA abundance in that particular sampling time point significantly differed from the original abundance at the first sampling (day 3). Significance values (P_{FDR}) are only indicated on rRNA and mRNA level for the taxon-specific abundance peak. The complete set of P_{FDR} values obtained by DESeq2 analysis for all sampling time points is shown in Tables S4.5 (rRNA) and S4.6 (mRNA).

4.5 Defining the dominant *Methanosarcina* populations

Assembled from the rRNA Illumina reads, near full-length 16S rRNA sequences grouped into five distinct *Methanosarcina* populations (I to V). These differed in their abundance dynamics (**Figure 4.6**). The Group III population was closely affiliated to *Methanosarcina barkeri* 3 and predominant throughout slurry incubation, with the peak abundance between days 35 and 60 (77% of total *Methanosarcina*-affiliated 16S rRNA). *Methanosarcina* Group I with close affiliation to *M. flavescens* and *M. thermophilia*, Group II with close affiliation to *Methanosarcina* sp. MSH10X1, and Group IV with close affililiation to *M. horonobensis* displayed similar rRNA abundances. These slowly declined with incubation time. Overall, the Group I, II, and IV populations showed 16S rRNA abundance dynamics opposite to those of the Group III population, with the Group III peak abundance but Groups I, II and IV minimal abundance on day 60 (4-8% [Group I, II and IV] versus 78% [Group III] of total

Methanosarcina-affiliated 16S rRNA) (**Figure 4.6b**). The *Methanosarcina* Group V population displayed low but relatively stable transcript abundances (collectively < 5% of total *Methanosarcina*-affiliated 16S rRNA) throughout slurry incubation (**Figure 4.6b**).

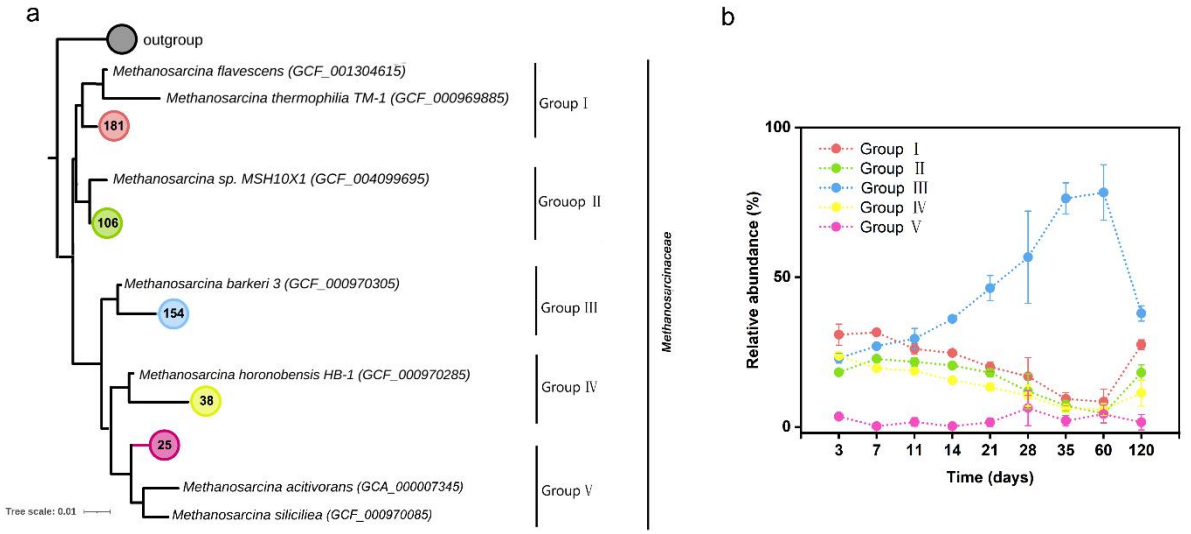

Figure 4.6: Phylogenetic tree of the five *Methanosarcina* populations detected in the paddy soil slurries at moderately themophilic temperature (45 °C). The Neighbor-joining tree was constructed based on near full-length 16S rRNA sequences (> 1200 bp) assembled by EMIRGE from the metatranscriptomic datasets (504 sequences) and reference sequences extracted from *Methanosarcina* genomes in GTDB.

4.6 Mapping-independent expression analysis of methanogenic pathways

The collective mRNA abundance of major methanogenesis pathways (**Figure 4.7a**) and the transcript abundance of particular pathway marker genes (**Figure 4.7b**) varied with incubation time. Acetoclastic methanogenesis was the dominant methane production pathway with the greatest transcript abundance (13.2% of total mRNA assigned to KEGG level 3 methane metabolism) in the early stage. This involved the peak abundance of the following pathway marker genes: c*dhAB*, *cdhCDE*, *ack*, *pta* (**Figure 4.7b**). Their changes in relative expression level agreed well with the overall abundance dynamics of the *Methanosarcinaceae* (**Figures 4.5b, 4.7c**). Transcripts of genes (*acs*) indicative of *Methanotrichaceae*-driven acetoclastic methanogenesis didn't show abundance in *Methanotrichaceae* over incubation time (**Figures 4.7c**).

Members of the *Methanocellaceae* were the prevailing H_2-CO_2-utilizing methanogens, with the key genes involved in hydrogenotrophic methanogenesis (*fwd*, *ftr*, *mch*, *mtd*, *mer*) being most expressed by this family-level group (**Figure 4.7b,c**). The gene expression

dynamics indicative of hydrogenotrophic methanogenesis agreed well with the overall abundance dynamics of *Methanocellaceae* (**Figures 4.5b, 4.7b**).

In addition, transcripts of genes (*mtaA*, *mtaBC*, *mtbA*, *mtbBC*, *mtmBC*, *mttBC*) indicative of methylotrophic methanogenesis were detected, with *mtaBC* exhibiting the greatest transcript abundance throughout slurry incubation. The relative abundance of transcripts involved in methylotrophic methanogenesis increased from day 3 and reached first peak abundance (4.2% of total mRNA assigned to KEGG level 3 'methane metabolism') on day 11, but then decreased towards day 14 (3.6%). Thereafter, the relative expression level of this pathway increased again and reached a second peak in relative transcript abundance (8.3% of total mRNA assigned to KEGG level 3 'methane metabolism') around day 60 (**Figure 4.7a, b**). This two-peak (11 and 60 days) abundance dynamics of methylotrophic mRNA agreed well with the overall abundance dynamics of *Methanosarcina*-affiliated rRNA (**Figure 4.5a**) and mRNA (**Figure 4.5b**), in both early and late stages. Indeed, the taxonomic assignment of transcripts involved in methylotrophic methanogenesis showed that they were entirely expressed by the *Methanosarcinaceae* (**Figure 4.7c**).

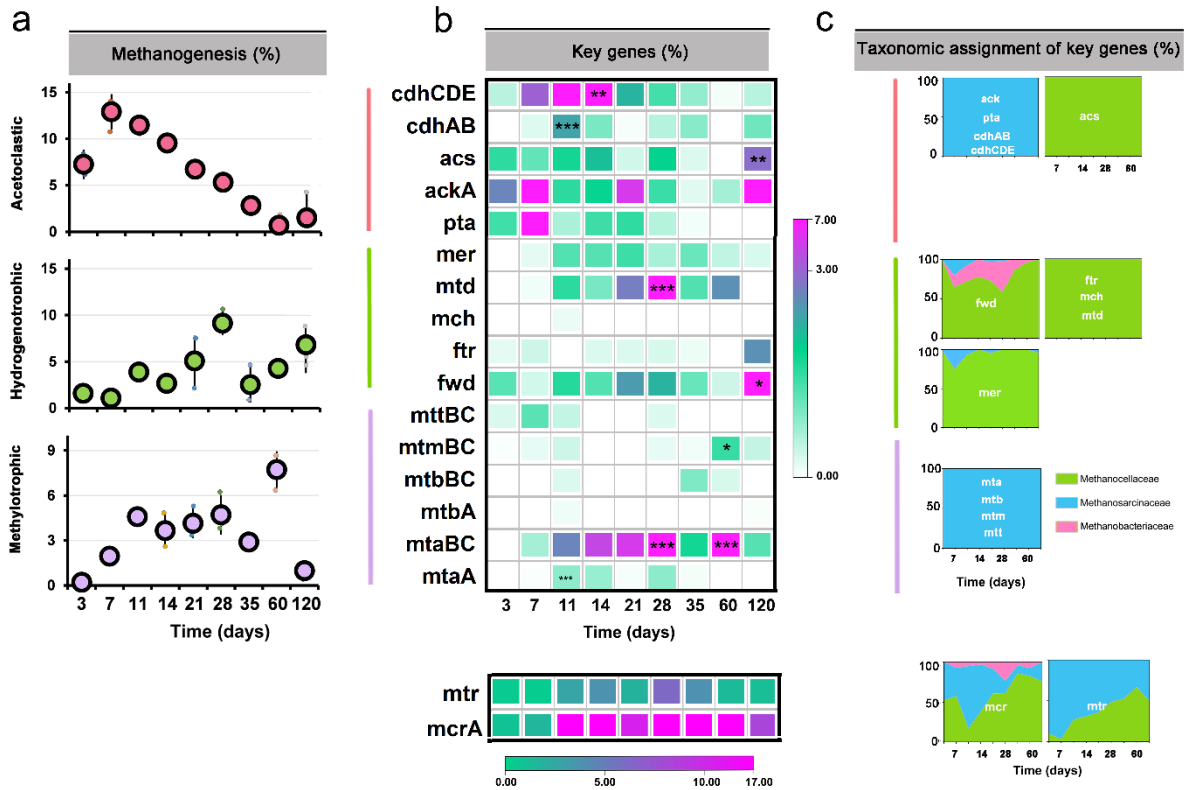

Figure 4.7: Relative mRNA abundance dynamics of individual methanogenic pathways over incubation time (a), transcript dynamics of related key pathway genes (b), and taxonomic assignment of the transcripts (c). The relative abundance values are given in relation to total mRNA affiliated to the KEGG level 3 category

'methane metabolism'. The relative expression levels were calculated based on TPM values. Data are means ± SE (n = 3). Asterisks * (P_{FDR}≤0.05), ** (P_{FDR}≤0.01), and *** (P_{FDR}≤0.001) indicate significant difference. Asterisks directly shown in the heatmap (b) indicate that in DESeq2, the mRNA abundance in that particular sampling time point significantly differed from the original abundance at the first sampling (day 3). Significance values (P_{FDR}) are only indicated for the peak transcript abundance(s) of each key pathway gene. The complete set of P_{FDR} values obtained in DESeq2 analysis for all sampling time points is shown in Table S4.7.

4.7 Competitive transcript mapping onto reference genomes

Simultaneous mRNA mapping against the composite reference genomes of *Methanosarcina* Groups I to IV revealed that the vast majority of transcripts involved in acetoclastic methanogenesis were mapped onto the genome of *Methanosarcina flavescens* (Group I), with the peak abundance on day 7. On that day, a certain number of transcripts of the acetoclastic pathway were also mapped onto the genomes of *Methanosarcina* sp. MSH10X1 (Group I) and *Methanosarcina barkeri* 3 (Group III) (**Figure 4.8a**). Transcripts involved methylotrophic methanogenesis were mapped onto the genome of *Methanosarcina thermophilia* (Group I), with the peak abundance on day 7, and *Methanosarcina barkeri* 3 (Group III) with two abundance peaks, namely on days 11 and 60. (**Figure 4.8b**).

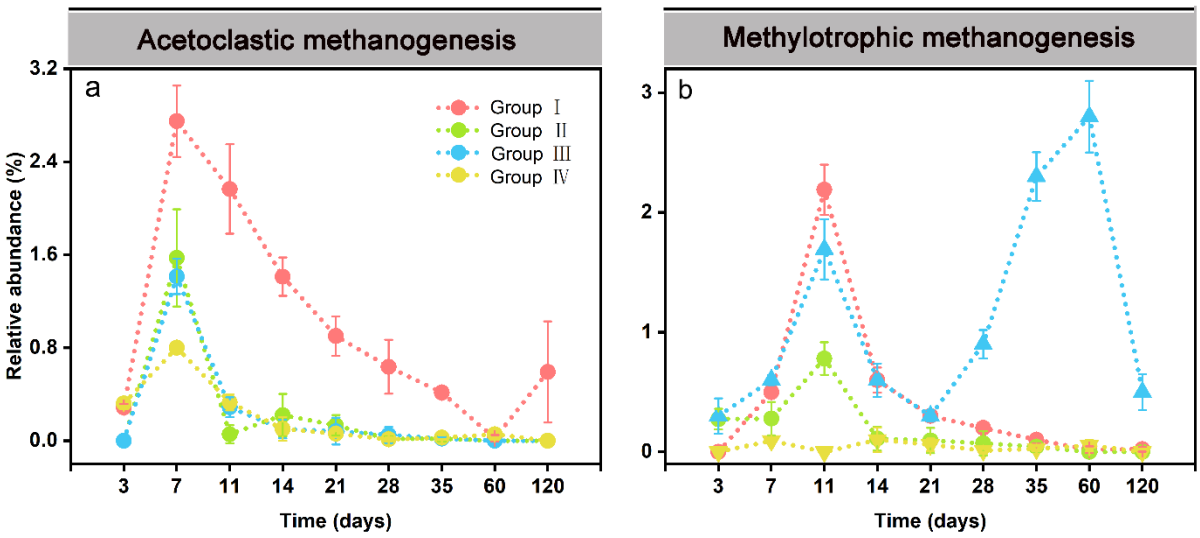

Figure 4.8: Relative transcript dynamics of acetoclastic and methylotrophic methanogen pathways inferred from transcript mapping simultaneously onto a mix of *Methanosarcina* Group I to IV reference genomes (competitive mapping approach). The relative mapping efficiencies were calculated based on TPM values. Data are means ± SE (n = 3).

4.8 *Methanosarcina* MAGs

Metagenomic sequencing yielded a total of 485,006,271reads after quality control (**Table S2.2**). The assembly of quality-filtered reads generated a total of 1,239,041contigs greater than 1,000 bp and 449,028 contigs greater than 5,000 bp. This resulted in six medium-quality metagenome-assembled *Methanosarcina* genomes, ranging in completeness from 62% to 94% (**Table S4.8**). These will be referred to as *Methanosarcina* MAGs. Three each were obtained from slurry material sampled on day 28 (MAGs_28_1;_2;_3) and day 60 (MAGs_60_1;_2;_3). Four MAGs (MAGs 28_1 and 28_2; as well as MAGs 60_2 and 60_3) shared high average nucleotide identity (ANI) values (> 98%). When compared to *Methanosarcina* genomes in GTDB, the above four MAGs shared greatest ANI values with *Methanosarcina flavescens* (89%) (**Figure 4.9**). In addition, MAG_28_3 and MAG_60_1 shared highest ANI values with *Methanosarcina barkeri* 3 and *Methanosarcina horonobensis* HB-1, respectively (86% and 85%). The inclusion of a near full-length 16S rRNA gene sequence (1,400 nt) from MAG_28_2 and MAG_60_3 in the *Methanosarcina* 16S rRNA tree confirmed that the four MAGs (MAGs 28_1 and 28_2; as well as MAGs 60_2 and 60_3) belong to *Methanosarcina* Group I and are most closely related to *Methanosarcina flavescens* (**Figure 4.10**). In addition, the *Methanosarcina* 16S rRNA tree confirmed that MAG_28_3 is affiliated to *Methanosarcina* Group IV and most closely related to *Methanosarcina horonobensis* HB-1 (**Figure 4.10**).

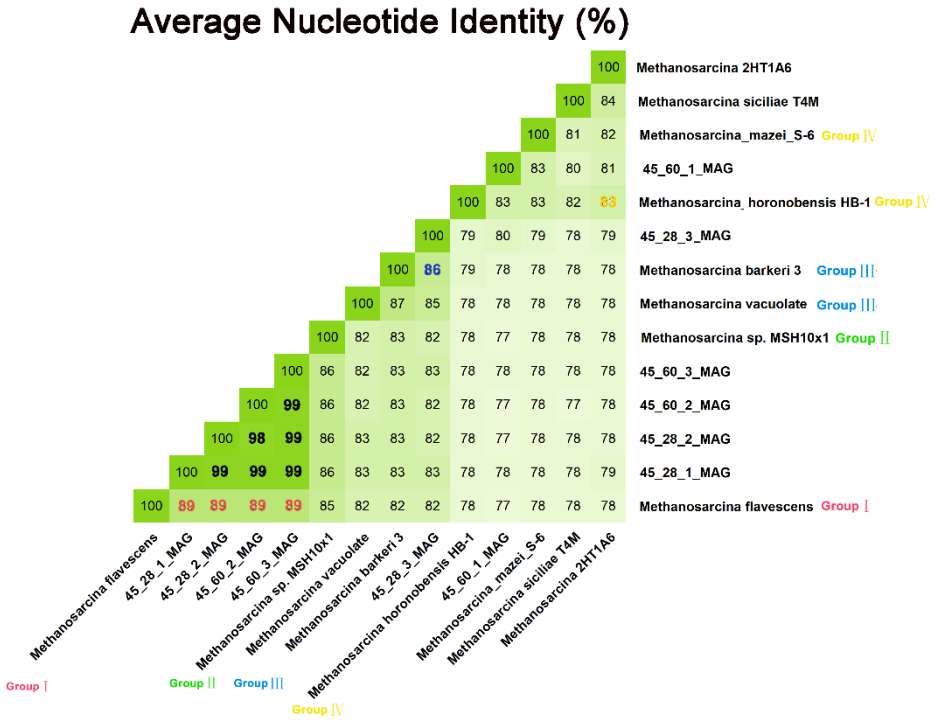

Figure 4.9: Average nucleotide identity (ANI) values calculated for *Methanosarcina* MAGs (MAGs 28_1;_2;_3 and 60_1;_2;_3) and reference genomes downloaded from GTDB.

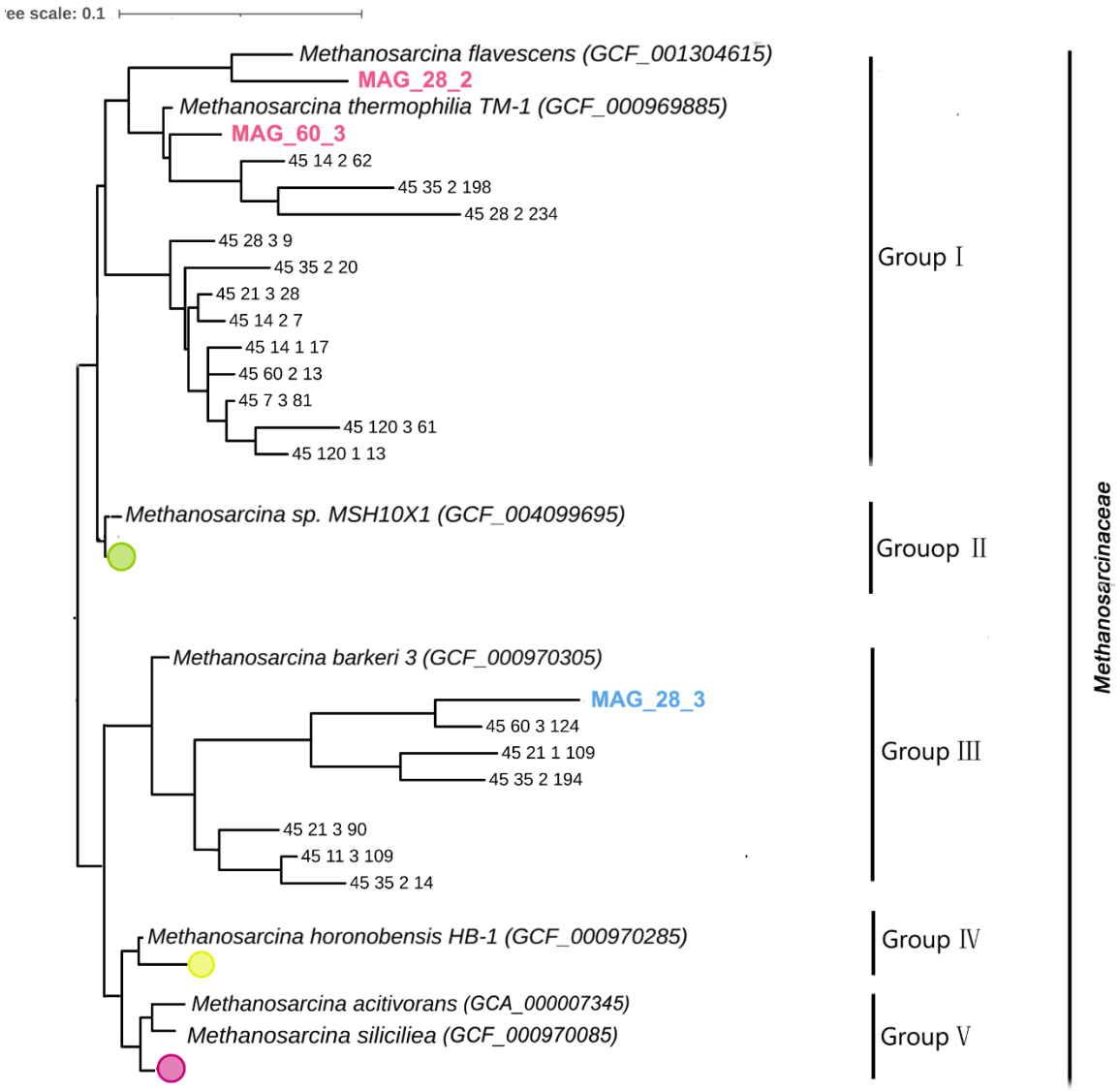

Figure 4.10: Neighbor-joining tree of 16S rRNA gene sequences from MAGs 28_1 and 28_3 as well as MAG_60_3 in relation to 16S rRNA (gene) sequences obtained in this study and *Methanosarcina* reference genomes.

5 Discussion

Microbial composition and functioning in rice field soil under anoxic conditions has been frequently studied over the last two decades using paddy soils from different geographic locations [e.g., from Italy (Conrad et al., 2009; Fey et al., 2004) and China (Peng et al., 2008; Yue et al., 2015)]. However, contrary to previous PCR-based research, our study is based on a major effort of random metatranscriptomic and metagenomic sequencing, thereby providing deeper insights into the community responses. In particular, we aimed to disentangle the structural and functional responses of paddy soil microbial communities to a long-term incubation period of 120 days under anoxic conditions. Rice straw was added to the slurries as a major source of organic matter. It is well known that rice straw addition strongly enhances CH_4 production in and emission from rice field soils (Glissmann and Conrad, 2000; Peng et al., 2008; Liu et al., 2014). Our study revealed distinct successional changes of methanogens over incubation time, which will be discussed in greater detail in the following text.

5.1 The methanogenic community responses to mesophilic temperature

5.1.1 Linking metabolite turnover with methanogen dynamics

Typical intermediates (i.e., acetate, propionate, butyrate) of the methanogenic food chain transiently accumulated and were then consumed fast. Acetate is the most abundant intermediate during the anaerobic organic matter breakdown (Fey and Conrad, 2000; Glissmann and Conrad, 2000). Generally, it is the direct substrate of acetoclastic methanogens, including *Methanosarcinaceae* and *Methanotrichaceae* (Chin et al., 1999; Fey and Conrad, 2000; Lueders and Friedrich, 2000). The transient accumulation of acetate with highest peak concentration on day 7 followed by its fast methanogenic consumption was closely linked to the increase in both the activity (defined by increased mRNA abundance) of *Methanosarcinaceae* (days 7 to 14, **Figure 3.5b**) and the CH_4 production rate (days 11-21, **Figures 3.5b and 3.1d**). Thereafter, the decline in *Methanosarcinaceae*'s activity (days 14 to 28, Fig. 3) corresponded well to a transient decrease in CH_4 production (days 21 to 28, **Figure 3.1d**).

Propionate and butyrate are the two next important intermediates of organic matter conversion under anoxic conditions (Krylova et al., 1997). Acetate, H_2, and CO_2 generated by syntrophic conversion of propionate and butyrate are able to feed acetoclastic and hydrogenotrophic methanogens. The process is highly endergonic under standard conditions

(G°= +76.1 kJ/mol), but it can be accomplished by syntrophy with an H_2-utilizing methanogen, which maintains a low H_2 partial pressure (Schink and Stams, 2002). The rapid consumption of butyrate between days 7 and 11 (**Figure 3.1b**) corresponds well to the initial activity increase of H_2-utilizing *Methanocellaceae* (**Figure 3.5b**). The net consumption of propionate from day 14 towards day 28 indicates that in addition to butyrate, propionate fuels acetoclastic methanogenesis (**Figure 3.1c**).

5.1.2 Composition and activity dynamics of the bacterial community

The bacterial community anaerobically degrades organic matter to yield the main methanogenic precursors including acetate, propionate, butyrate, H_2, and CO_2. Like methanogens, the bacterial community composition and activity also showed successional changes during the subsequent stages of organic matter decomposition (**Figure 3.3**). The *Geobacteraceae* family comprises members able to operate various anaerobic energy-yielding pathways: fermentation, syntrophic degradation of fermentation intermediates, and anaerobic respiration. The peak abundances of *Geobacteraceae* at days 7 (**Figure 3.3a,b**) relate well to the initial reductive phase of rice straw degradation, which is characterized by the limited availability of alternative electron acceptors (Achtnich et al., 1995; Chidthaisong and Conrad, 2000). Collectively, these organisms are able to use a large variety of electron acceptors, including nitrate, nitrite, nitrous oxide, Fe(III), sulfur, fumarate and malate (Straub and Buchholz-Cleven, 2001). In anoxic rice field soil, alternative electron acceptors are completely exhausted during the first few days upon flooding. In addition, it has been revealed that *Geobacteraceae* can be involved in the syntrophic conversion of butyrate (Li et al., 2014). Linking butyrate turnover with the dynamics of *Geobacteraceae*, it is reasonable to propose that *Geobacteraceae* is responsible for the syntrophic oxidation of butyrate. Moreover, the mRNA dynamics of *Geobacteraceae* corresponded exactly to those of the *Methanosarcinaceae* and *Methanotrichaceae* (**Figure 3.5b**). A possible explanation for this might be that *Geobacteraceae*, *Methanosarcinaceae*, and *Methanotrichaceae* be involved in the direct interspecies electron transfer (DIET). Certain methanogens, including *Methanosarcina* and *Methanothrix* species, are capable of directly accepting electrons from *Geobacteraceae* members for the reduction of carbon dioxide to methane, having been demonstrated as DIET (Rotaru et al., 2013, 2014). Members of the *Peptococcaceae* are considered as possible candidates for the syntrophic conversion of propionate (de Bok et al., 2001) and were previously detected with high abundance in paddy soil (Lueders et al., 2004; Gan et al., 2012;

Wegner and Liesack, 2016; Peng et al., 2018). A perfect correspondence between the propionate turnover and the mRNA dynamics of both *Peptococcaceae* and *Methanocellaceae* suggests that *Peptococcaceae* members were the major players in the syntrophic propionate conversion (**Figures 3.1c, 3.3d, and 3.5b**).

Previous studies have shown that changes in the chemical composition of straw affects structure and functioning of the decomposing bacterial community. For example, it was found that litter quality explained 16% of the variation in bacterial community composition (Cleveland et al., 2014). It has been observed that glycosyl hydrolase transcripts involved in cellulose and chitin breakdown were predominantly expressed by the phylum *Firmicutes*, whereas those involved in hemicellulose breakdown exhibited more diverse taxonomic sources, including the phyla *Acidobacteria*, *Bacteriodetes*, and *Chloroflexi* (Wegner and Liesack, 2016). *Clostridiaceae* presumably acted as primary fermenters, resulting in the temporary accumulation of short chain fatty acids (Glissmann and Conrad, 2002). Propionate and butyrate that transiently accumulated during the first 14 days were observed in our study (Fig. 1). The breakdown of complex polymer substances was increasingly the rate-limiting step in microbial activity after two weeks, with the easily degradable compounds becoming exhausted (Glissmann and Conrad, 2002). This may explain the peak abundance of *Clostridiaceae* at day 21, given that CAZymes were dominantly expressed by the *Firmicutes* (**Figure 3.4b**). Presence of the *Lachnospiraceae* with peak abundances at day 28 reflects its ecophysiology. Members of the *Lachnospiraceae* are known as homoacetogens (Gagen et al., 2010) and to be involved in biopolymer breakdown (Turnbaugh et al., 2009; Biddle et al., 2013). As already discussed for the *Clostridiaceae*, one reason for the strong increase in the relative abundance of the *Lachnospiraceae* from days 21 to 28 may be that the breakdown of complex polymer substances became the rate-limiting step in microbial activity, making the members of this family more competitive in the paddy soil. Organisms of *Anaerolineaceae* (within the phylum *Chloroflexi*) were dominant, indicating that their syntrophic cooperation with *Methanothrix* spp. may be involved in the process of methanogenic degradation of alkanes (Liang et al., 2015). *Acidobacteriaceae* as the major functional bacteria would have not only played an important role in the process of fermentation and also to be able oxidize alkanes, thereby leading to the release of small molecules like formate, acetate, hydrogen, carbon dioxide (Liang et al., 2015; Sun et al., 2016; McIlroy et al., 2017). According to previous research (Cantarel et al., 2009; Ward et al., 2009; Rawat et al., 2012), members of the *Acidobacteriaceae* habor a large number of genes associated with the breakdown of plant polysaccharides and the degradation or synthesis of microbial polysaccharides. The rRNA and mRNA abundance increase of

Anaerolineaceae and *Acidobacteriaceae* in the late stage may indicate that members both phyla have been involved in the decomposition of more recalcitrant biopolymer (**Figure 3.3c,d**).

5.1.3 Composition and activity dynamics of the methanogenic community

The dominant methanogen groups were – in the order of abundance - *Methanosarcinaceae*, *Methanocellaceae*, and *Methanotrichaceae*. This is in good agreement with previous studies on the composition of microbial communities in rice field soils from the Philippines (Breidenbach and Conrad, 2015; Liu et al., 2018b), Italy (Weber et al., 2001a; Conrad and Klose, 2006; Wegner and Liesack, 2016) and Asia (Sugano et al., 2005; Peng et al., 2008; Yue et al., 2015; Bao et al., 2016). Our study identified three successional stages defined by two activity peaks separated by an intermittent decrease of methanogenic activity (**Figure 3.5**). Methanogenic archaea obtain energy for growth by converting C1 and C2 compounds, including CO_2, formate, acetate, ethanol, methanol, and other methylated compounds, to methane (Garcia et al., 2000; Liu and Whitman, 2008; Evans et al., 2019). Accordingly, the succession of methanogen guilds is due to changes in available substrates and their utilization for energy conservation. *Methanosarcinaceae* were the first methanogens to be stimulated in response to substrates (acetate) released by the anaerobic bacterial degradation of rice straw and may be considered early- or rapid-responding methanogens (**Figures 3.1a and 3.5b**). With the ongoing anaerobic degradation of complex carbon, the activity of *Methanocellaceae* as intermediate responders is stimulated, primarily due to their role as syntrophic methanogen partner in the bacterial conversion of propionate to acetate, H_2, and CO_2 (**Figures 3.1c and 3.5b**)

Methanosarcinaceae and *Methanotrichaceae* are an excellent example of how two family-level groups compete for the same substrate. *Methanosarcinaceae* was prevailing in acetoclastic methanogenesis at relatively high acetate concentrations, but after acetate declined to a very low level, the late-responding *Methanotrichaceae* significantly increased in competitiveness and acetoclastic activity (**Figures 3.1a and 3.5b**). The mRNA abundance of *Methanosarcinaceae* and *Methanotrichaceae* were in accordance with transcripts indicative of actoclastic methanogenesis (**Figure 3.5b**). With a higher maximum rate of acetate utilization and maximum growth rate ($Y * k$), a higher half-saturation coefficient (KS), and a higher yield coefficient compared with *Methanotrichaceae*, elevated acetate concentrations are favorable for growth and activity of *Methanosarcinaceae*. By contrast, *Methanotrichaceae* are superior at low acetate concentrations due to the investment of energy to activate acetate, thereby leading to a lower k and KS (Conklin et al., 2006; Großkopf et al., 1998a; Jetten et al., 1992).

These results are consistent with the concept that both substrate availability and substrate concentration (threshold concept) are key factors controlling structure and function of methanogenic communities.

A transient activity decline around day 28 was observed not only in the absolute abundance of biomarkers but also in the metatranscriptome analysis (**Figures 3.2 and 3.5**). One possible driving factor for this activity pattern is substrate availability and concentration. Previous research has shown that the hydrolytic release of labile compounds occurs over the first four weeks much faster than recalcitrant compounds; with the latter having a longer residence time (Fey and Conrad, 2000; Glissmann and Conrad, 2002). The transition from the degradation of labile organic matter to the decomposition of recalcitrant C compounds may lead to a temporary decline in the community activity around day 28 until critical sizes of substrate pools and functional populations are re-established, thereby leading to the second activity peak during the late stage. Furthermore, a shift in the microbial colonization from rice straw to bulk soil may be another reason for the intermittent decline in microbial activity around day 28. The organic matter in our anaerobic microcosms include two pools: rice straw and the organic matter in bulk soil. The study by Wegner and Liesack (2016) revealed *Clostridiaceae* to act as primary fermenters. Indeed, they primarily colonized rice straw during the first 7 days but then declined in abundance on rice straw from day 14 onwards, while their abundance greatly increased in bulk soil between days 14 and 28. Thus, it is reasonable to assume that microorganisms attached to the rice straw surface are released to the bulk soil due to the gradual degradation of certain straw fractions.

5.1.4 Characterization of dominant *Methanosarcina* populations

The intra-family analysis of *Methanosarcinaceae* identified four distinct populations, with the Group II population prevailing over the complete 120-day incubation period (**Figure 3.6**). This implies that the same methanogen population with close affiliation to *Methanosarcina* sp. MSH10X1 dominated *Methanosarcinaceae* during the early and late activity stages (**Figures 3.5 and 3.6**). The cutoff of 93% and 75% in ANI values are generally considered as species and genus demarcation, respectively (M. Kim et al., 2014). Thus, the ANI values of around 95% among our *Methanosarcina* MAGs suggest they belong to the same species. The highest ANI value between *Methanosarcina* MAGs and *Methanosarcina* sp. MSH10X1 (around 85%) indicates that they represent different species of the same genus (**Figure 3.8a**). Phylogenetic analysis of the 16S rRNA gene located on the *Methanosarcina* MAG "Day-21" and representative full-length 16S rRNA sequences assembled from our metatranscriptomic

datasets further confirmed that the *Methanosarcina* MAGs obtained from Philippine paddy soil slurries during mesophilic incubation are closely affiliated to *Methanosarcina* sp. MSH10X1, thereby providing further evidence for the dominant role of the *Methanosarcina* Group II population (**Figure 3.9**).

Microbes compete for limited nutrients and space with various species in their surrounding (Ghoul and Mitri, 2016). Competition strategies affect their functional role in the microbial ecosystem. Given the metabolic potential of different *Methanosarcina* species, they overlap in their capacity to utilize the same substrates (i.e., acetate, methanol, CO_2 and H_2). However, *Methanosarcina* Group II was the most competitive population among the four distinct *Methanosarcina* populations detectable over the 120-day incubation period. Thus, the unambiguous reason for the prevailing role of the Group II population in our study remains elusive, but its predominant activity may be generally explained by the following considerations. On the one hand, increased nutrients utilization by altering metabolic activity and thus improving growth rate is known to be one of the effective competitive strategies. This may involve a higher affinity to particular substrates than competitors (Pfeiffer et al., 2001; MacLean and Gudelj, 2006). The upregulation of key genes of multiple methanogen pathways by the Group II population may have allowed its members to utilize a broader spectrum of substrates. Moreover, the high proportion of unique genes in the *Methanosarcina* MAGs revealed great variations in the genetic potential related to the KEGG level 2 categories "processing" as well as "carbohydrate, amino acid, and energy metabolisms". This may imply higher growth dynamics compared with the other *Methanosarcina* populations due to faster nutrient utilization (**Figure 3.10, Table S3.11**). On the other hand, microbes also compete for prime locations within a niche (W. Kim et al., 2014). This can be accomplished either by rapidly colonizing unpopulated spaces or by killing or pushing out already colonized cells (Bucci et al., 2011). Indeed, KEGG annotation of our *Methanosarcina* MAGs revealed the genetic potential to produce type IV pili, to form biofilms and to produce antimicrobials, all of which could help the Group II population to access new niches due to enhanced motility and to protect themselves from environmental hazards and inhibition of their competitors.

5.1.5 Expression of methanogenic pathways by *Methanosarcinaceae*

Methanosarcina species are the metabolically most versatile methanogens and have a broad substrate spectrum (acetate, methanol, CO_2 and H_2). They can utilize all the methanogenic substrates discussed above (except formate) and operate all three traditionally known methane production pathways (acetoclastic, hydrogenotrophic, and methylotrophic methanogenesis)

(Embree et al., 2015). Our mRNA expression analysis of key genes involved in the expression of these three methanogenesis pathways by *Methanosarcinaceae* confirmed their broad substrate spectrum for methane production (**Figure 3.7b**). Previous studies have demonstrated that acetoclastic methanogenesis is the major methane production pathway in *Methanosarcinaceae*. Indeed, we observed a high expression level of key genes (*ack*, *pta*, and *cdhA-E*) related to acetoclastic methanogenesis in *Methanosarcinaceae* (**Figure 3.7b**). The expression of *ack* and *pta* reached their peak abundance in the early stage, while their transcripts were detected only on a low level in the late stage. Oviously, acetoclastic methanogenesis was the major functional pathway of the *Methanosarcinaceae* in the early stage (**Figure 3.7a**). The competitive mapping results confirmed the major role of acetoclastic methanogenesis in *Methanosarcina* populations (including Group I, II, and IV) during the early stage (**Figure 3.13a**).

However, contrary to our expectation, we also detected the expression of key genes encoding methylotrophic methanogenesis *(mta*, *mtb*, *mtm* and *mtt*); but in particular transcripts of *mtaBC* (accounting for 0.8% to 5.2% of total mRNA affiliated to the KEGG level 3 category 'methane metabolism'), whose enzyme products are highly indicative of methanol-dependent methanogenesis (**Figure 3.7b**). The transcripts involved in methylotrophic methanogenesis were affiliated with *Methanosarcinaceae* and their greatest expression level agreed largely with the two activity peaks of *Methanosarcinaceae* (**Figures 3.7c and 3.5b**). According to our findings, it is reasonable to conclude that *Methanosarcinaceae* produce CH_4 via both acetoclastic and methylotrophic methanogenesis in Philippine paddy soils during long-term incubation under anoxic conditions. The competitive mapping approach resulted in the mapping of nearly all methylotrophic mRNA to the Group II representatives. It implies that *Methanosarcina* Goup II population was the major player of methylotrophic methanogenesis in our study (**Figure 3.13b**). Moreover, the detection of the genes encoding methylotrophic methanogenesis in our *Methanosarcina* MAGs also verified the above results (**Figure 3.12**). Previous research has actually shown that methanol and trimethylamine are more preferred substrates for *Methanosarcina* strain MSH10X1 than other methylated compounds, H_2/CO_2, and acetate, thereby resulting in the greatest methane yield (Mehta et al., 2021). This research finding agrees well with our detection of *Methanosarcina* Group II population being most competitive under methylotrophic methanogenesis conditions. It also needs to be noted that the expression dynamics of the acetoclastic and methylotrophic pathways by the Group II population strongly differ over the 120-day incubation period (**Figures 3.7 and 3.13)**. This provides strong evidence that the methylotrophic pathway plays a major metabolic role for the

Methanosarcina Group II population in Philippine paddy soil, rather than only to be co-expressed with the acetoclastic pathway.

Although methylotrophic methanogenesis is common in nature such as, for example, marine sediments, mangroves, or other sulfate-enriched environments (Strąpoć et al., 2008; Carr et al., 2018; Lyu et al., 2018; Zhang et al., 2020), the role of methylotrophic methanogenesis in rice field soil has not yet been highlighted. Methylotrophic methanogenesis was believed to contribute less than 5% to methane production in anoxic environments (Lovley and Klug, 1983). The ^{13}C-isotope labeling experiment by Conrad and Claus (2005) indicated that methanol-derived methane was only marginal in Italian rice field soil. However, studies have revealed that distinct microbial communities and functional processes most likely relate to different soil properties (including C/N content, humic acids, pH value, vegetation, etc.). The Philippine paddy soil contains higher contents of carbon (C) and nitrogen (N) than the Italian rice field soil (**Table S3.15**) (Pump and Conrad, 2014; Liu et al., 2018b). This may be one possible explanation for the increased occurrence of methylotrophic methanogenesis in our study. In addition, the higher relative expression level of methylotrophic methanogenesis (defined as the abundance of *mtaBC* transcripts related to total mRNA affiliated to KEGG level 3 category 'methane metabolism') in Philippine paddy soil relative to the Italian rice field soil may imply a higher contribution of methanol to methane production in the Philippine paddy soil (**Table S3.16**).

The high expression level of methylotrophic methanogenesis in our study raises questions about the methane sources. In general, methanol is a product of pectin degradation and can be utilized by methanogens (Schink and Zeikus, 1980; Dittoe et al., 2020). Pectin, a complex polymer composed of galacturonic acid and rhamnogalacturonans, is a common component of plants. The pectin methylesterase acts on methoxylesters of galacturonic acid to release methanol. Various CAZyme families involved in degrading pectin, including PL1, PL4, PL11, CE1, CE8, CE12, GH16, GH28, G43 and GH53, were all expressed in our study (**Table S3.7**) (Bonnin and Pelloux, 2020). Small amounts of methanol may also be released during the decomposition of xylan (Rosell and Svensson, 1975; Pang et al., 2021) and lignin (Ander et al., 2006; Khan and Ahring, 2019; Venkatesagowda, 2019). Lignin-degrading bacteria mainly belong to three classes: *Actinomycetes*, α-*Proteobacteria,* and γ-*Proteobacteria* (Bugg et al., 2011; Huang et al., 2013). Lignin is recalcitrant during the anaerobic degradation because the anaerobic bacteria do not possess the oxidative enzymes and pathways, which are required for the initial depolymerization of lignin (Achinas et al., 2017). To degrade lignin under anoxic conditions, it has to be anaerobically depolymerized into smaller polymer units to which the

enzyme pool of the anaerobic bacteria can get access to decompose them into monomers (Ko et al., 2009). Studies of lignin degradation under anaerobic condition have revealed that the anaerobic bacteria degrade the lignin in three steps with demethoxylation as the initial step, followed by ring cleavage and fermentation leading to precursors of methanogenesis (Mechichi et al., 2005; Wu and He, 2013; Kato et al., 2015; Khan and Ahring, 2019). In addition, phylogenic analysis has shown that representatives of the *Archaea* from four phyla possess genes encoding laccases (Sharma and Kuhad, 2009). Yet the greatest numbers of strains harboring laccase genes were identified in the *Proteobacteria*, *Actinobacteria* and *Firmicutes* (Janusz et al., 2017). Although known laccases are members of the multi-copper oxidoreductases that oxidize a variety of phenolic compounds, laccase-like genes were also found in anaerobic bacteria (Ausec et al., 2011). A putative bacterial laccase gene was identified by computational analysis in the genome of *Geobacter metallireducens*, which is a strict anaerobic bacterium (Berini et al., 2018). Members of these phyla showed high abundance over incubation time (**Figures 3.3b and 3.4b**). Thus, the degradation of pectin, xylan, and lignin may at least partially explain methanol-dependent methanogenesis.

Although methanol was found to be a less important methanogenic substrate than trimethylamine, which is another substrate of methylotrophic methanogenesis in some environments (Oremland et al., 1982), it may be an important precursor in particular ecosystems. One such example is wetwood, where wood pectin is anaerobically degraded by a methanogenic community (Schink et al., 1981). Methanogens in peat soil from the Zoige wetlands were also suggested to produce CH_4 mainly from methanol (Jiang et al., 2010). In our study, while consumed by members of the *Methanotrichaceae*, acetate was detectable at low but steady-state level during the late-stage incubation period (**Figures 3.1a and 3.5b**). This may indicate that in our Philippine paddy soil slurries, the anaerobic degradation of recalcitrant compounds, such as xylan and lignin, during the late stage primarily resulted in the production of methanol and to lesser extent in the release of acetate. It has been shown that methanol is being released by demethoxylation as the initial step of anaerobic lignin degradation, and the production of acetate occurs in the subsequent ring cleavage and fermentation, which need the cooperation between acetogens and ring-cleaving fermenters (Kato et al., 2015; Khan and Ahring, 2019). Thus, acetate may not necessarily accompany the production of methanol. It may explain the low but steady-state concentration of acetate during the late stage and, at least on the mRNA level, the presence of both acetoclastic and methylotrophic pathways.

5.2 The methanogenic community responses to moderately thermophilic temperature

Microbial community responses to increasing temperatures can be quite complex (Roussel et al., 2015). Temperature not only regulates each individual process by affecting the underlying thermodynamics and kinetics, but also affects population dynamics and the structuring of the entire microbial community (Conrad, 2008). The influence of two contrasting temperatures (30 ℃ and 45 ℃) on the anaerobic food chain was investigated in this study. The mesophilic temperature (30 °C) represents the present-day conditions in most rice paddies, while the moderately thermophilic temperature (45 °C) represents a near-future scenario that may occur in various tropical and subtropical rice paddies due to global warming. Our study revealed that both structural and functional dynamics of the methanogenic community differed between the mesophilic and moderately themophilic incubations.

5.2.1 Moderately thermophilic bacteria

The structure and function of the bacterial community displayed significant changes in response to the rising temperature. Compared with the mesophilic temperature, *Heliobacteriaceae* replaced *Geobacteraceae* to become the dominant bacterial population at moderately thermophilic temperature (**Figure 4.3**). Elevated temperature (45°C) has been reported to favor the proliferation of the *Heliobacteriaceae* in certain soils (Liu et al., 2018b; Peng et al., 2018). *Helicobacteraceae* may be involved in the anaerobic oxidation of propionate, possibly even acetate (Noll et al., 2010; Sattley and Madigan, 2014; Liu et al., 2018b; Peng et al., 2018). In addition, members of the *Thermoanaerobacteraceae* have been identified as being responsible for syntrophic acetate oxidation (Liu and Conrad, 2010; Liu et al., 2018b; Peng et al., 2018). If acetoclastic methanogenesis can't be performed in a methanogenic system as, for example, in Italian rice field soil at moderately thermophilic temperature, acetate utilization by syntrophic bacteria is the only possibility to oxidize acetate, which is syntrophically coupled to H_2-utilizing methanogens. In contrary, our study revealed high activity of acetoclastic methanogenesis in the Philippine paddy soil at moderately thermophilic temperature, but only low transcript level of mRNA affiliated to the *Thermoanaerobacteraceae*. Obviously, the syntrophic acetate oxidizers observed in Italian rice field soil were replaced by moderately thermophilic acetoclastic methanogens in the Philippine paddy soil (**Figure 4.3b**). Given this result, the *Heliobacteriaceae* were more likely involved in the syntrophic oxidation of propionate, rather than the syntrophic conversion of acetate.

Temperature significantly affects polymer breakdown in rice field soil by changing both the structure and the function of bacterial communities. The phylum-level analysis of CAZyme transcripts showed significantly differing taxonomic patterns between 30 °C and 45 ℃

(**Figures 3.4b and 4.4b**). The *Firmicutes* were the sole and predominant group over the complete incubation period at 45 °C (**Figures 4.4b**). This is in clear contrast to the mesophilic approach, at which members of multiple bacterial phyla (*Firmicutes* together with *Proteobacteria, Actinbacteria, Chloroflexi, Acidobacteria,* and *Planctomycetes*) were abundant over the complete incubation period time (**Figures 3.4b**). In addition, elevated temperature is known to increase the enzymatic activity, which is well reflected by the CAZyme transcript abundance that was significantly increased at 45 °C in Italian rice field soil (Peng et al., 2018). The relative abundances of transcripts encoding cellulases as well as alpha- and beta-glactosidases were greatest at day 60 and clearly higher than during the 30°C-incubation (**Figures 3.4a and 4.4a**). This implies that relative to the mesophilic temperature, the late-stage degradation of recalcitrant compounds, including lignin and lignocellulose, was strongly increased at the moderately thermophilic temperature. As discussed above, lignin degradation is one possible source of methanol to feed methylotrophic methanogenesis.

5.2.2 Moderately thermophilic methanogens

The moderately thermophilic methanogen community was composed of both acetoclastic *Methanosarcina* spp. and hydrogenotrophic *Methanocella* spp.; however, members of the *Methanotrichaceae* had vanished at 45 °C (**Figure 4.5**). The increasing mRNA abundance of *Methanosarcinaceae* (days 7-14, **Figure 4.5b**) was closely linked to a rapid consumption of acetate (days 7-14, **Figure 4.1a**) and an increase in the CH_4 production rate (days 14-28, **Figure 4.1d**). Thereafter, the gradual decline in *Methanosarcinaceae'*s mRNA abundance (days 14 to 120, **Figure 4.5b**) corresponded well to a transient decrease in CH_4 production (days 28 to 35, **Figure 4.1d**). Despite the presence of acetate in a low but detectable level (around 0.6 mM, **Figure 4.1a**), acetoclastic methanogenesis was not active after day 60 (**Figure 4.7a**). Thus, acetate was presumably utilized by members of the *Thermoanaerobacteraceae* through syntrophic acetate oxidation (**Figure 4.3b**). Earlier research has shown that syntrophic acetate oxidation is favored at low acetate concentrations, while acetoclastic methanogenesis is favored at high acetate concentrations under thermophilic conditions (Zinder and Koch, 1984). The mRNA dynamics of the H_2-utilizing *Methanocellaceae* between days 21 and 120 with a peak abundance at day 35 (**Figure 4.5b**) corresponds well to the rapid consumption of propionate (days 14-21) and its steady-state concentration between 0.3 and 0.5 mM during the late-stage incubation, thereby suggesting a balance between production through fermentative processes and consumption by syntrophic propionate oxidation (**Figure 4.1b**). The ongoing propionate oxidation may have replenished the low but detectable acetate pool. Thus, the

syntrophic oxidation of both propionate and acetate agrees well with the ongoing activity of H_2-utilizing *Methanocellaceae* (**Figure 4.5**) and the ongoing CH_4 production during the late-stage incubation until day 120 (**Figure 4.1d**). Previous studies have addressed that temperature may influence the relative contribution of acetoclastic and hydrogenotrophic methanogenesis to methane production. The methanogen community is usually composed of both acetoclastic (*Methanosarcinaceae*, *Methanotrichaceae*) and hydrogenotrophic (*Methanocellaceae*, *Methanobacteriaceae*) taxa within a temperature range of 4 to 40 °C (Oren, 2014), but the relative contribution of hydrogenotrophic methanogenesis has been found to increase with rising temperature (Schulz and Conrad, 1996; Glissman et al., 2004; (Fey and Conrad, 2000). Above a soil temperature above 40°C (actually 40 to 50 °C), hydrogenotrophic methanogens prevailed as the sole methanogen group in various Chinese and Italian paddy soils (Conrad et al., 2009; Liu et al., 2018b; Peng et al., 2018). However, certain paddy soil are known to contain moderately thermophilic acetoclastic methanogens (Wu et al., 2006). In such soils, the active methanogenesis pathways do not change significantly with temperature rise above 40 °C (Liu et al., 2018b, 2019) and both acetoclastic and hydrogenotrophic methanogenesis operate at the common ratio (Conrad, 2020b). Our results are in good agreement with those paddy soil studies that revealed the presence of moderately thermophilic *Methanosarcinaceae*, thereby explaining that acetoclastic methanogenesis majorly contributed to methane production in Philippine rice field soil at 45 °C. By contrast, members of the *Methanotrichaceae* were strictly mesophilic and did not contribute to acetoclastic methanogenesis at 45 °C. This finding is consistent with the results of previous studies (Conrad et al., 2009; Liu et al., 2018b, 2019).

The intra-family analysis of *Methanosarcinaceae* identified five distinct populations with varying mRNA abundances during the 120-day incubation period (**Figures 4.6 and 4.8**). *Methanosarcina* populations (I to III) displayed similar dynamics until day 11. Later (days 11 to 120), mRNA transcripts indicative of acetoclastic methanogenesis were predominated by *Methanosarcina* Group I population, while those indicative of methylotrophic methanogenesis were only affiliated to *Methanosarcina* Group III population. This implies that multiple methanogen populations contributed to CH_4 production during the 120-day incubation period (**Figure 4.8**). Furthermore, the ANI values among our *Methanosarcina* MAGs suggest taxonomic differentiation at the species level. The ANI values among four *Methanosarcina* MAGs (MAGs 28_1 and 28_2; as well as MAGs 60_2 and 60_3, ANI > 98%) and the highest ANI value between these four MAGs and *Methanosarcina flavescens* (around 89%) indicate that they belong to the same species closely affiliated to *Methanosarcina* Group I (**Figure 4.9**). In addition, MAG_28_3 and MAG_60_1 shared highest ANI values with *Methanosarcina*

barkeri 3 (*Methanosarcina* Group III) and *Methanosarcina horonobensis* HB-1 (*Methanosarcina* Group IV), respectively (86% and 85%) (**Figure 4.9**). Phylogenetic analysis of the 16S rRNA genes located on MAG_28_2 and MAG_60_3 and representative full-length 16S rRNA sequences assembled from our metatranscriptomic datasets further confirmed that the *Methanosarcina* MAGs (MAGs 28_1 and 28_2; as well as MAGs 60_2 and 60_3) obtained from Philippine paddy soil are closely affiliated to *Methanosarcina flavescens* (**Figure 4.10**). Similarly, phylogenetic analysis of the 16S rRNA gene located on MAG_28_3 and representative full-length 16S rRNA sequences assembled from our metatranscriptomic datasets further confirmed that *Methanosarcina* MAG (MAGs 28_3) is closely affiliated to *Methanosarcina barkeri* 3 (**Figure 4.10**). Thereby, these results provide further evidence that in our study, the *Methanosarcina* Group I and III populations predominate at 45 ℃ (**Figure 4.6**). By contrast, the *Methanosarcina* Group II population (*Methanosarcina* sp. MSH10X1) was solely predominant during the whole incubation period at 30 ℃. It has previously been shown that elevated temperature may dramatically change structure and activity of the methanogenic community (Liu et al., 2018b, 2019; Peng et al., 2018; Chen et al., 2022). The adjustments in soil microbial structure and function to temperature change may involve acclimation (i.e., physiological responses of individuals), adaptation (i.e., genetic variation within species) and/or species turnover (i.e., shifts in the species composition of the community) (Bradford, 2013; Karhu et al., 2014; Wei et al., 2014). *Methanosarcina* sp. MSH10X1 (*Methanosarcina* Group II population) is able grow between 5 °C and 40 °C with the optimal temperature being 37 °C (Mehta et al., 2021). Some other species of the family *Methanosarcinaceae* are moderately thermophilic microorganisms. The optimal growth temperature of *Methanosarcina flavescens* (*Methanosarcina* Group I) is reported to be around 45 °C (Kern et al., 2016). Another member of *Methanosarcina* Group I, *Methanosarcina thermophila* TM-1, is known as thermophilic methanogen with a temperature optimum for methanogenesis near 50°C and growth at 55°C (Zinder and Mah, 1979). Earlier research has shown that members of *Methanosarcina barkeri* (*Methanosarcina* Group III) grow most rapidly at 37 to 42 °C (Maestrojuan' and Boone, 1991). Thus, the temperature preferences of the *Methanosarcina* Group I and III populations explain well the abundance and activity shifts among *Methanosarcina* after rise of the temperature from 30 ℃ to 45 ℃.

Furthermore, the mRNA expression analysis of key genes involved in the dominant methanogenesis pathways (i.e., acetoclastic, hydrogenotrophic, and methylotrophic methanogenesis) further confirmed the functional role of the methanogen community in Philippine paddy soil under moderately thermophilic condition. High expression of key genes

(*ack*, *pta* and *cdhA-E*) related to acetoclastic methanogenesis by *Methanosarcinaceae* was observed (**Figure 4.7b,c**). The mRNA expression of the acetoclastic pathway reached its peak abundance in the early stage (around 7 days) followed by a steady mRNA abundance decline until 120 day; thus indicating that acetoclastic methanogenesis was the major functional pathway in *Methanosarcinaceae* during the early stage, but was operated only on low level during the late stage (**Figure 4.7a**). The competitive mapping results confirmed the major role of acetoclastic methanogenesis in *Methanosarcina* populations during the early stage, with Group I, II, III and IV contributing collectively to this activity (**Figure 4.8b).** Furthermore, the high relative expression level of key genes encoding methylotrophic methanogenesis, including *mta*, *mtb*, *mtm*, *mtt* and in particular *mtaBC*, revealed that methylotrophic methanogenesis was a major pathway to produce CH_4, in addition to acetoclastic methanogenesis. Like observed for the mesophilic approach, the transcripts involved in methylotrophic methanogenesis were affiliated with *Methanosarcinaceae*. However, contrary to the mesophilic conditions, the competitive mapping approach resulted in the mapping of nearly all methylotrophic mRNA to the Group I and III representatives, and only few methylotrophic mRNA transcripts were mapped onto the genome of the Group II population after the incubation under moderately thermophilic conditions. This mapping result further corroborates that at 45 °C, methylotrophic methanogenesis was predominantly performed by *Methanosarcina* Group I and III populations; contrary to the Group II population at 30 °C (**Figure 4.6b**). Methane production was exclusively dominated by methylotrophic methanogenesis during the late stage, with the *Methanosarcina* Group III population having its greatest mRNA peak abundance at day 60 (**Figures 4.6a and 4.7b**).

5.3 Conclusions

Understanding the sources and controls of microbial methane production and the response mechanisms of methanogenic communities in rice field soils is critical for modeling predictions of global methane emission. Metatranscriptomics, coupled in part with metagenomics, provided more detailed insights into the role and dynamics of key functional guilds participating in the methanogenic organic matter breakdown in Philippine paddy soil when compared to previous research. Particular links between the active microbial community members and their potential functions could be revealed. Our transcript analysis provided evidence that methylotrophic methanogenesis in the family *Methanosarcinaceae* occurs in flooded rice field soils, in addition to acetoclastic methanogenesis. Given the substrate specificity of MtaBC, the methylotrophic activity is most likely driven by methanol, rather than

other methylated compounds. Another major finding is that the expression of the methanogenesis pathways didn't significantly differ between mesophilic (30 °C) and moderately thermophilic (45 °C) temperature. All three traditionally known pathways, i.e., acetoclastic, hydrogenotrophic and methylotrophic methanogenesis, were active at both temperature regimes. However, the intra-family analysis of *Methanosarcinaceae* revealed that different *Methanosarcina* populations became active at either 30 °C or 45 °C. Likewise, structure and activity of the bacterial community differed between 30 °C and 45 °C. The phylum-level analysis of CAZyme transcripts showed significantly differing taxonomic patterns between 30 °C and 45 °C. The *Firmicutes* were the sole and predominant group over the complete incubation period at 45 °C. This is in clear contrast to the mesophilic approach, at which members of multiple bacterial phyla (*Firmicutes* together with *Proteobacteria, Actinbacteria, Chloroflexi, Acidobacteria,* and *Planctomycetes*) were abundant over the complete incubation time period. In addition, the syntrophically propionate-oxidizing bacteria differed between 30 °C and 45 °C. Thus, a more systemic understanding of the temperature-affected functional links between the bacterial and methanogenic community dynamics was gained in this study. In conclusion, the detection of methylotrophy, in addition to the occurrence of acetoclastic and hydrogenotrophic methanogenesis, is a major new finding showing that the methanogenic community responses to straw fertilization in flooded rice field soils are more complex than previously thought. The temperature rise significantly affected the community structure of both bacteria and methanogens, but had no major impact on the methanogenesis pathways being expressed.

5.4 Final critical remarks

The findings presented in our study highlight that high-throughput sequencing approaches, such as metagenomics and metatranscriptomics, allow us to generate and test ecological hypotheses (Jansson and Prosser, 2013). Unfortunately, meta-omic studies are strongly impaired by low assignment efficiencies of datasets affiliated to uncultured groups. Moreover, the taxonomic assignment of mRNA sequences could be biased towards the publicly available genomes. One possible solution may be to increase isolation efforts, especially for members that are poorly covered in public databases.

The current biogeochemical models take only sources of acetoclastic and hydrogenotrophic methanogenesis into consideration, but not those of methylotrophic methanogenesis. Thus, the methanogen contribution to the global methane flux may be underestimated(Ji et al., 2018c; Peng et al., 2018; Liu et al., 2019; Yuan et al., 2020). Our

transcript analysis revealed that methylotrophic methanogenesis was active during the 120-day incubation period, with methanol being the most likely substrate under the slurry conditions that had been applied. However, our metatranscriptome and metabolite analyses could not prove the transient presence of methanol in our slurries. In addition, the relative abundance and expression level of methanogenic pathway genes may not exactly reflect the actual contribution of the different methanogenesis pathways to methane formation. Thus, future research should be based on a complex multi-omics approach, including metagenomics, metatranscriptomics, metaproteomics, and metabolomics coupled to ^{13}C isotope labeling experiments, to disentangle the structural and functional performance of anaerobic microbial communities in rice field soils.

The changes in the anaerobic food chain in Philippine rice field soil in response to 45 °C slurry temperature may not only be a realistic near-future scenario for rice paddies but also represent the current situation in methanogenic wetlands in the tropics and subtropics; thereby, more detailed research is needed to elucidate the impact of the climate change-induced responses in anaerobic food chain functionality on CH_4 emission. Particularly, flux measurements in the native environment will be necessary to gain accurate estimates whether and how the change in microbial community functionality will influence the source strength of flooded rice fields and other methanogenic ecosystems for atmospheric CH_4.

Taken together, temperature is a major environmental factor that shapes structure and function of the anaerobic food chain in paddy soil. The knowledge of the methanogenic pathways being active at a particular temperature allows us to establish mechanistic models, predict future methane release scenarios, and develop moderation strategies. Additional experimental efforts under field conditions and more detailed metabolite analyses are required in future research. Finally, the increasing number of metagenome-assembled (environmental) genomes may help us to develop new cultivation and isolation strategies for the great diversity of so-called “unculturable microbes”, which would provide a better basis for the efficient ecological interpretation of the exponentially growing high-throughput environmental sequencing datasets.

6 References

Abdallah, R.Z., Wegner, C.-E., Liesack, W., 2019. Community transcriptomics reveals drainage effects on paddy soil microbiome across all three domains of life. Soil Biology and Biochemistry 132, 131–142. doi:10.1016/j.soilbio.2019.01.023

Abram, F., 2015. Systems-based approaches to unravel multi-species microbial community functioning. Computational and Structural Biotechnology Journal 13, 24–32. doi:10.1016/j.csbj.2014.11.009

Achinas, S., Achinas, V., Euverink, G.J.W., 2017. A Technological Overview of Biogas Production from Biowaste. Engineering 3, 299–307. doi:10.1016/J.ENG.2017.03.002

Achtnich, C., Bak, F., Conrad, R., 1995. Competition for electron donors among nitrate reducers, ferric iron reducers, sulfate reducers, and methanogens in anoxic paddy soil. Biology and Fertility of Soils.

Amann, R.I., Ludwig, W., Schleifer, K.H., 1995. Phylogenetic identification and in situ detection of individual microbial cells without cultivation. Microbiological Reviews 59, 143–169.

Ander, P., Eriksson, M., Eriksson, K., 2006. Methanol Production from Lignin-Related Substances by Phanerochaete chrysosporium. Physiologia Plantarum 65, 317–321. doi:10.1111/j.1399-3054.1985.tb02402.x

Angenent, L.T., Karim, K., Al-Dahhan, M.H., Wrenn, B.A., Domíguez-Espinosa, R., 2004. Production of bioenergy and biochemicals from industrial and agricultural wastewater. Trends in Biotechnology 22, 477–485. doi:10.1016/j.tibtech.2004.07.001

Anwar, Z., Gulfraz, M., Irshad, M., 2014. Agro-industrial lignocellulosic biomass a key to unlock the future bio-energy: A brief review. Journal of Radiation Research and Applied Sciences 7, 163–173. doi:10.1016/j.jrras.2014.02.003

Ausec, L., Zakrzewski, M., Goesmann, A., Schlüter, A., Mandic-Mulec, I., 2011. Bioinformatic Analysis Reveals High Diversity of Bacterial Genes for Laccase-Like Enzymes. PLoS ONE 6, e25724. doi:10.1371/journal.pone.0025724

Bao, Q., Huang, Y., Wang, F., Nie, S., Nicol, G.W., Yao, H., Ding, L., 2016. Effect of nitrogen fertilizer and/or rice straw amendment on methanogenic archaeal communities and methane production from a rice paddy soil. Applied Microbiology and Biotechnology 100, 5989–5998. doi:10.1007/s00253-016-7377-z

Bei, Q., Peng, J., Liesack, W., 2021. Shedding light on the functional role of the *Ignavibacteria* in Italian rice field soil: A meta-genomic/transcriptomic analysis. Soil Biology and Biochemistry 163, 108444. doi:10.1016/j.soilbio.2021.108444

Benjamini, Y., Hochberg, Y., 1995. Controlling the False Discovery Rate: A Practical and Powerful Approach to Multiple Testing. Journal of the Royal Statistical Society. Series B (Methodological) 57, 289–300.

Bentley, D.R., Balasubramanian, S., Swerdlow, H.P., Smith, G.P., Milton, J., Brown, C.G., Hall, K.P., Evers, D.J., Barnes, C.L., Bignell, H.R., Boutell, J.M., Bryant, J., Carter, R.J., Keira Cheetham, R., Cox, A.J., Ellis, D.J., Flatbush, M.R., Gormley, N.A., Humphray, S.J., Irving, L.J., Karbelashvili, M.S., Kirk, S.M., Li, H., Liu, X., Maisinger, K.S., Murray, L.J., Obradovic, B., Ost, T., Parkinson, M.L., Pratt, M.R., Rasolonjatovo, I.M.J., Reed, M.T., Rigatti, R., Rodighiero, C., Ross, M.T., Sabot, A., Sankar, S.V.,

Scally, A., Schroth, G.P., Smith, M.E., Smith, V.P., Spiridou, A., Torrance, P.E., Tzonev, S.S., Vermaas, E.H., Walter, K., Wu, X., Zhang, L., Alam, M.D., Anastasi, C., Aniebo, I.C., Bailey, D.M.D., Bancarz, I.R., Banerjee, S., Barbour, S.G., Baybayan, P.A., Benoit, V.A., Benson, K.F., Bevis, C., Black, P.J., Boodhun, A., Brennan, J.S., Bridgham, J.A., Brown, R.C., Brown, A.A., Buermann, D.H., Bundu, A.A., Burrows, J.C., Carter, N.P., Castillo, N., Chiara E Catenazzi, M., Chang, S., Neil Cooley, R., Crake, N.R., Dada, O.O., Diakoumakos, K.D., Dominguez-Fernandez, B., Earnshaw, D.J., Egbujor, U.C., Elmore, D.W., Etchin, S.S., Ewan, M.R., Fedurco, M., Fraser, L.J., Fuentes Fajardo, K.V., Scott Furey, W., George, D., Gietzen, K.J., Goddard, C.P., Golda, G.S., Granieri, P.A., Green, D.E., Gustafson, D.L., Hansen, N.F., Harnish, K., Haudenschild, C.D., Heyer, N.I., Hims, M.M., Ho, J.T., Horgan, A.M., Hoschler, K., Hurwitz, S., Ivanov, D.V., Johnson, M.Q., James, T., Huw Jones, T.A., Kang, G.-D., Kerelska, T.H., Kersey, A.D., Khrebtukova, I., Kindwall, A.P., Kingsbury, Z., Kokko-Gonzales, P.I., Kumar, A., Laurent, M.A., Lawley, C.T., Lee, S.E., Lee, X., Liao, A.K., Loch, J.A., Lok, M., Luo, S., Mammen, R.M., Martin, J.W., McCauley, P.G., McNitt, P., Mehta, P., Moon, K.W., Mullens, J.W., Newington, T., Ning, Z., Ling Ng, B., Novo, S.M., O'Neill, M.J., Osborne, M.A., Osnowski, A., Ostadan, O., Paraschos, L.L., Pickering, L., Pike, Andrew C., Pike, Alger C., Chris Pinkard, D., Pliskin, D.P., Podhasky, J., Quijano, V.J., Raczy, C., Rae, V.H., Rawlings, S.R., Chiva Rodriguez, A., Roe, P.M., Rogers, John, Rogert Bacigalupo, M.C., Romanov, N., Romieu, A., Roth, R.K., Rourke, N.J., Ruediger, S.T., Rusman, E., Sanches-Kuiper, R.M., Schenker, M.R., Seoane, J.M., Shaw, R.J., Shiver, M.K., Short, S.W., Sizto, N.L., Sluis, J.P., Smith, M.A., Ernest Sohna Sohna, J., Spence, E.J., Stevens, K., Sutton, N., Szajkowski, L., Tregidgo, C.L., Turcatti, G., Vandevondele, S., Verhovsky, Y., Virk, S.M., Wakelin, S., Walcott, G.C., Wang, J., Worsley, G.J., Yan, J., Yau, L., Zuerlein, M., Rogers, Jane, Mullikin, J.C., Hurles, M.E., McCooke, N.J., West, J.S., Oaks, F.L., Lundberg, P.L., Klenerman, D., Durbin, R., Smith, A.J., 2008. Accurate whole human genome sequencing using reversible terminator chemistry. Nature 456, 53–59. doi:10.1038/nature07517

Berger, S., Welte, C., Deppenmeier, U., 2012. Acetate Activation in *Methanosaeta thermophila*: Characterization of the Key Enzymes Pyrophosphatase and Acetyl-CoA Synthetase. Archaea 2012, 315153. doi:10.1155/2012/315153

Berini, F., Verce, M., Ausec, L., Rosini, E., Tonin, F., Pollegioni, L., Mandić-Mulec, I., 2018. Isolation and characterization of a heterologously expressed bacterial laccase from the anaerobe *Geobacter metallireducens*. Applied Microbiology and Biotechnology 102, 2425–2439. doi:10.1007/s00253-018-8785-z

Biddle, A., Stewart, L., Blanchard, J., Leschine, S., 2013. Untangling the Genetic Basis of Fibrolytic Specialization by *Lachnospiraceae* and *Ruminococcaceae* in Diverse Gut Communities. Diversity 5, 627–640. doi:10.3390/d5030627

Bodelier, P.L.E., 2015. Bypassing the methane cycle. Nature 523, 534–535. doi:10.1038/nature14633

Bolger, A.M., Lohse, M., Usadel, B., 2014. Trimmomatic: a flexible trimmer for Illumina sequence data. Bioinformatics (Oxford, England) 30, 2114–2120. doi:10.1093/bioinformatics/btu170

Bonnin, E., Pelloux, J., 2020. Pectin Degrading Enzymes, in: Kontogiorgos, V. (Ed.), Pectin: Technological and Physiological Properties. Springer International Publishing, Cham, pp. 37–60. doi:10.1007/978-3-030-53421-9_3

Borneman, J., Skroch, P.W., O'Sullivan, K.M., Palus, J.A., Rumjanek, N.G., Jansen, J.L., Nienhuis, J., Triplett, E.W., 1996. Molecular microbial diversity of an agricultural soil in Wisconsin. Applied and Environmental Microbiology 62, 1935–1943. doi:10.1128/aem.62.6.1935-1943.1996

Borrel, G., O'Toole, P.W., Harris, H.M.B., Peyret, P., Brugère, J.-F., Gribaldo, S., 2013. Phylogenomic data support a seventh order of Methylotrophic methanogens and provide insights into the evolution of Methanogenesis. Genome Biology and Evolution 5, 1769–1780. doi:10.1093/gbe/evt128

Borrel, G., Parisot, N., Harris, H., Peyretaillade, E., Gaci, N., Tottey, W., Bardot, O., Raymann, K., Gribaldo, S., Peyret, P., O'Toole, P., Brugère, J.-F., 2014. Comparative genomics highlights the unique biology of *Methanomassiliicoccales*, a *Thermoplasmatales*-related seventh order of methanogenic archaea that encodes pyrrolysine. BMC Genomics 15, 679. doi:10.1186/1471-2164-15-679

Bradford, M., 2013. Thermal adaptation of decomposer communities in warming soils. Frontiers in Microbiology 4.

Breidenbach, B., Conrad, R., 2015. Seasonal dynamics of bacterial and archaeal methanogenic communities in flooded rice fields and effect of drainage. Frontiers in Microbiology 5. doi:10.3389/fmicb.2014.00752

Bridgham, S.D., Cadillo-Quiroz, H., Keller, J.K., Zhuang, Q., 2013. Methane emissions from wetlands: biogeochemical, microbial, and modeling perspectives from local to global scales. Global Change Biology 19, 1325–1346. doi:10.1111/gcb.12131

Bucci, V., Nadell, C.D., Xavier, J.B., 2011. The Evolution of Bacteriocin Production in Bacterial Biofilms. The American Naturalist 178, E162–E173. doi:10.1086/662668

Buchfink, B., Xie, C., Huson, D.H., 2015. Fast and sensitive protein alignment using DIAMOND. Nature Methods 12, 59–60. doi:10.1038/nmeth.3176

Bugg, T.D., Ahmad, M., Hardiman, E.M., Singh, R., 2011. The emerging role for bacteria in lignin degradation and bio-product formation. Current Opinion in Biotechnology, Energy biotechnology – Environmental biotechnology 22, 394–400. doi:10.1016/j.copbio.2010.10.009

Burgess, J.E., Pletschke, B.I., 2008. Hydrolytic enzymes in sewage sludge treatment: A mini-review. Water SA 34, 343–350. doi:10.4314/wsa.v34i3

Bushnell, B., 2014. BBMap: A Fast, Accurate, Splice-Aware Aligner (No. LBNL-7065E). Lawrence Berkeley National Lab. (LBNL), Berkeley, CA (United States).

Cantarel, B.L., Coutinho, P.M., Rancurel, C., Bernard, T., Lombard, V., Henrissat, B., 2009. The Carbohydrate-Active EnZymes database (CAZy): an expert resource for Glycogenomics. Nucleic Acids Research 37, D233-238. doi:10.1093/nar/gkn663

Carr, S.A., Schubotz, F., Dunbar, R.B., Mills, C.T., Dias, R., Summons, R.E., Mandernack, K.W., 2018. Acetoclastic *Methanosaeta* are dominant methanogens in organic-rich Antarctic marine sediments. The ISME Journal 12, 330–342. doi:10.1038/ismej.2017.150

Chen, Y., Wu, N., Liu, C., Mi, T., Li, J., He, X., Li, S., Sun, Z., Zhen, Y., 2022. Methanogenesis pathways of methanogens and their responses to substrates and temperature in sediments from the South Yellow Sea. Science of The Total Environment 815, 152645. doi:10.1016/j.scitotenv.2021.152645

Chen, Y.-H., Prinn, R.G., 2005. Atmospheric modeling of high- and low-frequency methane observations: Importance of interannually varying transport. Journal of Geophysical Research (Atmospheres) 110, D10303. doi:10.1029/2004JD005542

Chidthaisong, A., Conrad, R., 2000. Pattern of non-methanogenic and methanogenic degradation of cellulose in anoxic rice field soil. FEMS Microbiology Ecology 31, 87–94. doi:10.1111/j.1574-6941.2000.tb00674.x

Chin, null, Lukow, null, Stubner, null, Conrad, null, 1999. Structure and function of the methanogenic archaeal community in stable cellulose-degrading enrichment cultures at two different temperatures (15 and 30 degrees C). FEMS Microbiology Ecology 30, 313–326. doi:10.1111/j.1574-6941.1999.tb00659.x

Chin, K.-J., Lueders, T., Friedrich, M.W., Klose, M., Conrad, R., 2004. Archaeal Community Structure and Pathway of Methane Formation on Rice Roots. Microbial Ecology 47, 59–67. doi:10.1007/s00248-003-2014-7

Cicerone, R.J., Oremland, R.S., 1988. Biogeochemical aspects of atmospheric methane. Global Biogeochemical Cycles 2, 299–327. doi:10.1029/GB002i004p00299

Cleveland, C.C., Reed, S.C., Keller, A.B., Nemergut, D.R., O'Neill, S.P., Ostertag, R., Vitousek, P.M., 2014. Litter quality versus soil microbial community controls over decomposition: a quantitative analysis. Oecologia 174, 283–294. doi:10.1007/s00442-013-2758-9

Collins, M., Knutti, R., Arblaster, J., Dufresne, J.-L., Fichefet, T., Friedlingstein, P., Gao, X., Gutowski, W.J., Johns, T., Krinner, G., Shongwe, M., Tebaldi, C., Weaver, A.J., Wehner, M.F., Allen, M.R., Andrews, T., Beyerle, U., Bitz, C.M., Bony, S., Booth, B.B.B., 2013. Long-term Climate Change: Projections, Commitments and Irreversibility. Climate Change 2013 - The Physical Science Basis: Contribution of Working Group I to the Fifth Assessment Report of the Intergovernmental Panel on Climate Change 1029–1136.

Conklin, A., Stensel, H.D., Ferguson, J., 2006. Growth Kinetics and Competition Between *Methanosarcina* and *Methanosaeta* in Mesophilic Anaerobic Digestion. Water Environment Research 78, 486–496. doi:10.2175/106143006X95393

Conrad, R., 2020. Importance of hydrogenotrophic, acetoclastic and methylotrophic methanogenesis for methane production in terrestrial, aquatic and other anoxic environments: A mini review. Pedosphere 30, 25–39. doi:10.1016/S1002-0160(18)60052-9

Conrad, R., 2009. The global methane cycle: recent advances in understanding the microbial processes involved. Environmental Microbiology Reports 1, 285–292. doi:10.1111/j.1758-2229.2009.00038.x

Conrad, R., 1999. Contribution of hydrogen to methane production and control of hydrogen concentrations in methanogenic soils and sediments. FEMS Microbiology Ecology 28, 193–202. doi:10.1111/j.1574-6941.1999.tb00575.x

Conrad, R., Bak, F., Seitz, H.J., Thebrath, B., Mayer, H.P., Schütz, H., 1989. Hydrogen turnover by psychrotrophic homoacetogenic and mesophilic methanogenic bacteria in anoxic paddy soil and lake sediment. FEMS Microbiology Ecology 5, 285–293. doi:10.1111/j.1574-6968.1989.tb03382.x

Conrad, R., Claus, P., 2005. Contribution of methanol to the production of methane and its ^{13}C-isotopic signature in anoxic rice field soil. Biogeochemistry 73, 381–393. doi:10.1007/s10533-004-0366-9

Conrad, R., Klose, M., 2006. Dynamics of the methanogenic archaeal community in anoxic rice soil upon addition of straw. European Journal of Soil Science 57, 476–484. doi:https://doi.org/10.1111/j.1365-2389.2006.00791.x

Conrad, R., Klose, M., Lu, Y., Chidthaisong, A., 2012. Methanogenic Pathway and Archaeal Communities in Three Different Anoxic Soils Amended with Rice Straw and Maize Straw. Frontiers in Microbiology 3. doi:10.3389/fmicb.2012.00004

Conrad, R., Klose, M., Noll, M., 2009. Functional and structural response of the methanogenic microbial community in rice field soil to temperature change. Environmental Microbiology 11, 1844–1853. doi:10.1111/j.1462-2920.2009.01909.x

Conrad, R., Wetter, B., 1990. Influence of temperature on energetics of hydrogen metabolism in homoacetogenic, methanogenic, and other anaerobic bacteria. Archives of Microbiology 155, 94–98. doi:10.1007/BF00291281

de Bok, F.A.M., Stams, A.J.M., Dijkema, C., Boone, D.R., 2001. Pathway of Propionate Oxidation by a Syntrophic Culture of *Smithella propionica* and *Methanospirillum hungatei*. Applied and Environmental Microbiology 67, 1800–1804. doi:10.1128/AEM.67.4.1800-1804.2001

Dittoe, D.K., Barabote, R.D., Rothrock, M.J., Ricke, S.C., 2020. Assessment of a Potential Role of Dickeya dadantii DSM 18020 as a Pectinase Producer for Utilization in Poultry Diets Based on in silico Analyses. Frontiers in Microbiology 11, 751. doi:10.3389/fmicb.2020.00751

Edgar, R.C., 2004. MUSCLE: multiple sequence alignment with high accuracy and high throughput. Nucleic Acids Research 32, 1792–1797. doi:10.1093/nar/gkh340

Ehhalt, D.H., 1979. Der atmosphärische Kreislauf von Methan. Naturwissenschaften 66, 307–311. doi:10.1007/BF00441273

Embree, M., Liu, J.K., Al-Bassam, M.M., Zengler, K., 2015. Networks of energetic and metabolic interactions define dynamics in microbial communities. Proceedings of the National Academy of Sciences 112, 15450–15455. doi:10.1073/pnas.1506034112

Evans, P.N., Boyd, J.A., Leu, A.O., Woodcroft, B.J., Parks, D.H., Hugenholtz, P., Tyson, G.W., 2019. An evolving view of methane metabolism in the Archaea. Nature Reviews Microbiology 17, 219–232. doi:10.1038/s41579-018-0136-7

Feng, L., Palmer, P.I., Parker, R.J., Lunt, M.F., Boesch, H., 2022. Methane emissions responsible for record-breaking atmospheric methane growth rates in 2020 and 2021 (preprint). Gases/Remote Sensing/Troposphere/Chemistry (chemical composition and reactions). doi:10.5194/acp-2022-425

Ferry, J.G., 2011. Fundamentals of methanogenic pathways that are key to the biomethanation of complex biomass. Current Opinion in Biotechnology 22, 351. doi:10.1016/j.copbio.2011.04.011

Fey, A., Chin, K.J., Conrad, R., 2001. Thermophilic methanogens in rice field soil. Environmental Microbiology 3, 295–303. doi:10.1046/j.1462-2920.2001.00195.x

Fey, A., Conrad, R., 2000. Effect of Temperature on Carbon and Electron Flow and on the Archaeal Community in Methanogenic Rice Field Soil. Applied and Environmental Microbiology 66, 4790–4797.

Fu, B., Conrad, R., Blaser, M., 2018. Potential contribution of acetogenesis to anaerobic degradation in methanogenic rice field soils. Soil Biology and Biochemistry 119, 1–10. doi:10.1016/j.soilbio.2017.10.034

Fu, B., Jin, X., Conrad, R., Liu, Hongbo, Liu, He, 2019. Competition Between Chemolithotrophic Acetogenesis and Hydrogenotrophic Methanogenesis for Exogenous H_2/CO_2 in Anaerobically Digested Sludge: Impact of Temperature. Frontiers in Microbiology 10, 2418. doi:10.3389/fmicb.2019.02418

Gagen, E.J., Denman, S.E., Padmanabha, J., Zadbuke, S., Al Jassim, R., Morrison, M., McSweeney, C.S., 2010. Functional gene analysis suggests different acetogen populations in the bovine rumen and tammar wallaby forestomach. Applied and Environmental Microbiology 76, 7785–7795. doi:10.1128/AEM.01679-10

Gan, Y., Qiu, Q., Liu, P., Rui, J., Lu, Y., 2012. Syntrophic oxidation of propionate in rice field soil at 15 and 30°C under methanogenic conditions. Applied and Environmental Microbiology 78, 4923–4932. doi:10.1128/AEM.00688-12

Garcia, J.-L., Patel, B.K.C., Ollivier, B., 2000. Taxonomic, Phylogenetic, and Ecological Diversity of Methanogenic Archaea. Anaerobe 6, 205–226. doi:10.1006/anae.2000.0345

Ghoul, M., Mitri, S., 2016. The Ecology and Evolution of Microbial Competition. Trends in Microbiology 24, 833–845. doi:10.1016/j.tim.2016.06.011

Glissman, K., Chin, K.-J., Casper, P., Conrad, R., 2004. Methanogenic Pathway and Archaeal Community Structure in the Sediment of Eutrophic Lake Dagow: Effect of Temperature. Microbial Ecology 48, 389–399. doi:10.1007/s00248-003-2027-2

Glissmann, K., Conrad, R., 2002a. Saccharolytic activity and its role as a limiting step in methane formation during the anaerobic degradation of rice straw in rice paddy soil. Biology and Fertility of Soils 35, 62–67. doi:10.1007/s00374-002-0442-z

Glissmann, K., Conrad, R., 2002b. Saccharolytic activity and its role as a limiting step in methane formation during the anaerobic degradation of rice straw in rice paddy soil. Biology and Fertility of Soils 35, 62–67. doi:10.1007/s00374-002-0442-z

Glissmann, K., Conrad, R., 2000. Fermentation pattern of methanogenic degradation of rice straw in anoxic paddy soil. FEMS Microbiology Ecology 31, 117–126. doi:10.1111/j.1574-6941.2000.tb00677.x

Glissmann, K., Weber, S., Conrad, R., 2001. Localization of processes involved in methanogenic degradation of rice straw in anoxic paddy soil. Environmental Microbiology 3, 502–511. doi:10.1046/j.1462-2920.2001.00212.x

Großkopf, R., Janssen, P.H., Liesack, W., 1998a. Diversity and Structure of the Methanogenic Community in Anoxic Rice Paddy Soil Microcosms as Examined by Cultivation and Direct 16S rRNA Gene Sequence Retrieval. Applied and Environmental Microbiology 64, 960–969. doi:10.1128/AEM.64.3.960-969.1998

Großkopf, R., Janssen, P.H., Liesack, W., 1998b. Diversity and Structure of the Methanogenic Community in Anoxic Rice Paddy Soil Microcosms as Examined by Cultivation and Direct 16S rRNA Gene Sequence Retrieval. Applied and Environmental Microbiology 64, 960–969. doi:10.1128/AEM.64.3.960-969.1998

Haas, B.J., Papanicolaou, A., Yassour, M., Grabherr, M., Blood, P.D., Bowden, J., Couger, M.B., Eccles, D., Li, B., Lieber, M., MacManes, M.D., Ott, M., Orvis, J., Pochet, N., Strozzi, F., Weeks, N., Westerman, R., William, T., Dewey, C.N., Henschel, R., LeDuc, R.D., Friedman, N., Regev, A., 2013. De novo transcript sequence reconstruction from RNA-seq using the Trinity platform for reference generation and analysis. Nature Protocols 8, 1494–1512. doi:10.1038/nprot.2013.084

Hackstein, J.H.P., Langer, P., Rosenberg, J., 1996. Genetic and evolutionary constraints for the symbiosis between animals and methanogenic bacteria. Environmental Monitoring and Assessment 42, 39–56. doi:10.1007/BF00394041

Hakobyan, A., Zhu, J., Glatter, T., Paczia, N., Liesack, W., 2020. Hydrogen utilization by *Methylocystis* sp. strain SC2 expands the known metabolic versatility of type IIa methanotrophs. Metabolic Engineering 61, 181–196. doi:10.1016/j.ymben.2020.05.003

Hanreich, A., Schimpf, U., Zakrzewski, M., Schlüter, A., Benndorf, D., Heyer, R., Rapp, E., Pühler, A., Reichl, U., Klocke, M., 2013. Metagenome and metaproteome analyses of microbial communities in mesophilic biogas-producing anaerobic batch fermentations indicate concerted plant carbohydrate degradation. Systematic and Applied Microbiology 36, 330–338. doi:10.1016/j.syapm.2013.03.006

Harmsen, P., Huijgen, W., Bermudez, L., Bakker, R., 2010. Literature review of physical and chemical pretreatment processes for lignocellulosic biomass .

Heyer, R., Kohrs, F., Reichl, U., Benndorf, D., 2015. Metaproteomics of complex microbial communities in biogas plants. Microbial Biotechnology 8, 749–763. doi:10.1111/1751-7915.12276

Himmel, M.E., Xu, Q., Luo, Y., Ding, S.-Y., Lamed, R., Bayer, E.A., 2010. Microbial enzyme systems for biomass conversion: emerging paradigms. Biofuels 1, 323–341. doi:10.4155/bfs.09.25

Holland, H.D., Lazar, B., McCaffrey, M., 1986. Evolution of the atmosphere and oceans. Nature 320, 27–33. doi:10.1038/320027a0

Huang, X.-F., Santhanam, N., Badri, D.V., Hunter, W.J., Manter, D.K., Decker, S.R., Vivanco, J.M., Reardon, K.F., 2013. Isolation and characterization of lignin-degrading bacteria from rainforest soils. Biotechnology and Bioengineering 110, 1616–1626. doi:10.1002/bit.24833

Huson, D.H., Beier, S., Flade, I., Górska, A., El-Hadidi, M., Mitra, S., Ruscheweyh, H.-J., Tappu, R., 2016. MEGAN Community Edition - Interactive Exploration and Analysis of Large-Scale Microbiome Sequencing Data. PLOS Computational Biology 12, e1004957. doi:10.1371/journal.pcbi.1004957

IPCC, 2013: Climate Change 2013: The Physical Science Basis. Contribution of Working Group I to the Fifth Assessment Report of the Intergovernmental Panel on Climate Change [Stocker, T.F., D. Qin, G.-K. Plattner, M. Tignor, S.K. Allen, J. Boschung, A. Nauels, Y. Xia, V. Bex and P.M. Midgley (eds.)]. Cambridge University Press, Cambridge, United Kingdom and New York, NY, USA, 1535 pp, doi:10.1017/CBO9781107415324.

Jain, C., Rodriguez-R, L.M., Phillippy, A.M., Konstantinidis, K.T., Aluru, S., 2018. High throughput ANI analysis of 90K prokaryotic genomes reveals clear species boundaries. Nature Communications 9, 5114. doi:10.1038/s41467-018-07641-9

Jansson, J.K., Prosser, J.I., 2013. The life beneath our feet. Nature 494, 40–41. doi:10.1038/494040a

Janusz, G., Pawlik, A., Sulej, J., Świderska-Burek, U., Jarosz-Wilkołazka, A., Paszczyński, A., 2017. Lignin degradation: microorganisms, enzymes involved, genomes analysis and evolution. FEMS Microbiology Reviews 41, 941–962. doi:10.1093/femsre/fux049

Jetten, M.S.M., Stams, A.J.M., Zehnder, A.J.B., 1992. Methanogenesis from acetate: a comparison of the acetate metabolism in *Methanothrix soehngenii* and *Methanosarcina* spp. FEMS Microbiology Letters 88, 181–198. doi:10.1111/j.1574-6968.1992.tb04987.x

Jetten, M.S.M., Stams, A.J.M., Zehnder, A.J.B., 1990. Acetate threshold values and acetate activating enzymes in methanogenic bacteria. FEMS Microbiology Ecology 6, 339–344. doi:10.1111/j.1574-6968.1990.tb03958.x

Ji, Y., Liu, P., Conrad, R., 2018a. Change of the pathway of methane production with progressing anoxic incubation of paddy soil. Soil Biology and Biochemistry 121, 177–184. doi:10.1016/j.soilbio.2018.03.014

Ji, Y., Liu, P., Conrad, R., 2018b. Response of fermenting bacterial and methanogenic archaeal communities in paddy soil to progressing rice straw degradation. Soil Biology and Biochemistry 124, 70–80. doi:10.1016/j.soilbio.2018.05.029

Ji, Y., Liu, P., Conrad, R., 2018c. Response of fermenting bacterial and methanogenic archaeal communities in paddy soil to progressing rice straw degradation. Soil Biology and Biochemistry 124, 70–80. doi:10.1016/j.soilbio.2018.05.029

Jiang, N., Wang, Y., Dong, X., 2010. Methanol as the primary methanogenic and acetogenic precursor in the cold Zoige wetland at Tibetan plateau. Microbial Ecology 60, 206–213. doi:10.1007/s00248-009-9602-0

Kang, D.D., Froula, J., Egan, R., Wang, Z., 2015. MetaBAT, an efficient tool for accurately reconstructing single genomes from complex microbial communities. PeerJ. doi:10.7717/peerj.1165

Karhu, K., Auffret, M.D., Dungait, J.A.J., Hopkins, D.W., Prosser, J.I., Singh, B.K., Subke, J.-A., Wookey, P.A., Ågren, G.I., Sebastià, M.-T., Gouriveau, F., Bergkvist, G., Meir, P., Nottingham, A.T., Salinas, N., Hartley, I.P., 2014. Temperature sensitivity of soil respiration rates enhanced by microbial community response. Nature 513, 81–84. doi:10.1038/nature13604

Kato, S., Chino, K., Kamimura, N., Masai, E., Yumoto, I., Kamagata, Y., 2015. Methanogenic degradation of lignin-derived monoaromatic compounds by microbial enrichments from rice paddy field soil. Scientific Reports 5, 14295. doi:10.1038/srep14295

Kern, T., Fischer, M., Deppenmeier, U., Schmitz, R., Rother, M., 2016. *Methanosarcina flavescens* sp. nov., a methanogenic archaeon isolated from a full-scale anaerobic digester. International Journal of Systematic and Evolutionary Microbiology 66. doi:10.1099/ijsem.0.000894

Khan, M.U., Ahring, B.K., 2019. Lignin degradation under anaerobic digestion: Influence of lignin modifications -A review. Biomass and Bioenergy 128, 105325. doi:10.1016/j.biombioe.2019.105325

Kim, M., Oh, H.-S., Park, S.-C., Chun, J., 2014. Towards a taxonomic coherence between average nucleotide identity and 16S rRNA gene sequence similarity for species demarcation of prokaryotes. International Journal of Systematic and Evolutionary Microbiology 64, 346–351. doi:10.1099/ijs.0.059774-0

Kim, W., Racimo, F., Schluter, J., Levy, S.B., Foster, K.R., 2014. Importance of positioning for microbial evolution. Proceedings of the National Academy of Sciences 111. doi:10.1073/pnas.1323632111

Kimura, M., Murase, J., Lu, Y., 2004. Carbon cycling in rice field ecosystems in the context of input, decomposition and translocation of organic materials and the fates of their end products (CO2 and CH4). Soil Biology and Biochemistry 36, 1399–1416. doi:10.1016/j.soilbio.2004.03.006

Kimura, M., Tun, C.C., 1999. Microscopic observation of the decomposition process of leaf sheath of rice straw and colonizing microorganisms during the cultivation period of paddy rice. Soil Science and Plant Nutrition 45, 427–437. doi:10.1080/00380768.1999.10409357

Kirschke, S., Bousquet, P., Ciais, P., Saunois, M., Canadell, J.G., Dlugokencky, E.J., Bergamaschi, P., Bergmann, D., Blake, D.R., Bruhwiler, L., Cameron-Smith, P., Castaldi, S., Chevallier, F., Feng, L., Fraser, A., Heimann, M., Hodson, E.L., Houweling, S., Josse, B., Fraser, P.J., Krummel, P.B., Lamarque, J.-F., Langenfelds, R.L., Le Quéré, C., Naik, V., O'Doherty, S., Palmer, P.I., Pison, I., Plummer, D., Poulter,

B., Prinn, R.G., Rigby, M., Ringeval, B., Santini, M., Schmidt, M., Shindell, D.T., Simpson, I.J., Spahni, R., Steele, L.P., Strode, S.A., Sudo, K., Szopa, S., van der Werf, G.R., Voulgarakis, A., van Weele, M., Weiss, R.F., Williams, J.E., Zeng, G., 2013. Three decades of global methane sources and sinks. Nature Geoscience 6, 813–823. doi:10.1038/ngeo1955

Klass, D.L., 1998. Biomass for Renewable Energy, Fuels, and Chemicals. Elsevier.

Ko, J.-J., Shimizu, Y., Ikeda, K., Kim, S.-K., Park, C.-H., Matsui, S., 2009. Biodegradation of high molecular weight lignin under sulfate reducing conditions: Lignin degradability and degradation by-products. Bioresource Technology 100, 1622–1627. doi:10.1016/j.biortech.2008.09.029

Koch, C., Müller, S., Harms, H., Harnisch, F., 2014. Microbiomes in bioenergy production: From analysis to management. Current Opinion in Biotechnology, Energy biotechnology • Environmental biotechnology 27, 65–72. doi:10.1016/j.copbio.2013.11.006

Kong, Y., Kuzyakov, Y., Ruan, Y., Zhang, J., Wang, T., Wang, M., Guo, S., Shen, Q., Ling, N., 2020. DNA Stable-Isotope Probing Delineates Carbon Flows from Rice Residues into Soil Microbial Communities Depending on Fertilization. Applied and Environmental Microbiology 86, e02151-19, /aem/86/7/AEM.02151-19.atom. doi:10.1128/AEM.02151-19

Kopylova, E., Noé, L., Touzet, H., 2012. SortMeRNA: fast and accurate filtering of ribosomal RNAs in metatranscriptomic data. Bioinformatics 28, 3211–3217. doi:10.1093/bioinformatics/bts611

Kotsyurbenko, O.R., Glagolev, M.V., Nozhevnikova, A.N., Conrad, R., 2001. Competition between homoacetogenic bacteria and methanogenic archaea for hydrogen at low temperature. FEMS Microbiology Ecology 38, 153–159. doi:10.1111/j.1574-6941.2001.tb00893.x

Krüger, M., Eller, G., Conrad, R., Frenzel, P., 2002. Seasonal variation in pathways of CH_4 production and in CH_4 oxidation in rice fields determined by stable carbon isotopes and specific inhibitors. Global Change Biology 8, 265–280. doi:10.1046/j.1365-2486.2002.00476.x

Krumböck, M., Conrad, R., 1991. Metabolism of position-labelled glucose in anoxic methanogenic paddy soil and lake sediment. FEMS Microbiology Ecology 8, 247–256. doi:10.1111/j.1574-6941.1991.tb01730.x

Krylova, N.I., Janssen, P.H., Conrad, R., 1997. Turnover of propionate in methanogenic paddy soil. FEMS Microbiology Ecology 23, 107–117. doi:10.1111/j.1574-6941.1997.tb00395.x

Kumar, S., Stecher, G., Li, M., Knyaz, C., Tamura, K., 2018. MEGA X: Molecular Evolutionary Genetics Analysis across Computing Platforms. Molecular Biology and Evolution 35, 1547–1549. doi:10.1093/molbev/msy096

Kurth, J.M., Op den Camp, H.J.M., Welte, C.U., 2020. Several ways one goal—methanogenesis from unconventional substrates. Applied Microbiology and Biotechnology 104, 6839–6854. doi:10.1007/s00253-020-10724-7

Lane, D.J., Pace, B., Olsen, G.J., Stahl, D.A., Sogin, M.L., Pace, N.R., 1985. Rapid determination of 16S ribosomal RNA sequences for phylogenetic analyses. Proceedings of the National Academy of Sciences 82, 6955–6959. doi:10.1073/pnas.82.20.6955

Langmead, B., Trapnell, C., Pop, M., Salzberg, S.L., 2009. Ultrafast and memory-efficient alignment of short DNA sequences to the human genome. Genome Biology 10, R25. doi:10.1186/gb-2009-10-3-r25

Lawson, C., Wu, S., Bhattacharjee, A.S., Hamilton, J., Mcmahon, K., Goel, R., Noguera, D., 2017. Metabolic network analysis reveals microbial community interactions in anammox granules. Nature Communications 8. doi:10.1038/ncomms15416

Li, A., Chu, Y., Wang, X., Ren, L., Yu, J., Liu, X., Yan, J., Zhang, L., Wu, S., Li, S., 2013. A pyrosequencing-based metagenomic study of methane-producing microbial community in solid-state biogas reactor. Biotechnology for Biofuels 6, 3. doi:10.1186/1754-6834-6-3

Li, B., Dewey, C.N., 2011. RSEM: accurate transcript quantification from RNA-Seq data with or without a reference genome. BMC Bioinformatics 12, 323. doi:10.1186/1471-2105-12-323

Li, H., Chang, J., Liu, P., Fu, L., Ding, D., Lu, Y., 2014. Direct interspecies electron transfer accelerates syntrophic oxidation of butyrate in paddy soil enrichments: Syntrophic butyrate oxidation facilitated by nanoFe_3O_4. Environmental Microbiology 17. doi:10.1111/1462-2920.12576

Liang, B., Wang, L.-Y., Mbadinga, S.M., Liu, J.-F., Yang, S.-Z., Gu, J.-D., Mu, B.-Z., 2015. *Anaerolineaceae* and *Methanosaeta* turned to be the dominant microorganisms in alkanes-dependent methanogenic culture after long-term of incubation. AMB Express 5, 37. doi:10.1186/s13568-015-0117-4

Liesack, W., Stackebrandt, E., 1992. Occurrence of novel groups of the domain Bacteria as revealed by analysis of genetic material isolated from an Australian terrestrial environment. Journal of Bacteriology 174, 5072–5078. doi:10.1128/jb.174.15.5072-5078.1992

Liu, C., Lu, M., Cui, J., Li, B., Fang, C., 2014. Effects of straw carbon input on carbon dynamics in agricultural soils: a meta-analysis. Global Change Biology 20, 1366–1381. doi:10.1111/gcb.12517

Liu, F., Conrad, R., 2010. *Thermoanaerobacteriaceae* oxidize acetate in methanogenic rice field soil at 50°C. Environmental Microbiology 12, 2341–2354. doi:10.1111/j.1462-2920.2010.02289.x

Liu, P., Conrad, R., 2017. *Syntrophobacteraceae*-affiliated species are major propionate-degrading sulfate reducers in paddy soil. Environmental Microbiology 19, 1669–1686. doi:10.1111/1462-2920.13698

Liu, P., Klose, M., Conrad, R., 2019. Temperature-Dependent Network Modules of Soil Methanogenic Bacterial and Archaeal Communities. Frontiers in Microbiology 10, 496. doi:10.3389/fmicb.2019.00496

Liu, P., Klose, M., Conrad, R., 2018a. Temperature effects on structure and function of the methanogenic microbial communities in two paddy soils and one desert soil. Soil Biology and Biochemistry 124, 236–244. doi:10.1016/j.soilbio.2018.06.024

Liu, P., Klose, M., Conrad, R., 2018b. Temperature effects on structure and function of the methanogenic microbial communities in two paddy soils and one desert soil. Soil Biology and Biochemistry 124, 236–244. doi:10.1016/j.soilbio.2018.06.024

Liu, Y., Whitman, W.B., 2008. Metabolic, Phylogenetic, and Ecological Diversity of the Methanogenic Archaea. Annals of the New York Academy of Sciences 1125, 171–189. doi:10.1196/annals.1419.019

Lovley, D.R., Klug, M.J., 1983. Methanogenesis from methanol and methylamines and acetogenesis from hydrogen and carbon dioxide in the sediments of a eutrophic lake. Applied and Environmental Microbiology 45, 1310–1315. doi:10.1128/aem.45.4.1310-1315.1983

Lueders, T., Friedrich, M., 2000. Archaeal population dynamics during sequential reduction processes in rice field soil. Applied and Environmental Microbiology 66, 2732–2742. doi:10.1128/AEM.66.7.2732-2742.2000

Lueders, T., Pommerenke, B., Friedrich, M., 2004. Stable-Isotope Probing of Microorganisms Thriving at Thermodynamic Limits: Syntrophic Propionate Oxidation in Flooded Soil. Applied and Environmental Microbiology 70, 5778–86. doi:10.1128/AEM.70.10.5778-5786.2004

Lyu, Z., Shao, N., Akinyemi, T., Whitman, W.B., 2018. Methanogenesis. Current Biology: CB 28, R727–R732. doi:10.1016/j.cub.2018.05.021

Ma, K., Conrad, R., Lu, Y., 2012. Responses of Methanogen *mcrA* Genes and Their Transcripts to an Alternate Dry/Wet Cycle of Paddy Field Soil. Applied and Environmental Microbiology 78, 445–454. doi:10.1128/AEM.06934-11

MacLean, R.C., Gudelj, I., 2006. Resource competition and social conflict in experimental populations of yeast. Nature 441, 498–501. doi:10.1038/nature04624

Maestrojuan', G.M., Boone, D.R., n.d. Characterization of *Methanosarcina barkeri* MST and 227, Methanosarcina mazei S-6T,and Methanosarcina vacuolata Z-76IT 8.

Mah, R.A., Xun, L.-Y., Boone, D.R., Ahring, B., Smith, P.H., Wilkie, A., 1990. Methanogenesis from Propionate in Sludge and Enrichment Systems, in: Bélaich, J.-P., Bruschi, M., Garcia, J.-L. (Eds.), Microbiology and Biochemistry of Strict Anaerobes Involved in Interspecies Hydrogen Transfer, Federation of European Microbiological Societies Symposium Series. Springer US, Boston, MA, pp. 99–111. doi:10.1007/978-1-4613-0613-9_8

Manyi-Loh, C.E., Mamphweli, S.N., Meyer, E.L., Okoh, A.I., Makaka, G., Simon, M., 2013. Microbial Anaerobic Digestion (Bio-Digesters) as an Approach to the Decontamination of Animal Wastes in Pollution Control and the Generation of Renewable Energy. International Journal of Environmental Research and Public Health 10, 4390–4417. doi:10.3390/ijerph10094390

McIlroy, S.J., Kirkegaard, R.H., Dueholm, M.S., Fernando, E., Karst, S.M., Albertsen, M., Nielsen, P.H., 2017. Culture-Independent Analyses Reveal Novel Anaerolineaceae as Abundant Primary Fermenters in Anaerobic Digesters Treating Waste Activated Sludge. Frontiers in Microbiology 8, 1134. doi:10.3389/fmicb.2017.01134

McInerney, M.J., Rohlin, L., Mouttaki, H., Kim, U., Krupp, R.S., Rios-Hernandez, L., Sieber, J., Struchtemeyer, C.G., Bhattacharyya, A., Campbell, J.W., Gunsalus, R.P., 2007. The genome of Syntrophus aciditrophicus: Life at the thermodynamic limit of microbial growth. Proceedings of the National Academy of Sciences 104, 7600–7605. doi:10.1073/pnas.0610456104

Mechichi, T., Patel, B.K.C., Sayadi, S., 2005. Anaerobic degradation of methoxylated aromatic compounds by *Clostridium methoxybenzovorans* and a nitrate-reducing bacterium *Thauera* sp. strain Cin3,4. International Biodeterioration & Biodegradation 56, 224–230. doi:10.1016/j.ibiod.2005.09.001

Mehta, P., Deshmukh, K., Dagar, S.S., Dhakephalkar, P.K., Lanjekar, V.B., 2021. Genome sequencing and analysis of a psychrotrophic methanogen *Methanosarcina* sp. nov. MSH10X1 cultured from methane hydrate deposits of Krishna Godavari Basin of India. Marine Genomics 59, 100864. doi:10.1016/j.margen.2021.100864

Miller, C.S., Baker, B., Thomas, B.C., Singer, S., Banfield, J., 2011. EMIRGE: reconstruction of full-length ribosomal genes from microbial community short read sequencing data. Genome Biology. doi:10.1186/gb-2011-12-5-r44

Min, H., Zinder, S.H., 1989. Kinetics of Acetate Utilization by Two Thermophilic Acetotrophic Methanogens: *Methanosarcina* sp. Strain CALS-1 and Methanothrix sp. Strain CALS-1. Applied and Environmental Microbiology 55, 488–491. doi:10.1128/aem.55.2.488-491.1989

Müller, N., Worm, P., Schink, B., Stams, A.J.M., Plugge, C.M., 2010. Syntrophic butyrate and propionate oxidation processes: from genomes to reaction mechanisms. Environmental Microbiology Reports 2, 489–499. doi:10.1111/j.1758-2229.2010.00147.x

Noll, M., Klose, M., Conrad, R., 2010. Effect of temperature change on the composition of the bacterial and archaeal community potentially involved in the turnover of acetate and propionate in methanogenic rice field soil: Effect of temperature on microbial acetate turnover. FEMS Microbiology Ecology 73, 215–225. doi:10.1111/j.1574-6941.2010.00883.x

Nozhevnikova, A.N., Kotsyurbenko, O.R., Simankova, M.V., 1994. Acetogenesis at Low Temperature, in: Drake, H.L. (Ed.), Acetogenesis, Chapman & Hall Microbiology Series. Springer US, Boston, MA, pp. 416–431. doi:10.1007/978-1-4615-1777-1_15

Nozhevnikova, A.N., Nekrasova, V., Ammann, A., Zehnder, A.J.B., Wehrli, B., Holliger, C., 2007. Influence of temperature and high acetate concentrations on methanogenensis in lake sediment slurries. FEMS Microbiology Ecology 62, 336–344. doi:10.1111/j.1574-6941.2007.00389.x

Nurk, S., Meleshko, D., Korobeynikov, A., Pevzner, P.A., 2017. metaSPAdes: a new versatile metagenomic assembler. Genome Research 27, 824–834. doi:10.1101/gr.213959.116

Oremland, R.S., Marsh, L.M., Polcin, S., 1982. Methane production and simultaneous sulphate reduction in anoxic, salt marsh sediments. Nature 296, 143–145. doi:10.1038/296143a0

Oren, A., 2014. The Family Methanotrichaceae, in: Rosenberg, E., DeLong, E.F., Lory, S., Stackebrandt, E., Thompson, F. (Eds.), The Prokaryotes: Other Major Lineages of Bacteria and The Archaea. Springer, Berlin, Heidelberg, pp. 297–306. doi:10.1007/978-3-642-38954-2_277

Pang, Y.X., Foo, D.C.Y., Yan, Y., Sharmin, N., Lester, E., Wu, T., Pang, C.H., 2021. Analysis of environmental impacts and energy derivation potential of biomass pyrolysis via Piper diagram. Journal of Analytical and Applied Pyrolysis 154, 104995. doi:10.1016/j.jaap.2020.104995

Parks, D.H., Imelfort, M., Skennerton, C.T., Hugenholtz, P., Tyson, G., 2015. CheckM: assessing the quality of microbial genomes recovered from isolates, single cells, and metagenomes. Genome Research. doi:10.1101/gr.186072.114

Peng, J., Lü, Z., Rui, J., Lu, Y., 2008. Dynamics of the Methanogenic Archaeal Community during Plant Residue Decomposition in an Anoxic Rice Field Soil. Applied and Environmental Microbiology 74, 2894–2901. doi:10.1128/AEM.00070-08

Peng, J., Wegner, C.-E., Bei, Q., Liu, P., Liesack, W., 2018. Metatranscriptomics reveals a differential temperature effect on the structural and functional organization of the anaerobic food web in rice field soil. Microbiome 6, 169. doi:10.1186/s40168-018-0546-9

Penning, H., Conrad, R., 2007. Quantification of carbon flow from stable isotope fractionation in rice field soils with different organic matter content. Organic Geochemistry 38, 2058–2069. doi:10.1016/j.orggeochem.2007.08.004

Pfeiffer, T., Schuster, S., Bonhoeffer, S., 2001. Cooperation and Competition in the Evolution of ATP-Producing Pathways. Science 292, 504–507. doi:10.1126/science.1058079

Prinn, R.G., 1994. Global Atmospheric-Biospheric Chemistry, in: Prinn, R.G. (Ed.), Global Atmospheric-Biospheric Chemistry, Environmental Science Research. Springer US, Boston, MA, pp. 1–18. doi:10.1007/978-1-4615-2524-0_1

Pruesse, E., Peplies, J., Glöckner, F.O., 2012. SINA: accurate high-throughput multiple sequence alignment of ribosomal RNA genes. Bioinformatics (Oxford, England) 28, 1823–1829. doi:10.1093/bioinformatics/bts252

Pump, J., Conrad, R., 2014. Rice biomass production and carbon cycling in $^{13}CO_2$ pulse-labeled microcosms with different soils under submerged conditions. Plant and Soil 384, 213–229. doi:10.1007/s11104-014-2201-y

Quast, C., Pruesse, E., Yilmaz, P., Gerken, J., Schweer, T., Yarza, P., Peplies, J., Glöckner, F.O., 2012. The SILVA ribosomal RNA gene database project: improved data processing and web-based tools. Nucleic Acids Research 41, D590–D596. doi:10.1093/nar/gks1219

Ramakrishnan, B., Lueders, T., Dunfield, P.F., Conrad, R., Friedrich, M.W., 2001. Archaeal community structures in rice soils from different geographical regions before and after initiation of methane production. FEMS Microbiology Ecology 37, 175–186. doi:10.1111/j.1574-6941.2001.tb00865.x

Ravin, N.V., Mardanov, A.V., Skryabin, K.G., 2015. Metagenomics as a tool for the investigation of uncultured microorganisms. Russian Journal of Genetics 51, 431–439. doi:10.1134/S1022795415050063

Rawat, S.R., Männistö, M.K., Bromberg, Y., Häggblom, M.M., 2012. Comparative genomic and physiological analysis provides insights into the role of Acidobacteria in organic carbon utilization in Arctic tundra soils. FEMS Microbiology Ecology 82, 341–355. doi:10.1111/j.1574-6941.2012.01381.x

Reeburgh, W.S., 2003. Global methane biogeochemistry. Treatise on geochemistry, 4, p.347. doi:10.1016/B0-08-043751-6/04036-6

Roger, P.A., Zimmerman, W.J., Lumpkin, T.A., 1993. Microbiological management of wetland rice fields. Soil microbial ecology: applications in agricultural and environmental management, 417-455.

Ronaghi, M., 2001. Pyrosequencing Sheds Light on DNA Sequencing. Genome Research 11, 3–11. doi:10.1101/gr.150601

Ronaghi, M., Karamohamed, S., Pettersson, B., Uhlén, M., Nyrén, P., 1996. Real-Time DNA Sequencing Using Detection of Pyrophosphate Release. Analytical Biochemistry 242, 84–89. doi:10.1006/abio.1996.0432

Rosell, K.-G., Svensson, S., 1975. Studies of the distribution of the 4-O-methyl-d-glucuronic acid residues in birch xylan. Carbohydrate Research 42, 297–304. doi:10.1016/S0008-6215(00)84271-8

Rotaru, A.-E., Shrestha, P.M., Liu, F., Markovaite, B., Chen, S., Nevin, K.P., Lovley, D.R., 2014. Direct Interspecies Electron Transfer between *Geobacter metallireducens* and *Methanosarcina barkeri*. Applied and Environmental Microbiology 80, 4599–4605. doi:10.1128/AEM.00895-14

Rotaru, A.-E., Shrestha, P.M., Liu, F., Shrestha, M., Shrestha, D., Embree, M., Zengler, K., Wardman, C., Nevin, K.P., Lovley, D.R., 2013. A new model for electron flow during anaerobic digestion: direct interspecies electron transfer to *Methanosaeta* for the reduction of carbon dioxide to methane. Energy & Environmental Science 7, 408–415. doi:10.1039/C3EE42189A

Roussel, E.G., Cragg, B.A., Webster, G., Sass, H., Tang, X., Williams, A.S., Gorra, R., Weightman, A.J., Parkes, R.J., 2015. Complex coupled metabolic and prokaryotic community responses to increasing temperatures

in anaerobic marine sediments: critical temperatures and substrate changes. FEMS Microbiology Ecology 91, fiv084. doi:10.1093/femsec/fiv084

Rui, J., Peng, J., Lu, Y., 2009. Succession of Bacterial Populations during Plant Residue Decomposition in Rice Field Soil. Applied and Environmental Microbiology 75, 4879–4886. doi:10.1128/AEM.00702-09

Sattley, W.M., Madigan, M.T., 2014. The Family *Heliobacteriaceae*, in: Rosenberg, E., DeLong, E.F., Lory, S., Stackebrandt, E., Thompson, F. (Eds.), The Prokaryotes: Firmicutes and Tenericutes. Springer, Berlin, Heidelberg, pp. 185–196. doi:10.1007/978-3-642-30120-9_362

Schink, B., 1997. Energetics of syntrophic cooperation in methanogenic degradation. Microbiology and Molecular Biology Reviews 61, 262–280. doi:10.1128/mmbr.61.2.262-280.1997

Schink, B., Stams, A.J.M., 2013. Syntrophism Among Prokaryotes, in: Rosenberg, E., DeLong, E.F., Lory, S., Stackebrandt, E., Thompson, F. (Eds.), The Prokaryotes. Springer Berlin Heidelberg, Berlin, Heidelberg, pp. 471–493. doi:10.1007/978-3-642-30123-0_59

Schink, B., Stams, A.J.M., 2002. Syntrophism among prokaryotes. The Prokaryotes.

Schink, B., Ward, J.C., Zeikus, J.G., 1981. Microbiology of Wetwood: Importance of Pectin Degradation and *Clostridium* Species in Living Trees. Applied and Environmental Microbiology 42, 526–532. doi:10.1128/aem.42.3.526-532.1981

Schink, B., Zeikus, J.G., 1980. Microbial methanol formation: A major end product of pectin metabolism. Current Microbiology 4, 387–389. doi:10.1007/BF02605383

Schulz, S., Conrad, R., 1996. Influence of temperature on pathways to methane production in the permanently cold profundal sediment of Lake Constance. FEMS Microbiology Ecology 20, 1–14. doi:10.1111/j.1574-6941.1996.tb00299.x

Schulz, S., Matsuyama, H., Conrad, R., 1997. Temperature dependence of methane production from different precursors in a profundal sediment (Lake Constance). FEMS Microbiology Ecology 22, 207–213. doi:10.1111/j.1574-6941.1997.tb00372.x

Schütz, H., Holzapfel-Pschorn, A., Conrad, R., Rennenberg, H., Seiler, W., 1989. A 3-year continuous record on the influence of daytime, season, and fertilizer treatment on methane emission rates from an Italian rice paddy. Journal of Geophysical Research 94, 16,405-16,416. doi:10.1029/JD094iD13p16405

Schutz, M.M., Hansen, L.B., Steuernagel, G.R., Reneau, J.K., Kuck, A.L., 1990. Genetic Parameters for Somatic Cells, Protein, and Fat in Milk of Holsteins1. Journal of Dairy Science 73, 494–502. doi:10.3168/jds.S0022-0302(90)78697-3

Seemann, T., 2014. Prokka: rapid prokaryotic genome annotation. Bioinformatics 30, 2068–2069. doi:10.1093/bioinformatics/btu153

Sharma, K., Kuhad, R., 2009. An evidence of laccases in archaea. Indian Journal of Microbiology 49, 142–50. doi:10.1007/s12088-009-0039-4

Sieber, J.R., McInerney, M.J., Gunsalus, R.P., 2012. Genomic Insights into Syntrophy: The Paradigm for Anaerobic Metabolic Cooperation. Annual Review of Microbiology 66, 429–452. doi:10.1146/annurev-micro-090110-102844

Sikora, A., Detman, A., Chojnacka, A., Blaszczyk, M., 2017. Anaerobic Digestion: I. A Common Process Ensuring Energy Flow and the Circulation of Matter in Ecosystems. II. A Tool for the Production of Gaseous Biofuels. doi:10.5772/64645

Smith, P.H., Mah, R.A., 1966. Kinetics of Acetate Metabolism during Sludge Digestion. Applied Microbiology 14, 368–371. doi:10.1128/am.14.3.368-371.1966

Smith-Unna, R., Boursnell, C., Patro, R., Hibberd, J.M., Kelly, S., 2016. TransRate: reference-free quality assessment of de novo transcriptome assemblies. Genome Research 26, 1134–1144. doi:10.1101/gr.196469.115

Stams, A.J.M., Plugge, C.M., 2009. Electron transfer in syntrophic communities of anaerobic bacteria and archaea. Nature Reviews Microbiology 7, 568–577. doi:10.1038/nrmicro2166

Steinberg, L.M., Regan, J.M., 2009. mcrA-Targeted Real-Time Quantitative PCR Method To Examine Methanogen Communities. Applied and Environmental Microbiology 75, 4435–4442. doi:10.1128/AEM.02858-08

Stothard, P., Wishart, D.S., 2005. Circular genome visualization and exploration using CGView. Bioinformatics (Oxford, England) 21, 537–539. doi:10.1093/bioinformatics/bti054

Strąpoć, D., Picardal, F.W., Turich, C., Schaperdoth, I., Macalady, J.L., Lipp, J.S., Lin, Y.-S., Ertefai, T.F., Schubotz, F., Hinrichs, K.-U., Mastalerz, M., Schimmelmann, A., 2008. Methane-Producing Microbial Community in a Coal Bed of the Illinois Basin. Applied and Environmental Microbiology 74, 3918. doi:10.1128/AEM.00856-08

Straub, K.L., Buchholz-Cleven, B.E. 2001. *Geobacter bremensis* sp. nov. and *Geobacter pelophilus* sp. nov., two dissimilatory ferric-iron-reducing bacteria. International Journal of Systematic and Evolutionary Microbiology 51, 1805–1808. doi:10.1099/00207713-51-5-1805

Stubner, S., 2004. Quantification of Gram-negative sulphate-reducing bacteria in rice field soil by 16S rRNA gene-targeted real-time PCR. Journal of Microbiological Methods 57, 219–230. doi:10.1016/j.mimet.2004.01.008

Sugano, A., Tsuchimoto, H., Cho, T.C., Kimura, M., Asakawa, S., 2005. Succession of methanogenic archaea in rice straw incorporated into a Japanese rice field: estimation by PCR-DGGE and sequence analyses. Archaea 1, 391–397. doi:10.1155/2005/582597

Sun, L., Toyonaga, M., Ohashi, A., Matsuura, N., Tourlousse, D.M., Meng, X.-Y., Tamaki, H., Hanada, S., Cruz, R., Yamaguchi, T., Sekiguchi, Y., 2016. Isolation and characterization of F*lexilinea flocculigen*. nov., sp. nov., a filamentous, anaerobic bacterium belonging to the class Anaerolineae in the phylum *Chloroflexi*. International Journal of Systematic and Evolutionary Microbiology 66, 988–996. doi:10.1099/ijsem.0.000822

Thauer, R.K., 1998. Biochemistry of methanogenesis: a tribute to Marjory Stephenson. 1998 Marjory Stephenson Prize Lecture. Microbiology (Reading, England) 144 (Pt 9), 2377–2406. doi:10.1099/00221287-144-9-2377

Thauer, R.K., Kaster, A.-K., Seedorf, H., Buckel, W., Hedderich, R., 2008. Methanogenic archaea: ecologically relevant differences in energy conservation. Nature Reviews Microbiology 6, 579–591. doi:10.1038/nrmicro1931

Tran, P., Ramachandran, A., Khawasik, O., Beisner, B.E., Rautio, M., Huot, Y., Walsh, D.A., 2018. Microbial life under ice: Metagenome diversity and in situ activity of Verrucomicrobia in seasonally ice-covered Lakes. Environmental Microbiology 20, 2568–2584. doi:10.1111/1462-2920.14283

Turnbaugh, P.J., Hamady, M., Yatsunenko, T., Cantarel, B.L., Duncan, A., Ley, R.E., Sogin, M.L., Jones, W.J., Roe, B.A., Affourtit, J.P., Egholm, M., Henrissat, B., Heath, A.C., Knight, R., Gordon, J.I., 2009. A core gut microbiome in obese and lean twins. Nature 457, 480–484. doi:10.1038/nature07540

Uritskiy, G.V., DiRuggiero, J., Taylor, J., 2018. MetaWRAP—a flexible pipeline for genome-resolved metagenomic data analysis. Microbiome 6, 158. doi:10.1186/s40168-018-0541-1

Vanwonterghem, I., Jensen, P.D., Ho, D.P., Batstone, D.J., Tyson, G.W., 2014. Linking microbial community structure, interactions and function in anaerobic digesters using new molecular techniques. Current Opinion in Biotechnology, Energy biotechnology • Environmental biotechnology 27, 55–64. doi:10.1016/j.copbio.2013.11.004

Venkatesagowda, B., 2019. Enzymatic demethylation of lignin for potential biobased polymer applications. Fungal Biology Reviews 33, 190–224. doi:10.1016/j.fbr.2019.06.002

Ward, N.L., Challacombe, J.F., Janssen, P.H., Henrissat, B., Coutinho, P.M., Wu, M., Xie, G., Haft, D.H., Sait, M., Badger, J., Barabote, R.D., Bradley, B., Brettin, T.S., Brinkac, L.M., Bruce, D., Creasy, T., Daugherty, S.C., Davidsen, T.M., DeBoy, R.T., Detter, J.C., Dodson, R.J., Durkin, A.S., Ganapathy, A., Gwinn-Giglio, M., Han, C.S., Khouri, H., Kiss, H., Kothari, S.P., Madupu, R., Nelson, K.E., Nelson, W.C., Paulsen, I., Penn, K., Ren, Q., Rosovitz, M.J., Selengut, J.D., Shrivastava, S., Sullivan, S.A., Tapia, R., Thompson, L.S., Watkins, K.L., Yang, Q., Yu, C., Zafar, N., Zhou, L., Kuske, C.R., 2009. Three genomes from the phylum *Acidobacteria* provide insight into the lifestyles of these microorganisms in soils. Applied and Environmental Microbiology 75, 2046–2056. doi:10.1128/AEM.02294-08

Watanabe, T., Kimura, M., Asakawa, S., 2009. Distinct members of a stable methanogenic archaeal community transcribe *mcrA* genes under flooded and drained conditions in Japanese paddy field soil. Soil Biology and Biochemistry 41, 276–285. doi:10.1016/j.soilbio.2008.10.025

Weber, S., Lueders, T., Friedrich, M.W., Conrad, R., 2001a. Methanogenic populations involved in the degradation of rice straw in anoxic paddy soil. FEMS Microbiology Ecology 38, 11–20. doi:10.1111/j.1574-6941.2001.tb00877.x

Weber, S., Stubner, S., Conrad, R., 2001b. Bacterial Populations Colonizing and Degrading Rice Straw in Anoxic Paddy Soil. Applied and Environmental Microbiology 67, 1318–1327. doi:10.1128/AEM.67.3.1318-1327.2001

Wegner, C.-E., Liesack, W., 2016. Microbial community dynamics during the early stages of plant polymer breakdown in paddy soil: Metatranscriptomics of rice straw decomposition. Environmental Microbiology 18, 2825–2842. doi:10.1111/1462-2920.12815

Wei, H., Guenet, B., Vicca, S., Nunan, N., AbdElgawad, H., Pouteau, V., Shen, W., Janssens, I.A., 2014. Thermal acclimation of organic matter decomposition in an artificial forest soil is related to shifts in microbial community structure. Soil Biology and Biochemistry 71, 1–12. doi:10.1016/j.soilbio.2014.01.003

Weller, S., Kraus, D., Wassmann, R., Ayag, K., Butterbach-Bahl, K., Kiese, R., Alberto, Ma.C., 2014. Methane and nitrous oxide emissions from rice and maize production in diversified rice cropping systems. Nutrient Cycling in Agroecosystems 100. doi:10.1007/s10705-014-9658-1

Welte, C., Deppenmeier, U., 2014. Bioenergetics and anaerobic respiratory chains of acetoclastic methanogens. Biochimica et Biophysica Acta (BBA) - Bioenergetics, 18th European Bioenergetics Conference 2014 Lisbon, Portugal 1837, 1130–1147. doi:10.1016/j.bbabio.2013.12.002

Westermann, P., Ahring, B.K., Mah, R.A., 1989. Temperature Compensation in *Methanosarcina barkeri* by Modulation of Hydrogen and Acetate Affinity. Applied and Environmental Microbiology 55, 1262–1266. doi:10.1128/aem.55.5.1262-1266.1989

Wiegel, J., 1990. Temperature spans for growth: Hypothesis and discussion*. FEMS Microbiology Reviews 6, 155–169. doi:10.1111/j.1574-6968.1990.tb04092.x

Wirth, R., Kovács, E., Maróti, G., Bagi, Z., Rákhely, G., Kovács, K.L., 2012. Characterization of a biogas-producing microbial community by short-read next generation DNA sequencing. Biotechnology for Biofuels 5, 41. doi:10.1186/1754-6834-5-41

Woese, C.R., Fox, G.E., 1977. Phylogenetic structure of the prokaryotic domain: The primary kingdoms. Proceedings of the National Academy of Sciences 74, 5088–5090. doi:10.1073/pnas.74.11.5088

Wofford, N.Q., Beaty, P.S., McInerney, M.J., 1986. Preparation of cell-free extracts and the enzymes involved in fatty acid metabolism in *Syntrophomonas wolfei*. Journal of Bacteriology 167, 179–185. doi:10.1128/jb.167.1.179-185.1986

Worm, P., Koehorst, J.J., Visser, M., Sedano-Núñez, V.T., Schaap, P.J., Plugge, C.M., Sousa, D.Z., Stams, A.J.M., 2014. A genomic view on syntrophic versus non-syntrophic lifestyle in anaerobic fatty acid degrading communities. Biochimica et Biophysica Acta (BBA) - Bioenergetics 1837, 2004–2016. doi:10.1016/j.bbabio.2014.06.005

Wu, X.-L., Friedrich, M.W., Conrad, R., 2006. Diversity and ubiquity of thermophilic methanogenic archaea in temperate anoxic soils. Environmental Microbiology 8, 394–404. doi:10.1111/j.1462-2920.2005.00904.x

Wu, Y.-R., He, J., 2013. Characterization of anaerobic consortia coupled lignin depolymerization with biomethane generation. Bioresource Technology 139, 5–12. doi:10.1016/j.biortech.2013.03.103

Wu, Y.-W., Simmons, B.A., Singer, S.W., 2016. MaxBin 2.0: an automated binning algorithm to recover genomes from multiple metagenomic datasets. Bioinformatics 32, 605–607. doi:10.1093/bioinformatics/btv638

Yan, X., Akiyama, H., Yagi, K., Akimoto, H., 2009. Global estimations of the inventory and mitigation potential of methane emissions from rice cultivation conducted using the 2006 Intergovernmental Panel on Climate Change Guidelines. Global Biogeochemical Cycles 23. doi:10.1029/2008GB003299

Yao, H., Conrad, R., 2000. Effect of temperature on reduction of iron and production of carbon dioxide and methane in anoxic wetland rice soils. Biology and Fertility of Soils 32, 135–141. doi:10.1007/s003740000227

Yao, H., Conrad, R., 1999. Thermodynamics of methane production in different rice paddy soils from China, the Philippines and Italy. Soil Biology and Biochemistry 31, 463–473. doi:10.1016/S0038-0717(98)00152-7

Yao, H., Conrad, R., Wassmann, R., Neue, H.U., 1999. Effect of soil characteristics on sequential reduction and methane production in sixteen rice paddy soils from China, the Philippines, and Italy. Biogeochemistry 47, 269–295. doi:10.1007/BF00992910

Yuan, Q., Huang, X., Rui, J., Qiu, S., Conrad, R., 2020. Methane production from rice straw carbon in five different methanogenic rice soils: rates, quantities and microbial communities. Acta Geochimica 39, 181–191. doi:10.1007/s11631-019-00391-5

Yue, L., Li, F., YaHai, L., Hugenholtz, F., Ke, M., 2015. Effect of temperature on the structure and activity of a methanogenic archaeal community during rice straw decomposition. Soil Biology & Biochemistry 81, 17–27.

Yvon-Durocher, G., Allen, A.P., Bastviken, D., Conrad, R., Gudasz, C., St-Pierre, A., Thanh-Duc, N., del Giorgio, P.A., 2014. Methane fluxes show consistent temperature dependence across microbial to ecosystem scales. Nature 507, 488–491. doi:10.1038/nature13164

Zhang, C.-J., Pan, J., Liu, Y., Duan, C.-H., Li, M., 2020. Genomic and transcriptomic insights into methanogenesis potential of novel methanogens from mangrove sediments. Microbiome 8, 94. doi:10.1186/s40168-020-00876-z

Zhang, G., Yu, H., Fan, X., Liu, G., Ma, J., Xu, H., 2015. Effect of rice straw application on stable carbon isotopes, methanogenic pathway, and fraction of CH_4 oxidized in a continuously flooded rice field in winter season. doi:10.1016/J.SOILBIO.2015.02.008

Zhang, M., Zhang, L., Huang, S., Li, W., Zhou, W., Philippot, L., Ai, C., 2022. Assessment of spike-AMP and qPCR-AMP in soil microbiota quantitative research. Soil Biology and Biochemistry 166, 108570. doi:10.1016/j.soilbio.2022.108570

Zinder, S.H., 1993. Physiological Ecology of Methanogens, in: Ferry, J.G. (Ed.), Methanogenesis: Ecology, Physiology, Biochemistry & Genetics, Chapman & Hall Microbiology Series. Springer US, Boston, MA, pp. 128–206. doi:10.1007/978-1-4615-2391-8_4

Zinder, S.H., Koch, M., 1984. Non-acetoclastic methanogenesis from acetate: acetate oxidation by a thermophilic syntrophic coculture. Archives of Microbiology 138, 263–272. doi:10.1007/BF00402133

Zinder, S.H., Mah, R.A., 1979. Isolation and Characterization of a Thermophilic Strain of Methanosarcina Unable to Use H_2-CO_2 for Methanogenesis. Applied and Environmental Microbiology 38, 996–1008.

7 Supporting information

Supplemental tables are available online under the link:
https://zenodo.org/record/7439280#.Y5pS_Z7MK5c

Supplemental tables for chapter2-Methodology

Table S2.1. Sequencing statistics of the metatranscriptomic datasets

Table S2.2 Sequencing statistics of the metagenomic data

Supplemental tables for chapter3-Methanogenic Community Dynamics at Mesophilic Temperature

Table S3.1 Significance analysis for the quantification of bacterial 16S rRNA gene copy numbers at 30 ℃.

Table S3.2 Significance analysis for the quantification of *mcrA* gene copy numbers at 30 ℃.

Table S3.3 Significance analysis for the quantification of bacterial 16S rRNA transcripts at 30 ℃.

Table S3.4 Significance analysis for the quantification of *mcrA* transcripts at 30 ℃.

Table S3.5 Analysis of taxon-specific abundances on rRNA level for the abundant families at 30 ℃.

Table S3.6 Analysis of taxon-specific abundances on mRNA level for the abundant families at 30 ℃.

Table S3.7 Transcript dynamics of CAZyme families (relative abundance related to mRNA reads assigned to all CAZyme familyies %).

Table S3.8 Analysis of the mapping-independent transcript abundances of particular methanogenesis genes at 30 ℃.

Table S3.9 Assembly statistics for the MAGs obtained at 30 ℃.

Table S3.10 KEGG-annotated genes copy numbers in *Methanosarcina* MAGs and *Methanosarcina* reference genomes at 30 ℃.

Table S3.11 List of KEGG-annotated genes only present in *Methnosarcina* MAGs at 30 ℃.

Table S3.12 Analysis of the mapping-dependent transcript abundances of particular methanogenesis genes at 30 ℃.

Table S3.13 KEGG level 2 assignment of mRNA mapped onto the *Methanosarcina* MAGs at 30 ℃.

Table S3.14 KEGG level 3 assignment of mRNA mapped onto the *Methanosarcina* MAGs at 30 ℃.

Table S3.15 Properties of Philippine paddy soil and Italian paddy soil.

Table S3.16 Comparison of the relative transcript abundances of methanogenic key genes between Philippine paddy soil (P) and Italian paddy soil (I) at 30 ℃.

Supplemental tables for chapter4-Methanogenic Community Dynamics at Moderately Mesophilic Temperature

Table S4.1 Significance analysis for the quantification of bacterial 16S rRNA gene copy numbers at 45 ℃.

Table S4.2 Significance analysis for the quantification of *mcrA* gene copy numbers at 45 ℃.

Table 4.3 Significance analysis for the quantification of bacterial 16S rRNA transcripts at 45 ℃.

Table S4.4 Significance analysis for the quantification of *mcrA* transcripts at 45 ℃.

Table S4.5 Analysis of taxon-specific abundances on rRNA level for the abundant families at 45 ℃.

Table S4.6 Analysis of taxon-specific abundances on mRNA level for the abundant families at 45 ℃.

Table S4.7 Analysis of the mapping-independent transcript abundances of particular methanogenesis genes at 45 ℃.

Table S4.8 Assembly statistics for the MAGs obtained at 45 ℃.

Supplemental figures for chapter3-Methanogenic Community Dynamics at Mesophilic Temperature

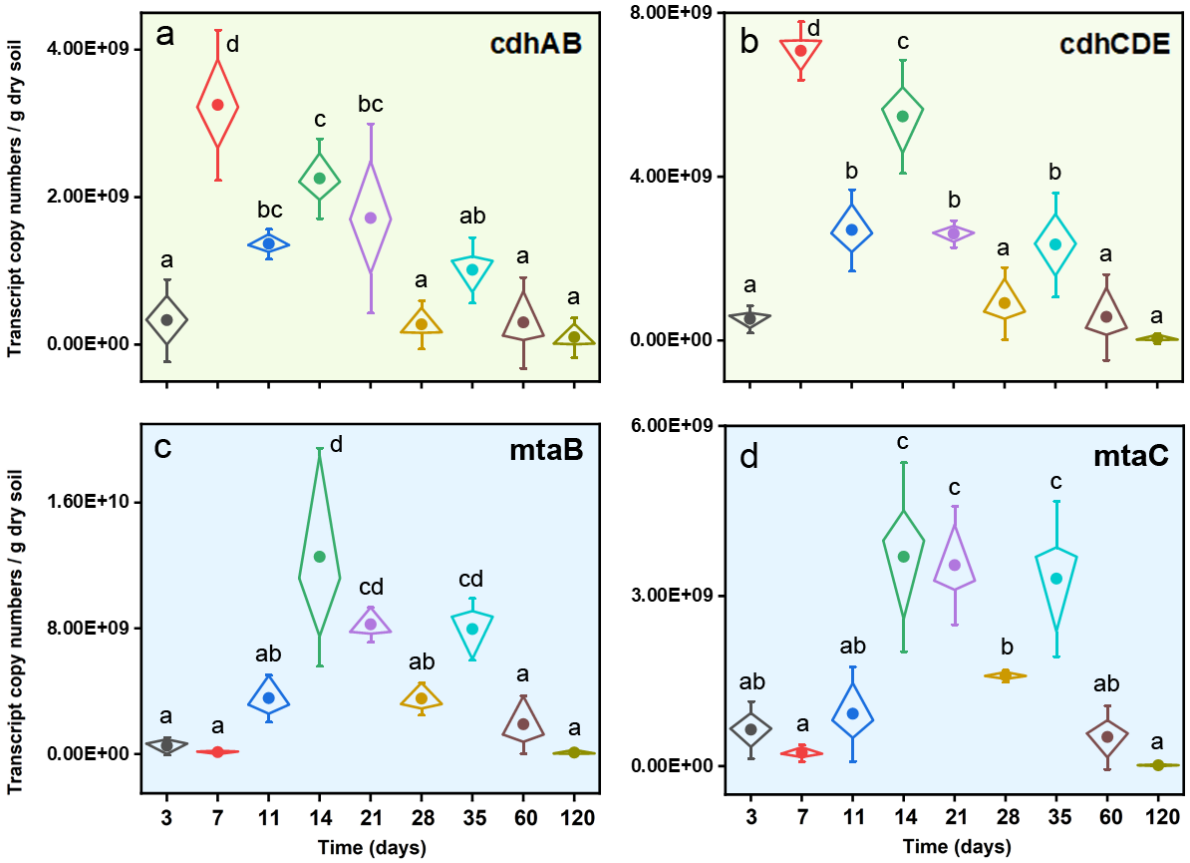

Figure S3.1: Absolute transcript abundances of acetoclastic and methylotrophic key pathway genes. The relative metatranscriptome abundances of particular transcript species were linked to the experimentally determined copy numbers of *mcrA* transcripts (RT-qPCR, Fig. 2d) to calculate the absolute transcript abundances expressed by marker genes indicative of acetoclastic (*cdhAB* and *cdhCDE* [a and b]) and methylotrophic (*mtaB* and *mtaC* [c and d]) methanogenesis. The calculation of the absolute transcript abundances followed a procedure described by Zhang et al. (2022) and is based on the following equation:

$$= \frac{\text{Metatranscriptomic transcript abundance of target gene (\%)}}{\text{Metatranscriptomic transcript abundance of mcrA (\%)}} \times \text{Transcript copy numbers of } \textit{mcrA} \text{ quantified by RT} - \text{qPCR}$$

Error bars represent standard errors. Data are means ± SE (n = 3).

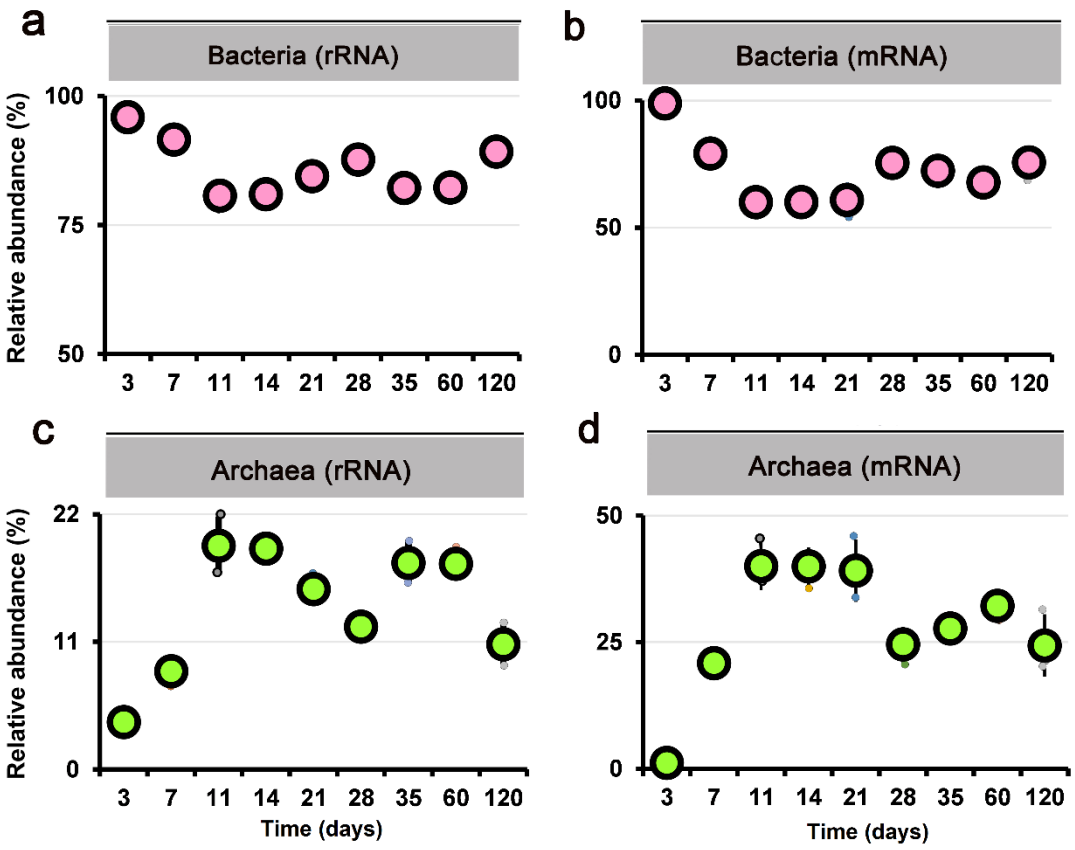

Figure S3.2: Metatranscriptomic abundance dynamics of bacterial and archaeal 16S rRNA (a and c) and mRNA (b and d) analyzed on domain level over the 120-day incubation period. The relative abundance values are given in relation to total bacterial and archaeal 16S rRNA and mRNA.

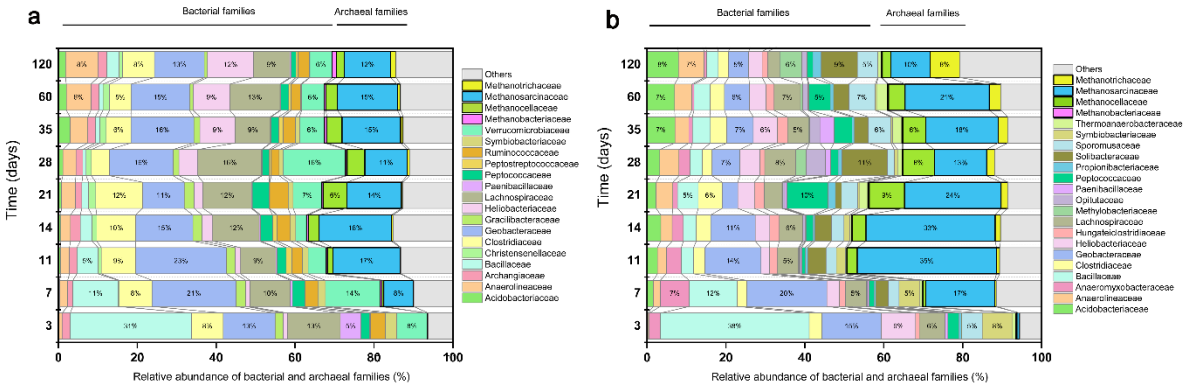

Figure S3.3: Metatranscriptomic abundance dynamics of bacterial and archaeal 16S rRNA (a) and mRNA (b) (cutoff > 2%) analyzed on family level over the 120-day incubation period. Taxonomic assignment of assembled 16S rRNA reads was performed using BLASTN algorithm implemented in DIAMOND against SILVA 132 SSU database with 0.90 sequence identity. Taxonomic assignment of mRNA reads was performed using BLASTX algorithm implemented in DIAMOND against NR database with 0.93 sequence identity. The relative abundance values are given in relation to total bacterial and archaeal 16S rRNA and mRNA.

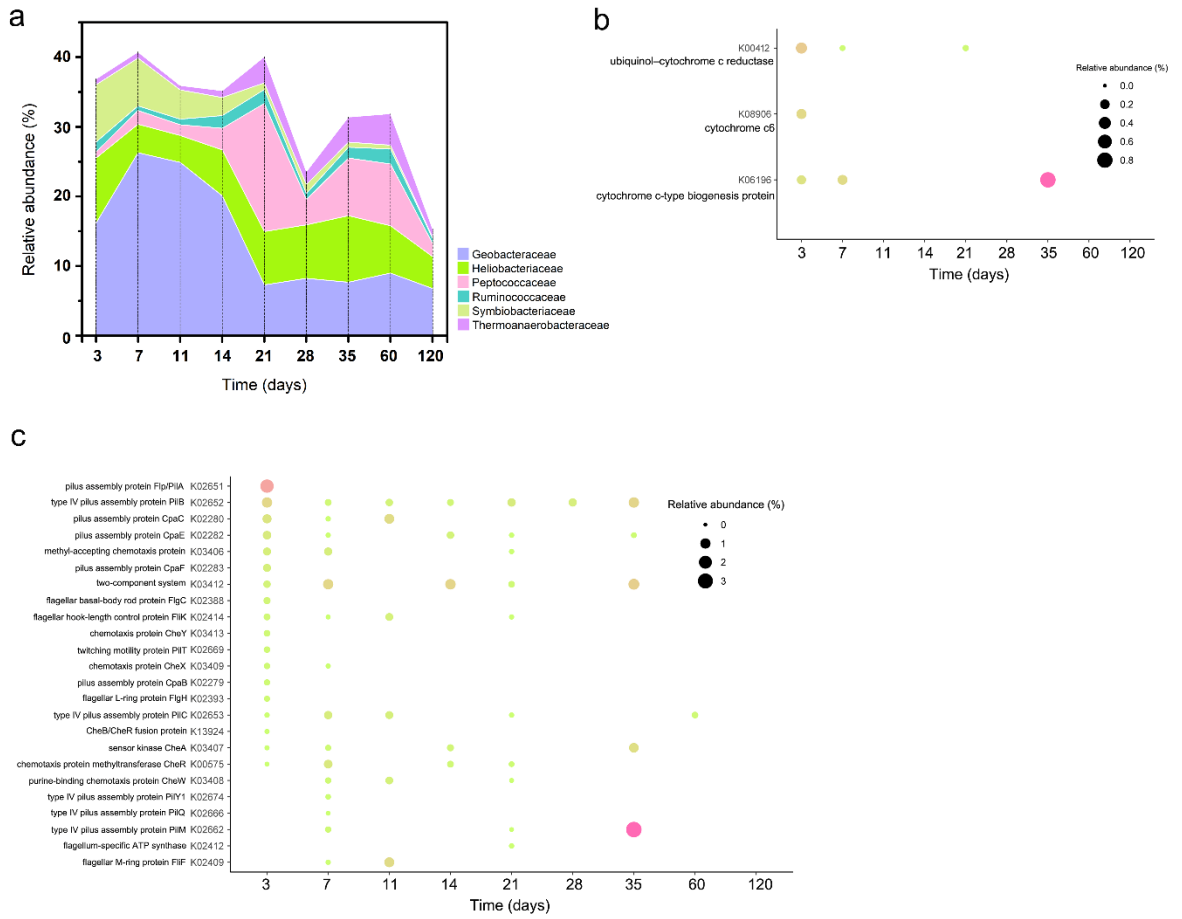

Figure S3.4: Metatranscriptomic mRNA abundance dynamics of putative syntrophic bacteria (cutoff > 2%) analyzed on family level over the 120-day incubation period at 30 °C (a). The relative abundance values are given in relation to total bacterial mRNA and are means of metatranscriptomic triplicate analysis. Transcript dynamics of genes affiliated to the family *Geobacteraceae* and involved either in the synthesis of *c*-type cytochromes (b) or in the KEGG category 'cell motility' (c). The relative abundance values are given in relation to total mRNA that could be functionally annotated in KEGG and is affiliated to the family *Geobacteraceae*.

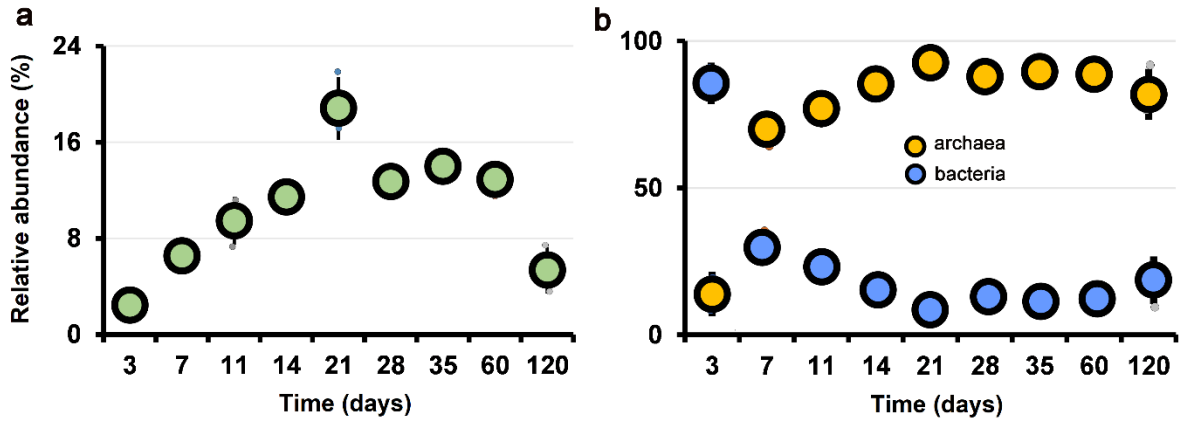

Figure S3.5: Metatranscriptomic abundance dynamics of transcripts affiliated with the KEGG category ‘methane metabolism’. The abundances were calculated in relation to total KEGG-assigned mRNA (a). Comparison of the relative abundance dynamics of bacterial and archaeal mRNA affiliated with the KEGG category ‘methane metabolism’ (b).

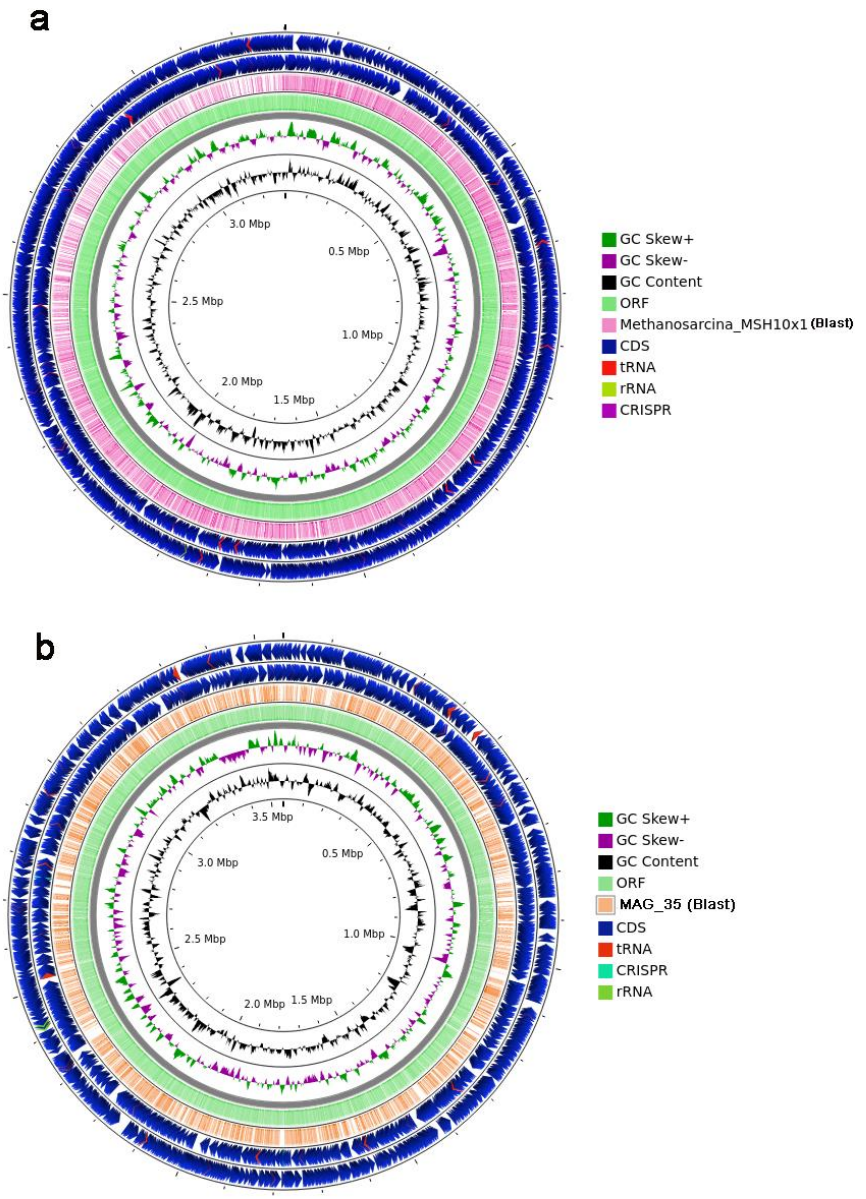

Figure S3.6: Circular genome maps for MAG_35 (a) and the most closely related reference genome (*Methanosarcina* sp. strain MSH10X1) (b). Circles from the outside to the inside show the positions of protein-coding sequences (blue), tRNA (red) and rRNA genes (green) on the positive (circle 1) and negative (circle 2) strands. Circles 3 shows the positions of BLAST hits detected through BLASTx (with an e-value cut-off of 1e-5) and circle 4 depicts the BLASTx results for the reciprocal search against the genome of strain MSH10X1 (a) and MAG_35 (b). Circles 5 and 6 show GC content and GC skew plotted as the deviation from the genomic average.

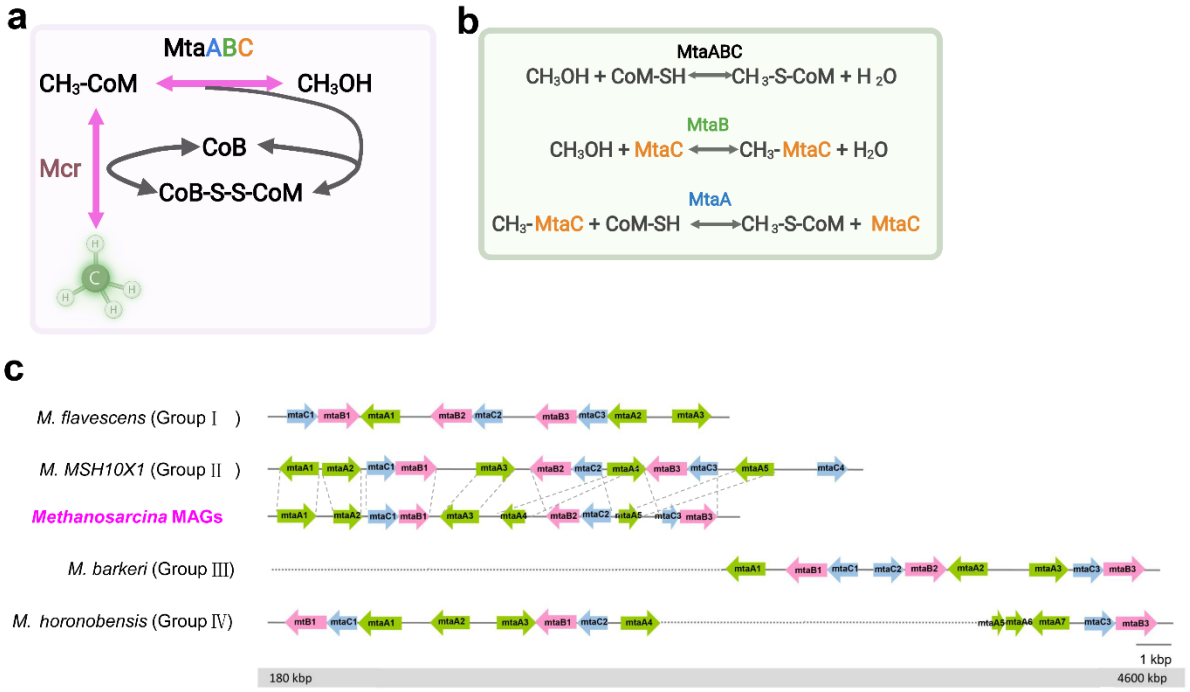

Figure S3.7: Methanol-dependent methanogenesis pathway in the three *Methanosarcina* MAGs (21, 28, 35) and the Group I to IV reference genomes (a and b). *Methanosarcina* populations produce the MtaABC enzyme complex to catalyze the methyl transfer from methanol to CoM to form methyl-CoM. (c) Comparison of the genetic organization of the *mta* gene cluster between the three *Methanosarcina* MAGs (21, 28, 35) and the Group I to IV reference genomes.

Supplemental figures for chapter4-Methanogenic Community Dynamics at Moderately Mesophilic Temperature

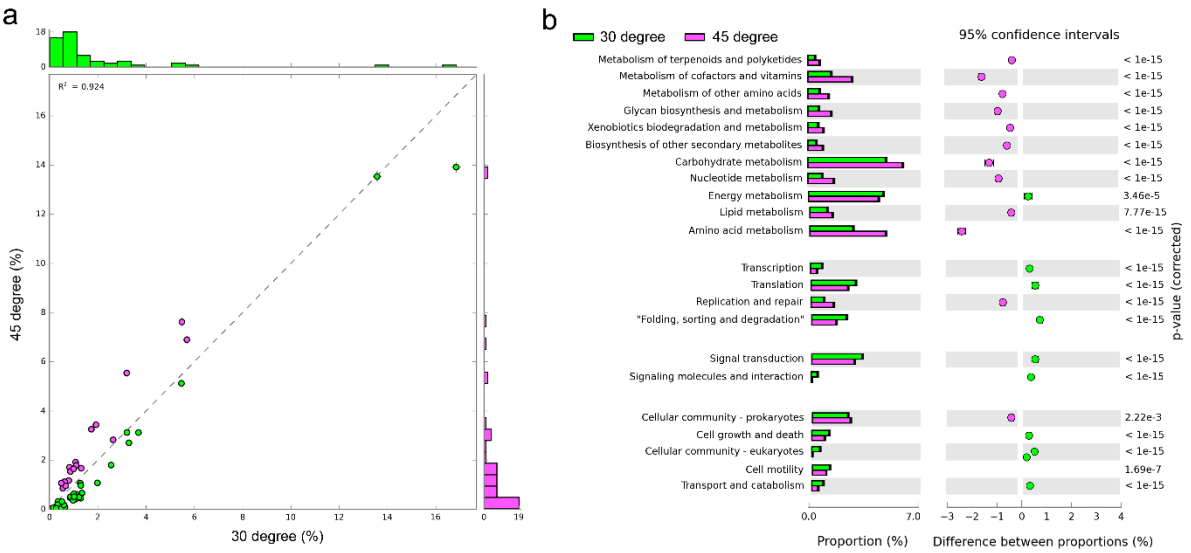

Figure S4.1: Comparison of the functional microbiome profiles between the 30 ℃ and 45 ℃ incubation treatments. The mean abundance of KEGG level 2 categories in the mRNA datasets (a) and the percentage difference in relative abundance among the categories with 95% confidence intervals (b).

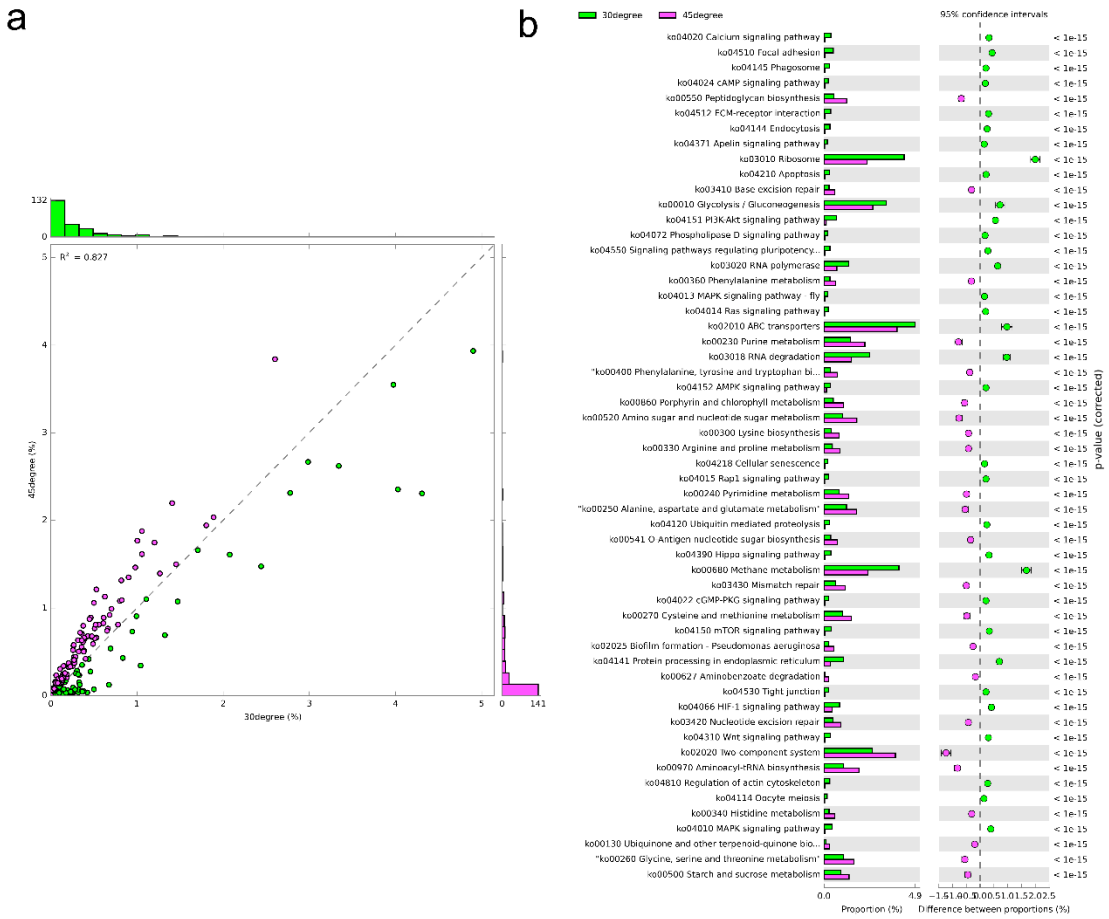

Figure S4.2: Comparison of the functional microbiome profiles between the 30 ℃ and 45 ℃ incubation treatments. The mean abundance of KEGG level 3 categories in the mRNA datasets (a) and the percentage difference in relative abundance among the categories with 95% confidence intervals (b).

List of abbreviations

Key pathways	Key enzymes	Full name of enzymes
Acetoclastic methsnogenesis	Cdh	acetyl-CoA decarbonylase/synthase complex
	Ack	acetate kinase
	Pta	phosphate acetyltransferase
	Acs	acetyl-CoA synthetase
Hydrogenotrophic methanogenesis	Fwd	formylmethanofuran dehydrogenase
	Ftr	formylmethanofuran-tetrahydromethanofuran dehydrogenase
	Mch	methenyl-H4MPT cyclohydrolase
	Mtd	F420-dependent methylene H4MPT dehydrogenase
	mer	5-10-methylenetetrahydromethanopterin reductase
Methylotrophic methanogenesis	MtaABC	methanol methyltransferase/methanol corrinoid protein
	MtbABC	methylamine methyltransferase/methylamine corrinoid protein
	MttABC	trimethylamine methyltransferase/trimethylamine corrinoid protein
	MtmABC	dimethylamine methyltransferase/dimethylamine corrinoid protein.
Common pathway genes	Mcr	methyl coenzyme M reductase
	Mtr	Na+-translocating methyl-H4MPT–coenzyme-M methyltransferase

Publication List

This thesis resulted in the following papers:

Li, X., Bei, Q.B., & Liesack, W. Methanogenic Community Dynamics in Philippine Rice Field Soil: A Metagenomic and Metatranscriptomic Analysis. (In preparation)

Li, X., Bei, Q.B., & Liesack, W. The effects of rising temperature on anaerobic food chain in Philippine Rice Field Soil. (In preparation)

Acknowledgements

This dissertation marks the end of a long and memorable journey, which I would not have been able to complete without the support of my supervisors and colleagues. First and foremost, I would like to express my sincere gratitude to my supervisor PD Dr. Werner Liesack for always being there when I needed his support, reviewing my progress constantly, and guiding me through my PhD studies.

I am grateful to my thesis advisory committee – Prof. Andreas Brune and Prof. Seigo Shima for their scientific support.

An immense thanks to Dr. Qicheng Bei for all his help during my PhD. It would have been quite tough without his support in the laboratory since day one. Thanks so much for all his help with the computational analysis and for the invaluable scientific discussions during my PhD study. I am also grateful to Dr. Nicole Paczia and Peter Claus for the metabolite analysis.

It has been an amazing experience working in Max Planck Institute for Terrestrial Microbiology. Sincere thanks to Kangli Guo, Dr. Jingjing Peng, Dr. Anna Hakobyan, Mehrdad Rabiei Nematabad, and all the members of Prof. Andreas Brune's group, for the pleasant work atmosphere. Over last four years, many people helped me relating to a lot of small and bigger problems thus making this PhD thesis possible.

I am deeply grateful to my family and my friends for their continuous and loving support.

ERKLÄRUNG

Ich versichere, dass ich meine Dissertation:

"**The impact of differential temperatures (30°C versus 45°C) on the methanogenic community in Philippine rice field soil**"

selbstständig und ohne unerlaubte Hilfe angefertigt habe und mich keiner als der von mir ausdrücklich bezeichneten Quellen und Hilfen bedient habe. Diese Dissertation wurde in der jetzigen oder ähnlichen Form noch bei keiner anderen Hochschule eingereicht und hat noch keinen sonstigen Prüfungszwecken gedient.

Marburg, 19.12.2022

Xin Li